ADSORPTION OF INORGANIC IONS AT THE TITANIUM OXIDE-SOLUTION INTERFACE

by

YVES GILLES BERUBE

B.A. Université de Montréal 1961
S.B. Massachusetts Institute of Technology 1963

Submitted in partial fulfillment of the requirements
for the degree of

DOCTOR OF SCIENCE

at the
Massachusett Institute of Technology
1967

Signature of Author
Department of Metallurgy _____

Signature of Professor
in Charge of Research _____

Signature of Chairman,
Departmental Committee on
Graduate Students _____

ABSTRACT

ADSORPTION OF INORGANIC IONS AT THE
TITANIUM OXIDE-SOLUTION INTERFACE

by

YVES GILLES BERUBE

Submitted to the Department of Metallurgy on January 9, 1967 in partial fulfillment of the requirements for the degree of Doctor of Science.

The existence of an electrical double layer at the oxide surface in contact with an aqueous electrolyte solution is a well substantiated fact. For these systems, it has been shown that the surface charge is due to the excess adsorption ($\Gamma_{H+} - \Gamma_{OH-}$) of the potential-determining ions, H^+ and OH^-.

In this dissertation, the effects of various monovalent inorganic ions, Li^+, Na^+, Ca^+, ClO_4^-, NO_3^-, Cl^-, I^-, on the surface charge of rutile has been investigated as a function of pH by means of potentiometric titrations. In order to characterize the structure of the interface and the mechanism of the adsorption processes, tracer exchange studies with tritium at the rutile and hematite interfaces were performed. In addition, the effect of temperature, as well as the importance of the past history of the surfaces on adsorption, were considered.

Adsorption of H^+ (OH^-) is found to occur in two steps; a fast adsorption followed by a slow exchange. This slow exchange is explained by an interaction between the ions in the inner plane of the ionic double layer and the surface hydroxyls. The behavior of the fast isotherm, obtained rapidly enough so as to prevent interference by the slow mechanism, is found to be consistent with the Gouy-Chapman treatment of the diffuse layer at low surface charges. Calculated capacities for the inner Helmholtz region suggest a penetration of counterions into the plane of surface charge, while specific adsorption is found to increase in the following order; $I^- < Cl^- = NO_3^- = ClO_4^- = Cs^+ < Na^+ < Li^+$. This is indeed a surprising result contrary to that normally observed with other materials.

Based on these findings, the following model of the rutile interface is proposed. The anhydrous oxide is assumed to be covered by tightly bonded, non-labile, hydroxyl groups. Superimposed on these groups is a second layer of strongly bonded water, the dissociation of which results in the formation of the surface charge as measured experimentally.

Such a model is also shown to be in agreement with the observed effects of temperature on adsorption, the heat-treatment of the surface, and with tracer exchange studies.

Complementary work on the hematite interface corroborates the postulate of Onoda and de Bruyn regarding the existence of water of hydration on the solid side of the interface. A thickness of 13 Å is calculated for this phase and a diffusion coefficient of 2.5×10^{-21} cm/sec^2 for tritium is found to be in agreement with the proton space charge theory.

Thesis Supervisor: P. L. de Bruyn
Professor of Metallurgy

TABLE OF CONTENTS

LIST OF FIGURES

ACKNOWLEDGMENTS

The author would like to express his gratitude to all those who contributed in helping him, but he cannot include them all.

Professor de Bruyn stands above all for his warm and friendly counseling throughout these many years at M.I.T. He has made this stay a rewarding and intellectually stimulating experience that will not be forgotten.

The author wishes also to express his appreciation to Professors Gaudin, Witt and Irvine, whose interests in various aspects of this research were of a direct help in bringing the investigation to a conclusion.

And there are all those friends of the Surface Chemistry Laboratory whose friendship will be missed: a very large part of this thesis has developed from the many exchanges of ideas that took place and the author would not want to forget in particular Lo Blok and George Onoda. The author owes his appreciation to Miss Pat Gavagan who typed the manuscript and Mr. Stan Mitchell who took care of the reproduction.

Finally, the author would like to thank his wife for the exemplary patience she showed during the preparation of this dissertation.

The author is indebted to the Office of Naval Research and the U. S. Army Research Office - Durham for having provided the financial support without which this study would not have been possible.

I. INTRODUCTION

Technology has often found itself way ahead of science in using properties of matter before they are understood. Oxide surfaces offer a good example of the discrepancy between how little we know about some properties and how useful they prove to be. The fact that an oxide interface in water carries around it an ionic atmosphere greatly dependent on pH has been exploited in many commercial processes for separating minerals. The fact that oxides show interesting ion exchange properties has also been applied to liquid chromatography.

Still, there has been comparatively little work done to establish the relationships between charges on oxides and their interaction with inorganic ions in solution. The purpose of this investigation is to study the origin of surface charges on rutile and the interaction taking place between these charges and some ionic components in solution. Such interactions have been characterized for the very well defined mercury interface[20]. But similar studies[6,13,16] on oxides do not appear to agree with the proposed model for mercury in any better than a qualitative way.

This dissertation will include both a kinetic and a thermodynamic analysis of the adsorption of potential-determining ions at the interface. The nature and concentration of the ionic population in solution, the temperature and the state of the surface will all be varied in an effort to resolve the mechanisms of adsorption. The nature of the interface itself will be investigated with the help of radioactive tracer exchanges.

II. REVIEW OF PAST WORK ON OXIDES

Interest in electrokinetic properties of oxides has been closely associated with their flotability and colloidal properties. Identification of the zero-point-of-charge (zpc) and of specific adsorption of organic and some inorganic complex ions constituted the primary purposes of most studies on rutile[1-4], for instance. We define here the zero-point-of-charge as the pH of the solution in equilibrium with the oxide where there is no net adsorption of hydrogen over hydroxyl ions.

Data on zpc's for a large number of oxides has been compiled recently[5]. Theoretical predictions of zpc's based on solubility data of oxides have been made[6]. A semi-theoretical correlation between zpc's and physical properties of the supporting oxide phase has recently been proposed by Parks[5], while a linear relation between zpc's and heats of immersion has also been suggested[7].

While surface charge as a function of pH can be derived indirectly[8] from zeta potential measurements, it was only recently that direct measurements by means of potentiometric titrations were attempted on ferric oxide[9]. Potentiometric titrations on oxides represent the extension of an idea first applied to silver iodide[10,11] and silver sulfide[12].

By drawing an analogy between an oxide system and these systems, hydrogen and hydroxyl ions were found to be potential-determining, while common monovalent inorganic ions were considered indifferent[9,13]. However, when Albrethsen[13]

attempted calculations of differential capacities following an approach well proven on other similar systems[10,14], he obtained capacities of an order of magnitude too large when compared with the AgI or mercury double layer systems. Also, irreproducibility of adsorption, hysteresis, and irreversibility of the system plagued the first experiments. Already in 1941, Troelstra[15] had observed similar complications.

The irreversibility of the hematite-water system was investigated by Onoda and de Bruyn[16]. These investigators explained the behavior in terms of a two-step adsorption process: a fast surface-exchange involving surface complexes, followed by a slow diffusion of protons in and out of the hydrated lattice. It was shown that reversible isotherms would be obtained if the slow step was prevented from interfering during a rapid titration of the suspension. A similar reaction on alumina was interpreted by Korpi[17] as a slow exchange between so-called indifferent anions and hydroxyl groups at the interface. Despite the fact that the hematite-water system has been better characterized, differential capacities derived from the fast isotherm and reported by Onoda[18] are still three times larger than would be predicted by the modified Stern-Grahame[20] model of the double layer. The same applies to Blok's results with zinc oxide.

Much less evidence has been accumulated on the titanium dioxide system. The properties of the double layer were evaluated by microelectrophoresis and streaming potential

measurements[1,2,3]. The value of the zpc was shown to vary with the nature of the preparation and the surface treatment to which the material was subjected[2,5]. The work done on a fully hydrated oxide was observed to give a zpc at pH 6.0, while a low value of pH 3.5 has been observed for fired material[4].

III. MATERIALS AND EXPERIMENTAL PROCECURE

1. Materials and Reagents

A. Titania

Various techniques, both wet and dry methods, are available for the production of titania. Dry methods, such as the Hautefeuille's method of preparation[21], were not used in this investigation because in most experiments, oxides that were fully in equilibrium with aqueous solutions were desired. For this reason, only methods of precipitation from aqueous phases were considered.

The influence of the methods of precipitation of titania on its properties has been the object of much interest in the past ten years[22-27]. Wilska[22] surveyed the methods of preparation and their effects on the crystallinity of the product. The diagram shown in Figure 1 illustrates this point.

For this particular research program, the bulk of the rutile was prepared by precipitation of a titanium tetrachloride salt (method 3). A mixture of ice prepared from conductivity water and the tetrachloride salt is made to yield 120 g of rutile per liter of solution and is brought slowly to room temperature. This procedure is intended to reduce the violence of liberation of hydrochloric vapors. Ten percent of the solution is removed and heated to boiling point. By this method, a very fine precipitate is obtained. The fine precipitate is again introduced in the bulk of the solution to provide nuclei for growth of larger particles. Precipi-

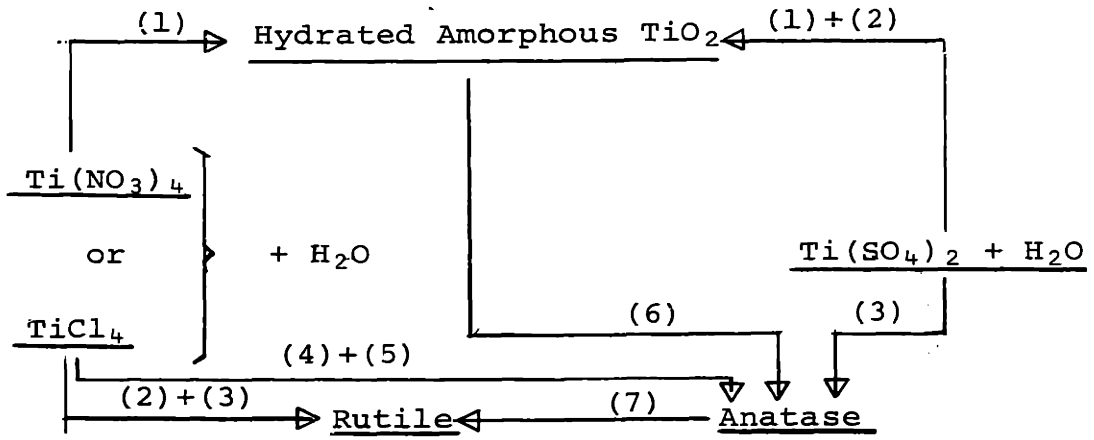

1: precipitation by alkaline hydrolysis

2: hydrolysis at room temperature

3: hydrolysis by boiling

4: hydrolysis by boiling in presence of SO_4^{-2}, PO_4^{-3} ions

5: hydrolysis by boiling in presence of excess Cl^- ions

6: dehydration at moderate temperatures (<150°C)

7: igniting*

FIGURE 1. SCHEMATIC DIAGRAM OF THE METHODS OF PREPARATION OF TITANIA.

*This method is questionable because of variations in stability of the anatase structure. For instance, anatase prepared by method 5 will convert rapidly to rutile by simple refluxing at 100°C.

tation occurs at a measurable rate at 80°C; the solution is kept for three hours at this temperature before it is refluxed at 105°C for 20 days. Refluxing is done by boiling the precipitate in the original highly acid solution (pH ≈ 1). A condenser prevents evaporation of the solution.

X-ray diffraction patterns on freeze-dried samples before and after refluxing indicate coarsening of the precipitate. The study also shows that while the initial precipitate consists of 70% rutile and 30% anatase, after refluxing it is transformed to a coarsened precipitate of pure (99%) rutile. Both crystal modifications have the tetragonal unit cell, where each titanium is coordinated by six oxygens. They differ in the way edges of adjacent octahedra are shared. In rutile, only two opposite edges per octahedron are shared, while in anatase, there are four edges which are shared. In Appendix 5, the crystal structures are described in more detail. Spectrographic analysis of the product showed traces of some heavy metal ions, all of which are present in concentrations below 10 ppm. Krypton adsorption measurements made by the BET method on freeze-dried precipitates, evacuated for 2 hours at 150°C, indicated surface areas of 43 M^2 up to 55 M^2 per gram.

Anatase was prepared from the hydrated sulfate salt, $Ti(SO_4)_2 \cdot 9\ H_2O$, according to method 3. This hydrated salt was very difficult to dissolve in cold water, while heating the solution only resulted in precipitation of anatase on the undissolved sulfate. It was found, however, that heating

overnight at 140°C dehydrates the salt to a glassy conglomerate which is then readily solubilized. A solution sufficiently concentrated to yield 120 gms of titania per liter was brought to the boiling point and precipitation of anatase resulted. Spectrographic analysis showed some contamination by silica (<0.1%) and potassium (<0.1%). X-ray patterns are characteristic of pure anatase without traces of rutile. Surface areas obtained from krypton adsorption were quite high, around 125 M^2/g.

In all cases, the precipitates were washed free of electrolyte contamination by repeated decantation of wash water. The material prepared from sulfate salts was, upon removal of most contamination, washed in ammonia[26] in order to remove adsorbed sulfate ions and then again equilibrated with conductivity water. At the end of the cleaning operation, conductivity of supernatant solution was 2×10^{-6} mho·cm^{-1}, or better. The material was stored in polyethylene bottles for a few months before experimentation.

B. Reagents

A list of reagents is given in Appendix 1 with their origin and chemical purity. Double-distilled water was used throughout these experiments with a minimum conductivity of 8×10^{-7} mho·cm^{-1}. Whenever possible, reactions cells were kept under a nitrogen atmosphere. Nitrogen was purified by bubbling it through two 37% solutions of caustic soda, followed by equilibration with water vapor at room tempera-

ture. Tenth normal solutions of acid and base were used; the alkaline solution was stored in polyethylene bottles to prevent silica contamination.

2. Experimental Equipment and Procedure

A. Potentiometric Titrations

The potentiometric titration is too familiar[14,12,6] a tool to be described here at any length. The titration consists in adding to an aqueous suspension known quantities of acid or base. The concentration of potential-determining species in solution (in this case hydrogen and hydroxyl ions) is recorded before and after the addition. What cannot be accounted for in the solution is assumed to be adsorbed.

(i) Apparatus. The titration cells, round pyrex flasks with five vertical ground-glass joints as described by Albrethsen[13], are kept in a constant temperature bath controlled to within 0.1°C of the desired temperature. Nitrogen is flowed through the cell at an overpressure of 2 inches of water.

The pH measuring system consists of two glass electrodes per cell and a reference electrode. For the work at room temperature, Beckman general purpose glass electrodes are coupled with the reference electrode, a saturated calomel electrode with an asbestos fiber junction. At temperatures above 35°C, a glass electrode (7-G-461 by Electrofact, Holland) with tamal (brand name for thallium amalgam/thallium chloride) internal is coupled with a

silver-silver chloride reference electrode in a saturated KCl solution. The leak rate of KCl through the junction varied from 10^{-5} moles of KCl per hour to 3.3×10^{-5} moles; hence, for measurements over extended periods of time, the reference electrode was removed from the cell between readings.

Calibration of electrodes is described in Appendix 2. In the same appendix, it is also shown how the calibration procedure can yield values for the mean ionic activity coefficient of the salt ($\gamma_{\pm}$) at different ionic strengths. The voltage output, directly proportional to pH, is measured by a vibrating Reed electrometer used as a null point indicator and is balanced against a Gebr. Ruhstrat potentiometer with an accuracy of ± 0.1 mV. The system is calibrated at frequent intervals against a standard cell. A Brown Electronik recorder was used to determined the point of constant emf output from the cell.

(ii) Calculation of Isotherms. The potentiometric titration consists in adding to a cell containing a known amount of precipitate and known volume of solution, aliquots of titrants and following the changes of concentrations in solution by means of the electrodes. A simple mass balance is obtained with

$$A\Delta\Gamma_{\pm} = \Delta M - \left[V_2\left(C_{H+}-C_{OH-}\right)_2 - V_1\left(C_{H+}-C_{OH-}\right)_1\right] \qquad (1)$$

where

$$\Delta\Gamma_{\pm} = \Delta\left(\Gamma_{H^+} - \Gamma_{OH^-}\right) = \text{change in relative surface excess of hydrogen over hydroxyl ions} \quad (2)$$

and

A = total surface area of suspension

ΔM = amount of acid or base added

V = volume of sclution

C_{H+} = concentration of hydrogen derived from pH

C_{OH-} = concentration of hydroxyl derived from pH.

Subscripts "1" and "2" refer to physical quantities before and after titrant addition.

The above equation gains its validity from the postulate that no side reactions such as CO_2 dissociation or dissolution of the precipitate take place. While the first condition is not easily met, the solubility of titania is so low[28,29] (solubility product is 10^{-55}) that it can be neglected. The volume dealt with in this equation is the total volume of added water and the solubility of water in the solid phase is assumed to be negligible.

The data is obtained as: changes in the emf of the pH electrodes, amount of reagent added, and total volume of water. To convert the voltage output into the proper concentration terms, two relations are used:

$$E = E^{\circ\prime} + k\ (-\log C_{H^+}) \qquad (3)$$

where

E = emf of the titration cell

$E^{\circ\prime}$ = standard reference potential determined by the calibration procedure. It is a function of ionic strength.

k = the pH-millivolt response of the electrodes as determined by the calibration (referred to as the "slope" of the electrodes; see Appendix 2).

and

$$(-\log C_{OH^-}) = (-\log K_w) + 2 \log \gamma_{\pm\,salt} + \log C_{H^+} \qquad (4)$$

where

K_w = the dissociation constant of water

$\gamma_\pm$ = mean activity coefficient of the salt in solution.

Values for C_{H^+} and C_{OH^-}, before and after an addition of reagent, can be introduced in equation (1), and, with the proper values for ΔM, V_1 and V_2, $\Delta\Gamma$ is calculated. Each $\Delta\Gamma$ is then related to the new pH of equilibrium reached after the reagent addition, ΔM, where pH is defined as $(-\log \gamma_\pm C_{H^+})$. A plot of $\sum\Delta\Gamma$ versus $(-\log \gamma_\pm C_{H^+})$ is obtained. The isotherms, obtained at various concentrations of salt in solution, normally intersect at one point; this point is given a value of $\Gamma_\pm = 0$. Appendix 2 describes the calibration procedure of the electrodes and the calculation of $\gamma_{\pm\,salt}$ when it is

not available in the literature. Appendix 3 gives a sample of data and a straightforward computer program to reduce the data to $\Gamma_{\pm}$, relative to the first experimental point rather than the intersection point, versus $(-\log C_{H^+})$.

(iii) Experimental Difficulties. Difficulties were encountered in measuring pH at elevated temperatures. With a large amount of precipitate in the cell, it was not possible to obtain stable pH readings. A discussion of this problem will be found in Appendix 4. Another difficulty comes from the variation in specific surface area introduced in sampling a precipitate. Two methods were used: (a) the suspension was centrifuged and the material spooned out, or (b) the suspension was stirred to give a uniform distribution of solids and fractions were poured into the cells. The latter of the two techniques is the most reproducible. It was observed that after a titration, a filtering operation tends to lower the surface area (loss of colloidal material). It is, for that reason, impossible to check the specific surface area for each titration. Repeated checks on the homogeneity of the suspension agree to within 6%, however, and a constant specific surface area for a batch of material is normally assumed.

B. pH Drift Experiments

On occasion, a different technique than the intersection of the isotherms was used to determine the zpc, the point of zero net adsorption of potential-determining ions. It consists

of dropping a dry material, which has no excess acid or base attached to its surface, into cells kept at various pH's, in order to find a pH at which adding material causes no pH change. The uncharged oxide is then in equilibrium with that particular pH, the pH of the zpc.

A precipitate is first heated to 500°C, under a vacuum of 10^{-3} mm of mercury for 20 hours to remove the reversible portion of physically and chemically adsorbed water. This, when done on a precipitate kept in a slightly acid pH, yields a precipitate free of any traces of excess acid. In a cell prepared at a fixed pH and ionic strength, the evacuated material is dumped in while the pH drift is recorded.

Various cells at different pH's and concentrations of salt are thus prepared. The same experiment is performed until a pH is found, whereupon with the addition of the precipitate, no change in pH can be observed. This is nothing more than a variation of the potentiometric titration, except that it is quite accurate at the zpc where surface concentrations are low and very small changes in pH are brought about by additions of material. Also, it gives directly the pH of the zpc, independently of the intersection of isotherms. This property is important when specific adsorption occurs and the zpc does not coincide with the apparent intersection of isotherms.

C. Radioactive Tracer Exchange

In an attempt to verify the structure of the interface of some oxides (TiO_2 and Fe_2O_3), the hydrogen on the surface of these oxides has been replaced with tritium. After evacuation to remove excess radioactive water non-bonded to the solid, the surface is contacted with pure water until equilibrium is established between the tritiated surface and the solution. The amount exchanged as a function of time should give an indication of the distribution and amount of water in the interphasal region.

One curie of tritiated water is diluted to give one liter of solution. Samples of wet oxides are centrifuged and introduced in the heavy water (one gram of material to an average 40 millicuries of tritium). The samples are kept at constant temperature (129°C) in sealed containers. The vial is of a design previously used by Van Lier, de Bruyn and Overbeek[30] in their studies of the solubility of quartz. An inner platinum sleeve with the opening reinforced by a ruthenium-gold ring is encased in a steel container. A screw-on cap for this outer container presses a teflon seal against the supporting ring. Equilibration time in this vial lasted normally one month, often more.

The treated oxide is then centrifuged to remove excess water. The wet precipitate is placed in an evacuator which is kept at 10^{-3} mm of Hg with the aid of a high-vacuum mechanical pump. The evacuated water is collected in a

liquid nitrogen trap. The duration of this operation depended on the desired results as will be discussed later.

On completion of this step, the oxide is left with only its surface water which may be present as chemisorbed water, water of hydration and other bonded water. While still under vacuum, the specimen is cooled to liquid nitrogen temperature to stop any further interaction with the environment. It can then be taken out and transferred to a reaction cell kept at constant temperature. The cell is a centrifuge tube with a 24/40 ground glass mouth that can be either stoppered when desorbing at 25°C or connected to a mercury manometer (with a large diameter arm) to allow for gas expansion when desorbing at 95°C. The tube contains approximately 35 cc of water. At varying time intervals, the cell is centrifuged to allow the precipitate to settle out and a sample (1 cc) is pipetted for analysis of the activity of the solution.

For experiments at 95°C, the cell is normally kept in an oven and is stirred only before and after sampling. However, for the first few hours of desorption when the rate is fast, the tube is kept unsealed (simply stoppered) in a temperature-controlled bath and stirred continuously; evaporation of the solution is then higher, but the tube is weighed after sampling and it is possible to calculate the loss through evaporation. It was found that no isotope effects were noticeable during evaporation of a radioactive solution. For experiments at room temperature, the cell is

simply stoppered and also stirred only before and after sampling, except for the first 10 hours.

The sample (1 cc of solution) is added to a low-sodium glass scintillation vial. Fifteen ml of scintillating solution is introduced in the vial before it is cooled to -16°C for the counting procedure. Difficulties were encountered at first with this procedure. In order to insure high counting efficiencies, one μmole of water being the desired limit of detection, large samples of solution had to be introduced in the counter (1 cc). Also, cooling the photomultiplier tube turned out to be the only means to lower thermal noise, unless an expensive coincidence circuit was used. A scintillation solvent that would dissolve large amounts of water (one cc of water per 15 cc of solvent) and which could also be cooled to -16°C had to be found. The standard toluene-methanol solvent does not dissolve water while the solvent in current use, a dioxane-anisole mixture, freezes at 4°C. In fact, there was at the time no known solvent available. After considerable experimentation, a solvent was developed that met all these requirements. A benzyl alcohol, with 10% methanol offers all possible advantages. It is a liquid phenyl alcohol, it dissolves water better than toluene because of the OH radical, it can be cooled down to -17°C without freezing and without precipitating the water phase, it is stable over periods of months and is considerably more efficient than the dioxane solvent often used. The

scintillator, PPO (see Appendix 1), is dissolved in it to a concentration of 4 grams per liter of solution, and a wavelength shifter, POPOP (see Appendix 1), is added to a concentration of 50 milligrams per liter.

The counting equipment consists of the Baird Atomic liquid scintillation system, #745. In most cases, integral counting is practised as it yields better efficiencies. Both photocathode and preamplifier are kept at -16°C to minimize background. The ratio of signal to background is kept usually around 25.

The data are recorded as sample activity versus elapsed time at sampling. To change from activity of a sample to the amount of water on the solid which is involved in radioactive exchange, a sample (1 cc) of the original solution already equilibrated with the oxide is diluted to one liter and will be called the mother sclution (M.S.). A sample (1 cc) from that diluted M.S. will give a thousandth of the activity per cc of the equilibrating tritiated water, and the solid that equilibrated with this water, therefore contains $(10^{+3} \cdot A_{M.S.}/f)$ of activity per ml of water, where $A_{M.S.}$ is the activity of the diluted M.S. and f some isotopic correction factor. "f" is assumed to be unity throughout this investigation. The amount of water exchanging on the solid can be directly related to the activity of the desorption cell at time "t" by the

following relation,

$$M_t = \frac{10^{-3} \cdot f}{Wt \cdot A_{M.S.}} \quad V_t \cdot A_t + \sum_{i=1}^{n-1} L_i A_i \qquad (5)$$

M_t = amount of water (in ml) per gram of precipitate

f = isotopic correction factor

W_t = weight of precipitate in grams

A_M = activity of the diluted M.S.

V_t = volume of water in the desorption cell at time "t"

A_t = activity of sample (1 cc) at time "t"

L_i = losses (in ml) of water during samplings "i"

A_i = activity of sample "i"

n = total number of samples at time "t".

It will be recalled that such an equation is valid for the case where A_t and $A_{M.S.}$ are determined under the same conditions of counting efficiency. Also, it will be stressed that the concentration of activity during desorption never exceeds 10^{+5} cpm (counts per minutes) per cc while the M.S. averages 2.10^8 cpm per cc. For all practical purposes, the activity of the solution is negligible by comparison with that of the solid. Finally, the limit of detection, as determined by $A_{M.S.}$, the volume of solution and BKD the background count, is given as 3 μmoles of water per sample.

The accuracy is high but another problem plagues liquid scintillation, namely internal quenching. Variation in scintillating properties (aging of solvent over six months), presence of suspended material, salts and many

other factors can "quench" the output of the scintillator and change the efficiency. The problem was overcome by adding samples of the diluted M.S. to each sample (100 λ). The activity is measured before and after this addition, and one can then compare directly the specimen count to the mother solution count and obtain concentrations of water under identical quenching conditions. It was checked that the increase of 100 λ of water could not affect quenching in any significant way. The maximum error was estimated at 5% including counting statistics.

The work on rutile was performed with the same material used in titrations. The hematite comes from a material prepared by Onoda[18] and used by him to analyze the slow equilibration of hematite with the solution. Prior to tritium exchange, it was further washed and its surface area was found to be 15.5 M^2 as opposed to the 21 M^2 that was previously reported. It is felt that loss of fines upon filtering and washing has caused this small change.

IV. RESULTS

1. Kinetics of Adsorption

A. Slow Step in Adsorption

The effect of time on abstraction of potential-determining ions from solution was first studied. The material, rutile, has been conditioned at pH 6.0, the approximate zpc, for at least six months, at a very low ionic strength (5×10^{-6} M). If ionic strength is increased and a known amount of base added to the suspension, a very rapid equilibrium is achieved within 2 minutes. However, the pH does not remain constant but starts drifting continuously toward increasing acid values.

This effect has been observed with two different salts, NaCl and $NaNO_3$, at various ionic strengths (10^{-3} M to 10^{-1} M). The magnitude of base addition was also varied so as to adjust pH at initial values of 7.5, 8.5, 9.5 and 10.5. Regardless of the initial pH to which the system was brought, the observed change of pH with time was similar. Typical variations are shown in Figures 2a and 2b where the oxide is brought from pH 6.1 to 7.85 and allowed to equilibrate (Figure 2a), while Figure 2b describes a material first taken to pH 4.1 and then brought to pH 9.7. It has also been found that conditioning an oxide on the acid side of the zpc does not result in a slow adsorption process detectable by a pH drift; equilibrium is reached instantaneously and no drift of any significant magnitude is observed. Figures 2a

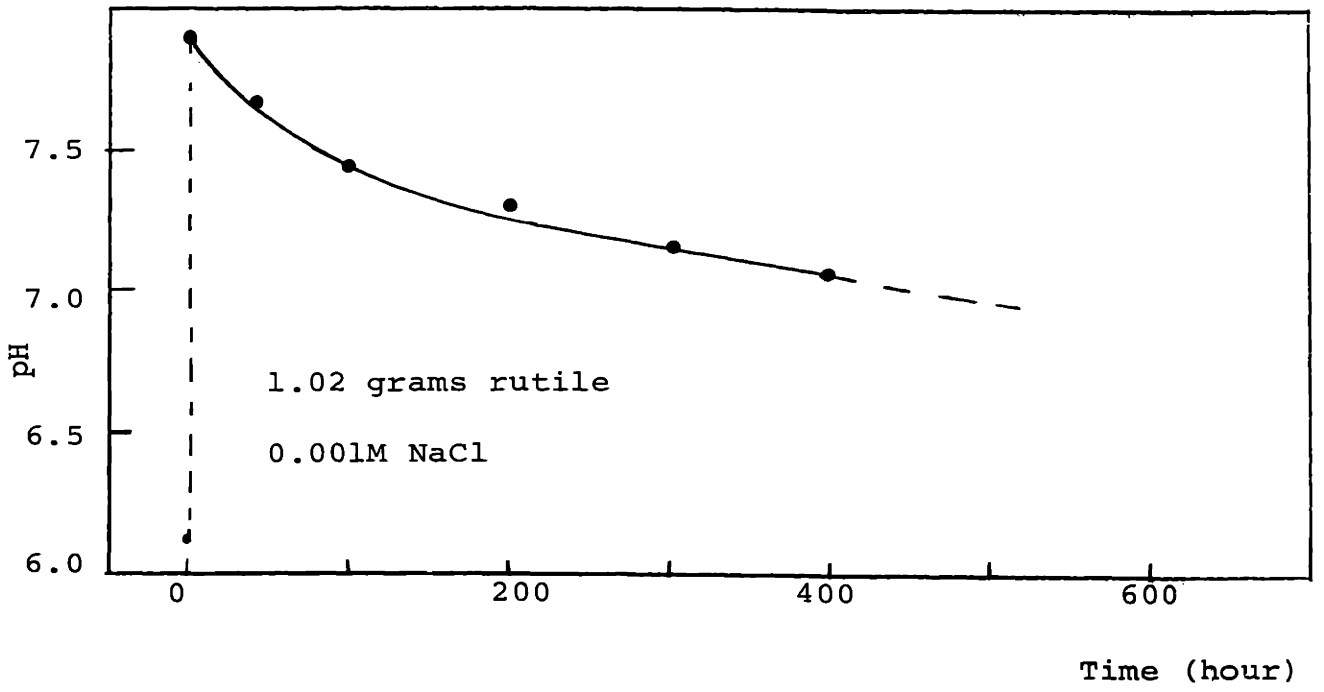

Figure 2a.

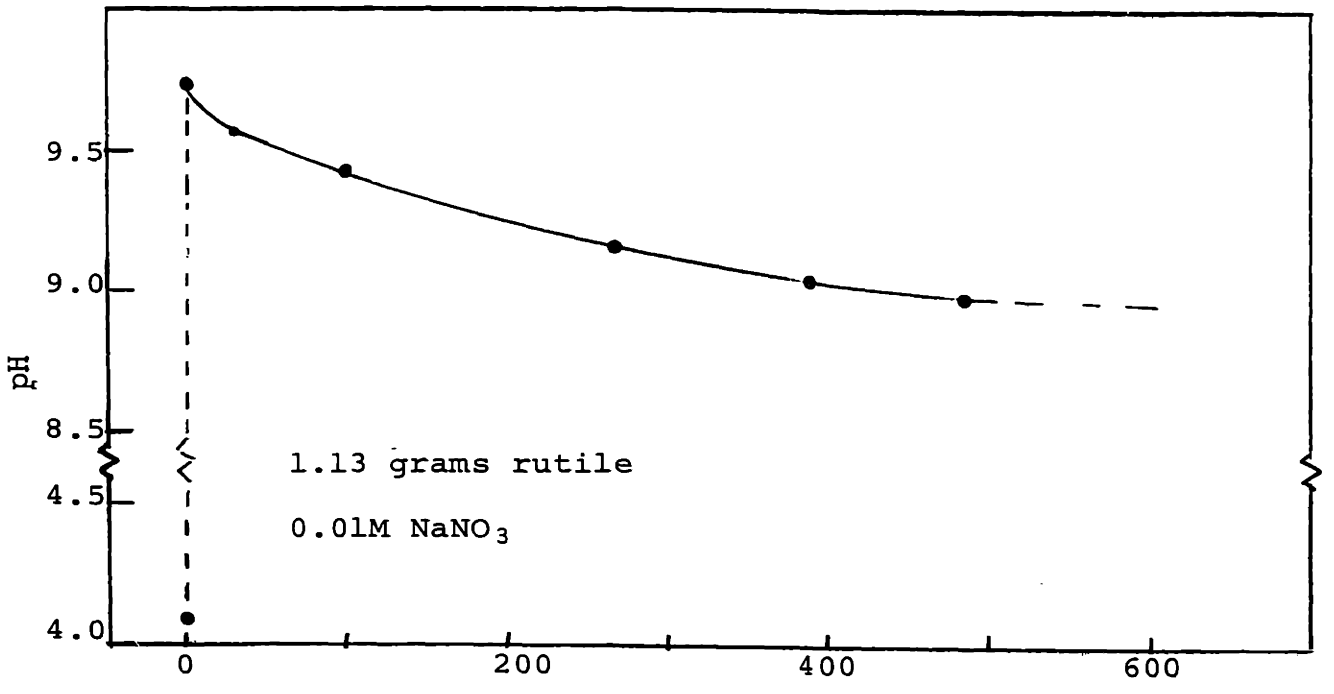

Figure 2b.

FIGURE 2. CONTINUOUS pH DRIFT DURING CONDITIONING OF A PRECIPITATE.

and 2b are described in the following way. An aliquot of base is added to a suspended material. The instantaneous pH change in the cell, indicated by the sudden rise in the curves, is far smaller than would be expected in pure water, due to adsorption on the solid. As pH drifts with time to more acid values, adsorption of hydroxyl ion is increased accordingly.

B. The Fast Isotherm

It is apparent from Figures 2a and 2b and all other work done on the system that the slow abstraction will only change pH by less than 0.2 units in the first 24 hours. If the material is never allowed to be in contact with extreme pH's (3 to 4 pH units away from the zpc) for more than a few minutes, the slow process can be inhibited. It becomes possible to titrate a suspension allowing 10 to 20 minutes per point, and obtain isotherms that are very little influenced by the slow step. Such a procedure yields a "fast" isotherm that has been well described by Onoda and de Bruyn[16]. Isotherms obtained in this way are reproducible to within 0.5 μmoles of reagent per sample or about 0.1 μcoul per cm^2.

If the slow abstraction is prevented from interfering during a given fast titration, there remains a possibility that conditioning a precipitate would alter its surface properties. In other words, the slow abstraction of potential-determining ions might change the surface properties involved in the fast exchange, even though the slow equilibrium itself is not disturbed during the establishment of a fast

isotherm. Fast titrations were performed on a precipitate which was conditioned at basic pH's to evaluate the effect of conditioning on successive fast isotherms spaced in time. The procedure consists in titrating a solid which originally had equilibrated at the zpc. A fast isotherm is thus obtained. The precipitate is then allowed to equilibrate on the basic side for long periods of time whereupon a new titration is run. This conditioning always results in a displacement of the initial isotherm. The precipitate can then be brought back to the acid side in an attempt to reverse the reaction and eventually retrace the original isotherm, or it can be conditioned even further at basic pH's. Multiple combinations are possible here.

Such isotherms are given for sodium nitrate and sodium chloride in Figures 3 and 4. In Figure 3, the original isotherm at icnic strength 0.01M is indicated by (1). The material was left at pH 9.45 for 11 days whereupon a shift in pH to a value of 9.0 was observed. Isotherm (2) is obtained by starting at that pH and ending at pH 4.1, where it is left for 5 hours before reproducibility is checked by running isotherm (3). The oxide is brought back to pH 4.1 for 4 days in an attempt to recover the original surface properties. A subsequent titration (4) showed little recovery (within experimental error) and was thereupon followed by further conditioning at pH 9.75 for 20 days. A final titration (5) starting at the new equilibrium pH

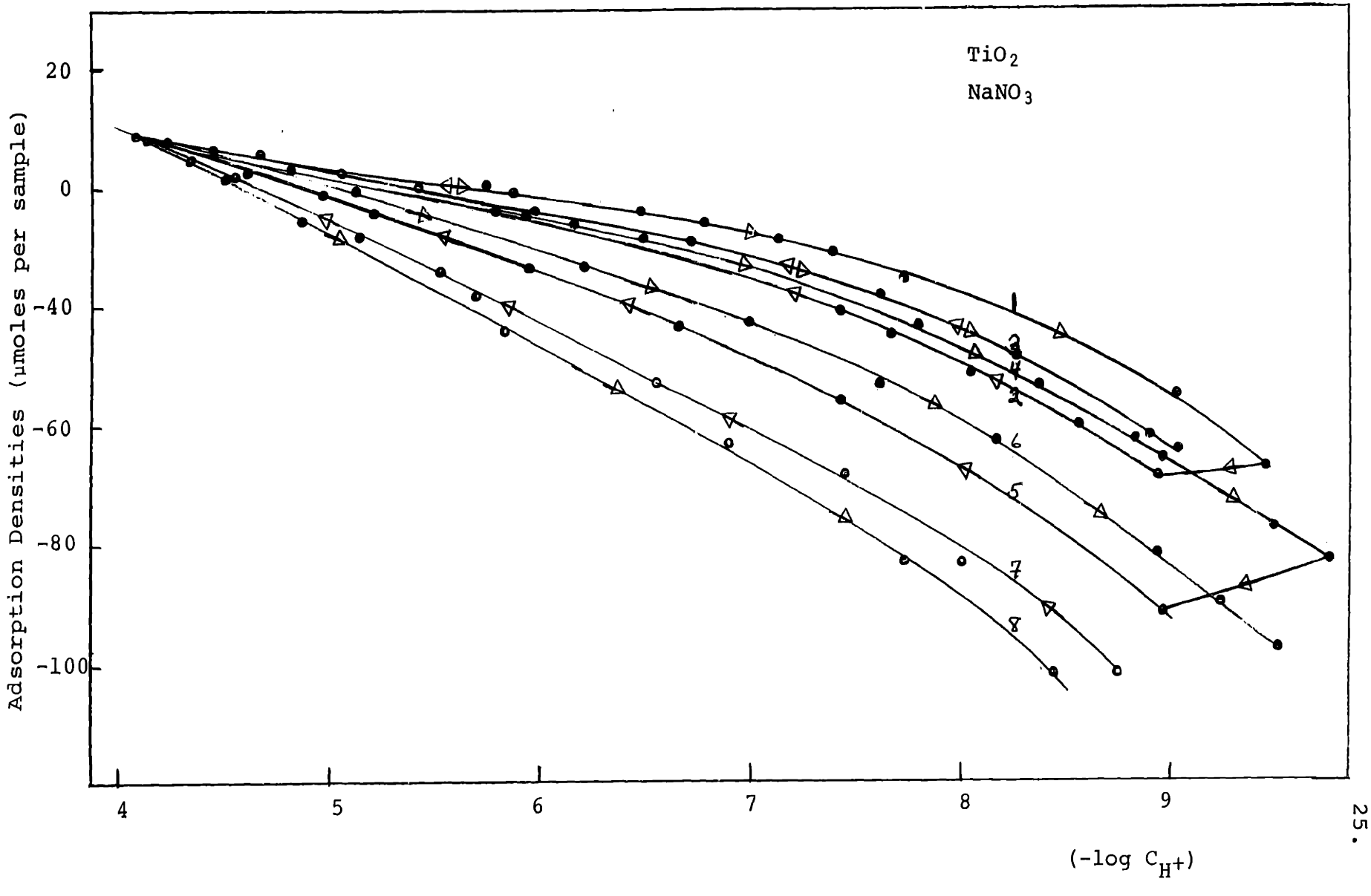

FIGURE 3. INFLUENCE OF CONDITIONING ON FAST ISOTHERMS AT 25°C IN PRESENCE OF $NaNO_3$.

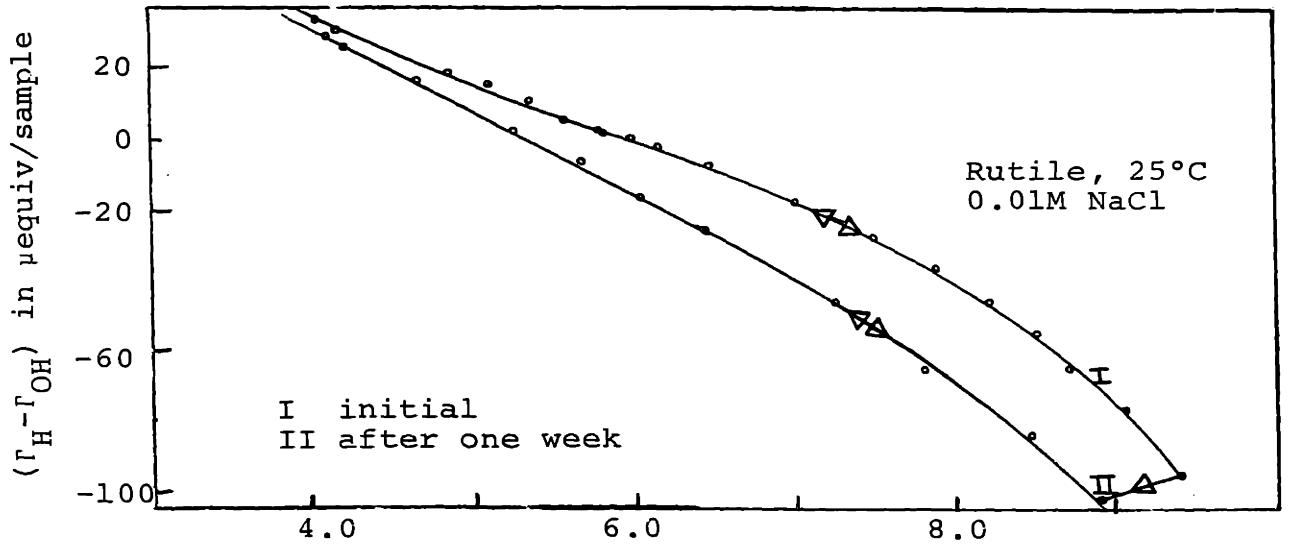

FIGURE 4. DISPLACEMENT OF FAST ISOTHERMS WITH CONDITIONING.

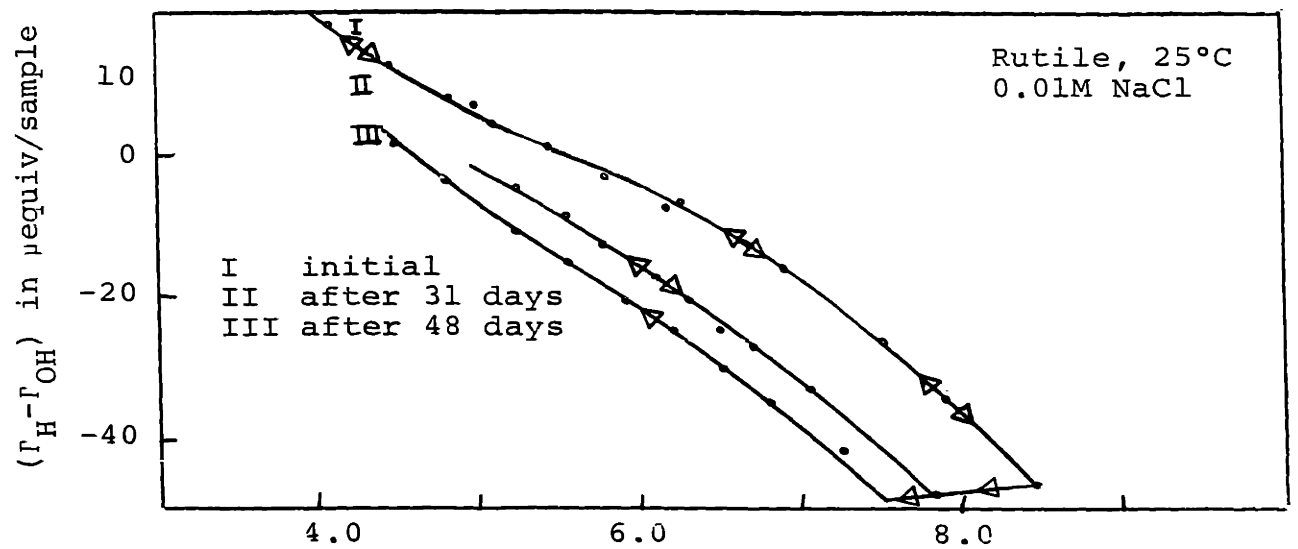

FIGURE 5. DISPLACEMENT OF FAST ISOTHERMS WITH CONDITIONING.

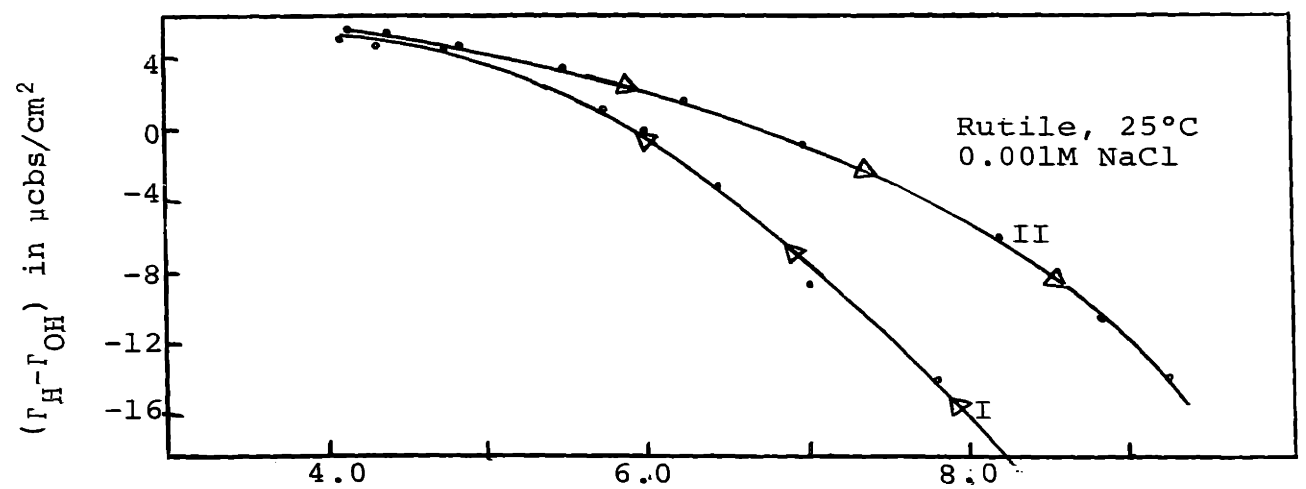

FIGURE 6. IRREVERSIBILITY OF FAST ISOTHERMS OBTAINED ON A MATERIAL CONDITIONED AT A BASIC pH.

of 9.0 brings the oxide to pH 4.1 is repeated (6) before ionic strength is changed to 0.1M (7) and 1M (8) to observe the new intercept of isotherms.

A similar procedure was followed with sodium chloride as the salt, the results of which are shown in Figure 4. An original isotherm (1) is repeated at the same ionic strength (10^{-2}M) after 7 days of conditioning at pH 9.5 (isotherm 2). Another displacement of isotherms at 10^{-1}M for sodium chloride upon basic conditioning is shown in Figure 5.

It is apparent from these figures that a fast isotherm is by no means indifferent to past conditioning. In fact, complete irreversibility can be found on a material aged at high pH's. An example is given in Figure 6 where a precipitate was kept one week in a normal sodium hydroxide solution before it was washed and introduced in a cell for titration (10 minutes per point) at an ionic strength of 10^{-3}M. Arrows on the isotherms indicate in all cases the direction of travel during titration.

It is of interest here to note that while conditioning at higher ionic strengths (10^{-1}M) leads to a parallel displacement of fast isotherms, at lower ionic strength conditioning will result in steeper isotherms. Also, prolonged conditioning is found to shift the intersection of isotherms, obtained with different concentrations of salts in solution, toward the acid side. Finally, it is found that an isotherm obtained after conditioning on the basic side is irreversible in the

sense that any subsequent titration will yield isotherms lying above this reference isotherm. The system behaves as if it were recovering its original properties.

2. pH Drift Experiments

The common intersection of isotherms serves as the usual criterion for establishing the zpc in the absence of specific adsorption. Under these conditions, it is normally expected that the zero point of ζ potential, to be referred to as the iep, coincides with the zpc. In the presence of specific adsorption, the zpc will also be a function of ionic strength and there will normally be no common intersection of isotherms. One way to verify the pH at which $\Gamma_{H^+} = \Gamma_{OH^-}$, is to have a dried material for which $\Gamma_{\pm} = 0$. Such a material can be introduced in a cell kept at a known pH. Only if this is the pH of the zpc will there be equilibrium between the added solid and the solution and will there be no pH drift in the cell upon addition of material.

Precipitates were heat-treated at 500°C for 20 hours under a vacuum of 10^{-3} mm of Hg and stored in a dessicator. It is assumed that such a heat-treatment leaves no excess acid or base on the solid (i.e., it may be assumed that $\Gamma_{H^+} = \Gamma_{OH^-}$). The postulate finds support in the fact that prior to evacuation, the specimen was kept at very low ionic strength and close to the expected zpc but on the acid pH side. Acids can evaporate but not alkalis. Excess titrant on the surface would, in a pH drift experiment, also permit

the determination of a pH of equilibrium between the solid and the solution. It would not be the pH of the zpc but the pH at which an equivalent surface charge must be adsorbed on the solid.

A series of drift experiments performed with solutions of 0.01M sodium perchlorate are given in Figure 7. Seven solutions of different pH values were prepared and each cell is identified by a number, from 1 to 7, at the top of the figure near the original pH of the cell. Variable amounts of solids are added to each cell individually while pH drift is recorded. On this figure, the abcissa represents pH while the ordinate, on the right-hand side of the figure, gives the amount of material added to a cell. At the zpc, no changes in pH take place upon addition of precipitate. Leaving the precipitate overnight in suspension results in no observable aging and corresponding change in pH.

In the same figure, a set of fast isotherms, also determined in the presence of sodium perchlorate, is given. Figure 7 clearly illustrates that the zpc lies at pH 5.8 and that the two independent measurements of the zpc give identical results.

3. Effect of Salts on Fast Isotherms

In the following sets of experiments, all variables except the nature of the indifferent electrolyte and pH are kept constant. Material (about 1.2 gram) from the same preparation is introduced in a cell, the suspension is stirred overnight in the vicinity of the zpc under a nitrogen atmos-

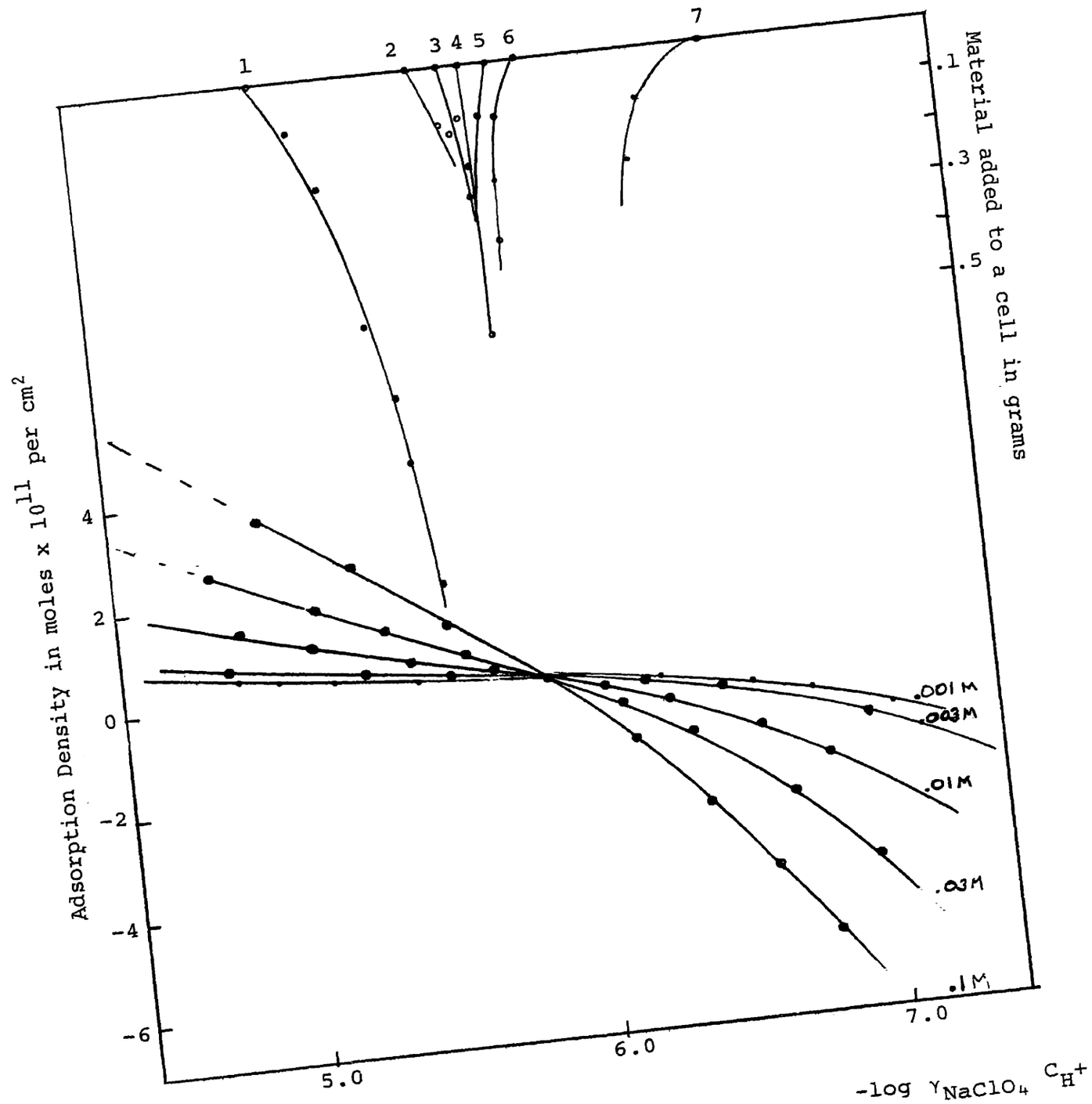

FIGURE 7. ADSORPTION ISOTHERMS IN THE PRESENCE OF $NaClO_4$ AND RESULTS OF pH DRIFT EXPERIMENTS IN 0.01M $NaClO_4$ AT 25°C.

phere. Rapid titrations are run with various inorganic salts as indifferent electrolytes. All isotherms are obtained within 10 hours.

The same titrating procedure applies to all experiments. The titration starts at the zpc, covers the acid side, comes back to the zpc, covers the basic side and ends again at the zpc. The ionic strength is changed at the zpc. It was observed that such a procedure would yield the best reproducible isotherms with a narrow intersection region (within 0.2 pH units). The results are given as $\Gamma_{\pm}$ vs. $-\log \gamma_{salt} \cdot C_{H^+}$.

Despite the care taken in reproducing the same experimental conditions, it has been observed that much fluctuation exists with regard to the intersection of isotherms, the exact position of an isotherm or its relative position with respect to isotherms at different ionic strength. This variation will not be apparent in the data since it would involve repeating isotherms obtained for a given salt with only minor modifications.

Suffice it to say that intersections of isotherms for sodium nitrate, for instance, will vary from pH 5.85 to pH 6.35 without any apparent reason, though a value of pH 6.0 $\pm$ 0.1 does definitely represent the normal value in 70% of the cases. Slopes ($d\Gamma_{\pm}/dpH$) at the zpc, expressed in μfarads per cm^2, have been observed to vary, again on sodium nitrate, between 6 μfarad/cm^2 and 12 μfarad/cm^2 at 0.001M or 66 μfarad/cm^2 and 74 μfarad/cm^2 at 0.1M. In general, the data at low ionic strengths show greater inaccuracies; this

is the range where adsorption is lowest and experimental error highest.

To study the specific influence of anions on the adsorption of potential-determining ions from the solution, a series of isotherms were determined in the presence of sodium salts of perchlorate, nitrate, chloride and iodide. The ionic strength is varied for each salt between 0.001M and 0.1M. The results are given in Figures 8 to 11. The influence of cations was also studied for a series of nitrate salts in the order, lithium, sodium and cesium. Corresponding isotherms are given in Figures 12 to 14.

Two sets of isotherms with sodium nitrate are offered with the data (Figures 9 and 13). They were specifically chosen so as to illustrate the worst case of irreproducibility. Isotherms in Figure 13 were determined at high concentrations of salts and will be used under Discussion of Results for a quantitative analysis of adsorption.

Rapid perusal of all these isotherms discloses but little information. They all have the same shapes, intersect in the same region, have essentially identical inflexion points in the vicinity of the common intersection. A more careful look, however, will disclose a general asymmetry of the isotherms; adsorption on the negative side of the isotherms ($\sigma < 0$) is always larger than on the positive side ($\sigma > 0$) for a fixed pH variation away from the intersection point. Adsorption at a fixed pH on the negative side of the isotherms increases in

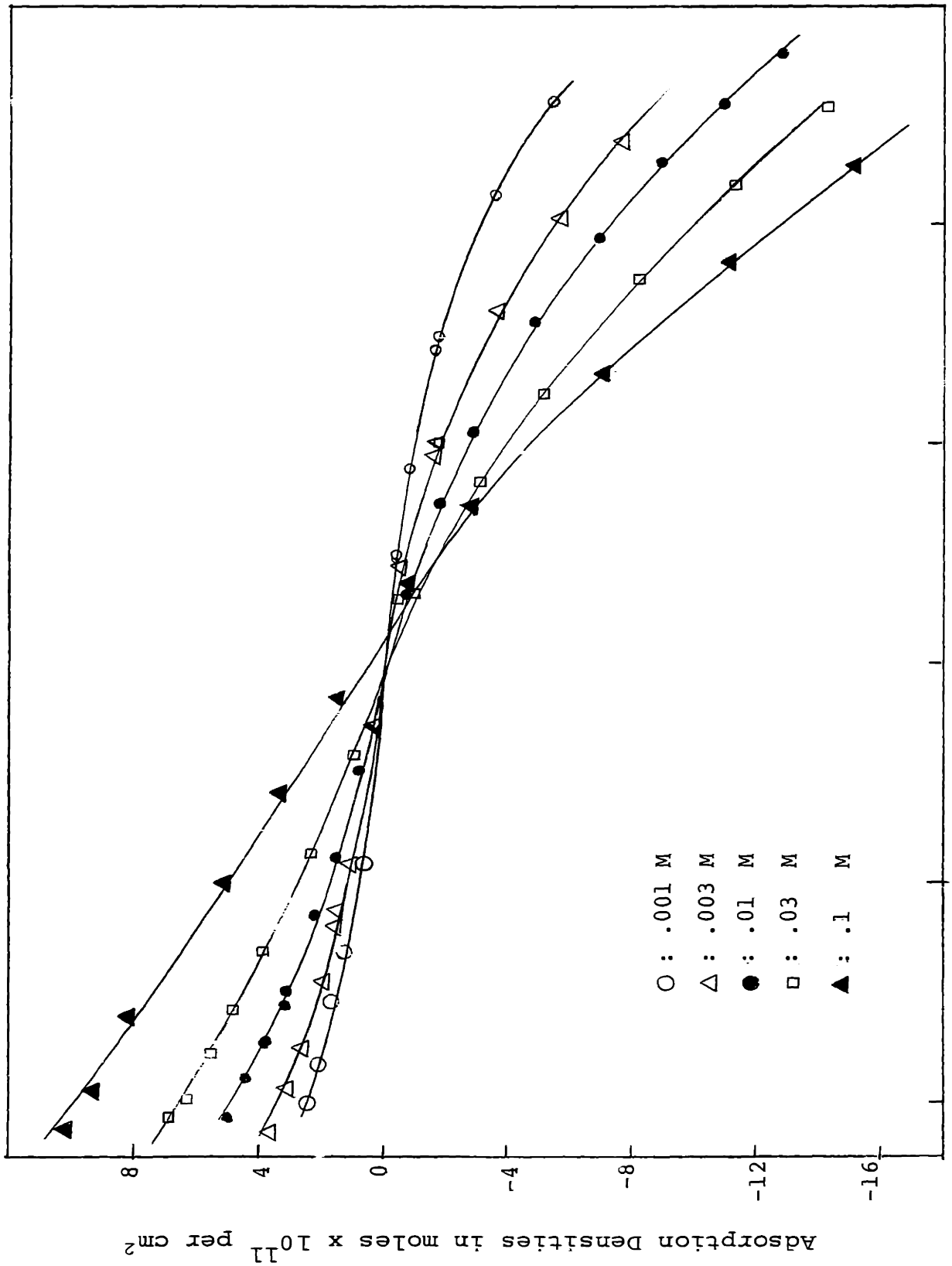

FIGURE 8. ADSORPTION ISOTHERMS ON RUTILE IN PRESENCE OF $NaClO_4$ AT 25°C.

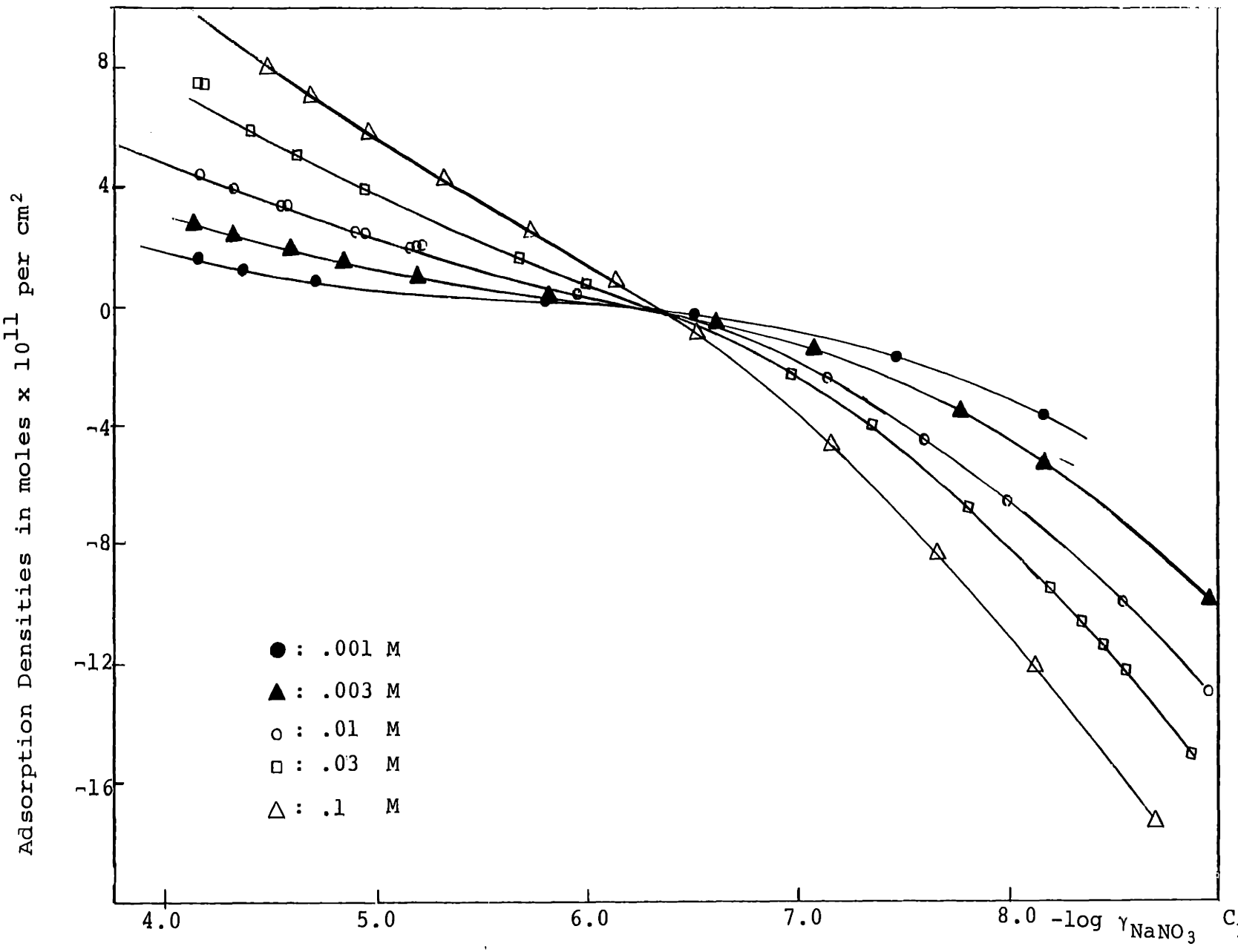

FIGURE 9. ADSORPTION ISOTHERMS ON RUTILE IN PRESENCE OF $NaNO_3$ AT 25°C.

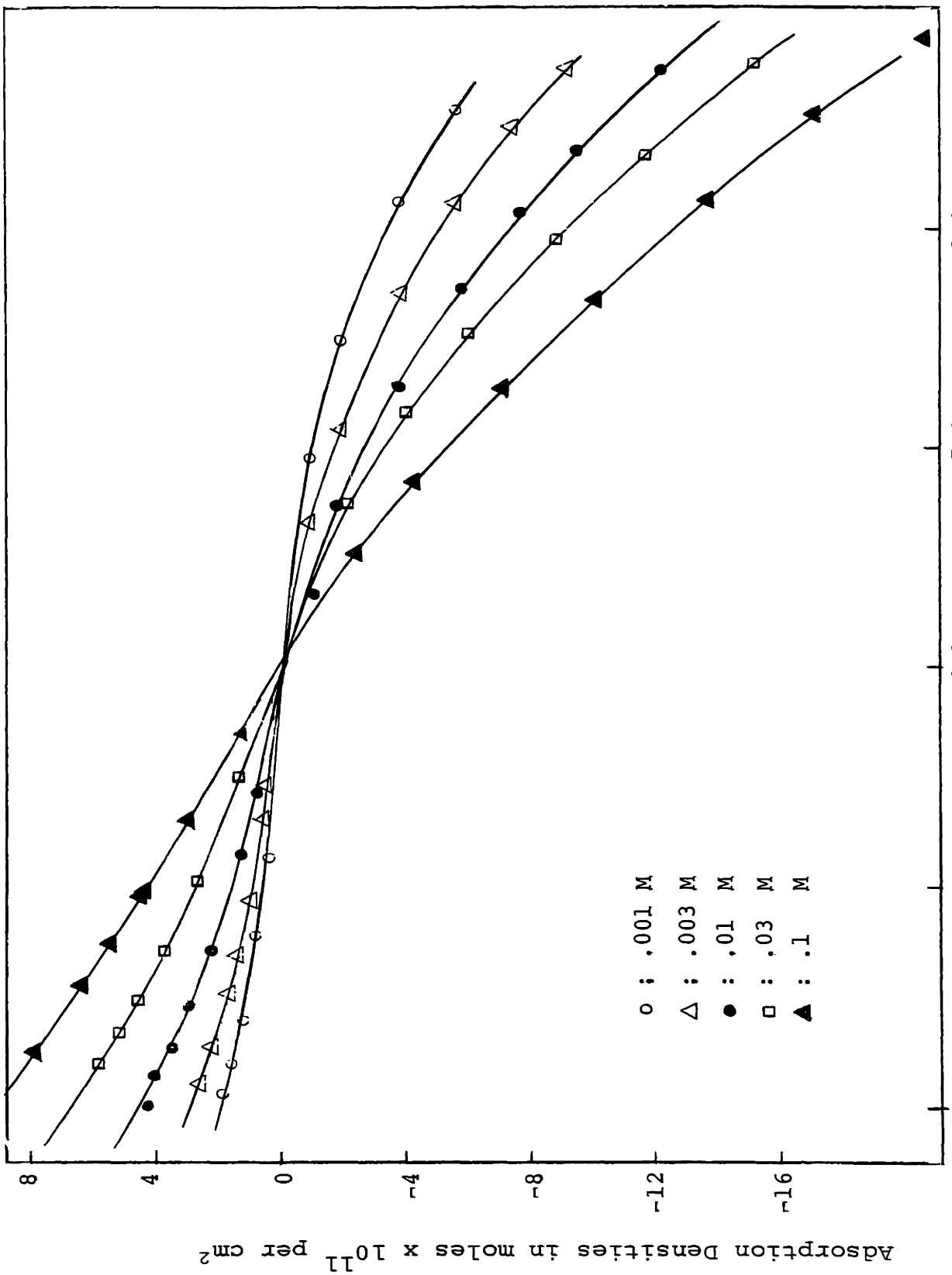

FIGURE 10. ADSORPTION ISOTHERMS ON RUTILE IN PRESENCE OF NaCl AT 25°C.

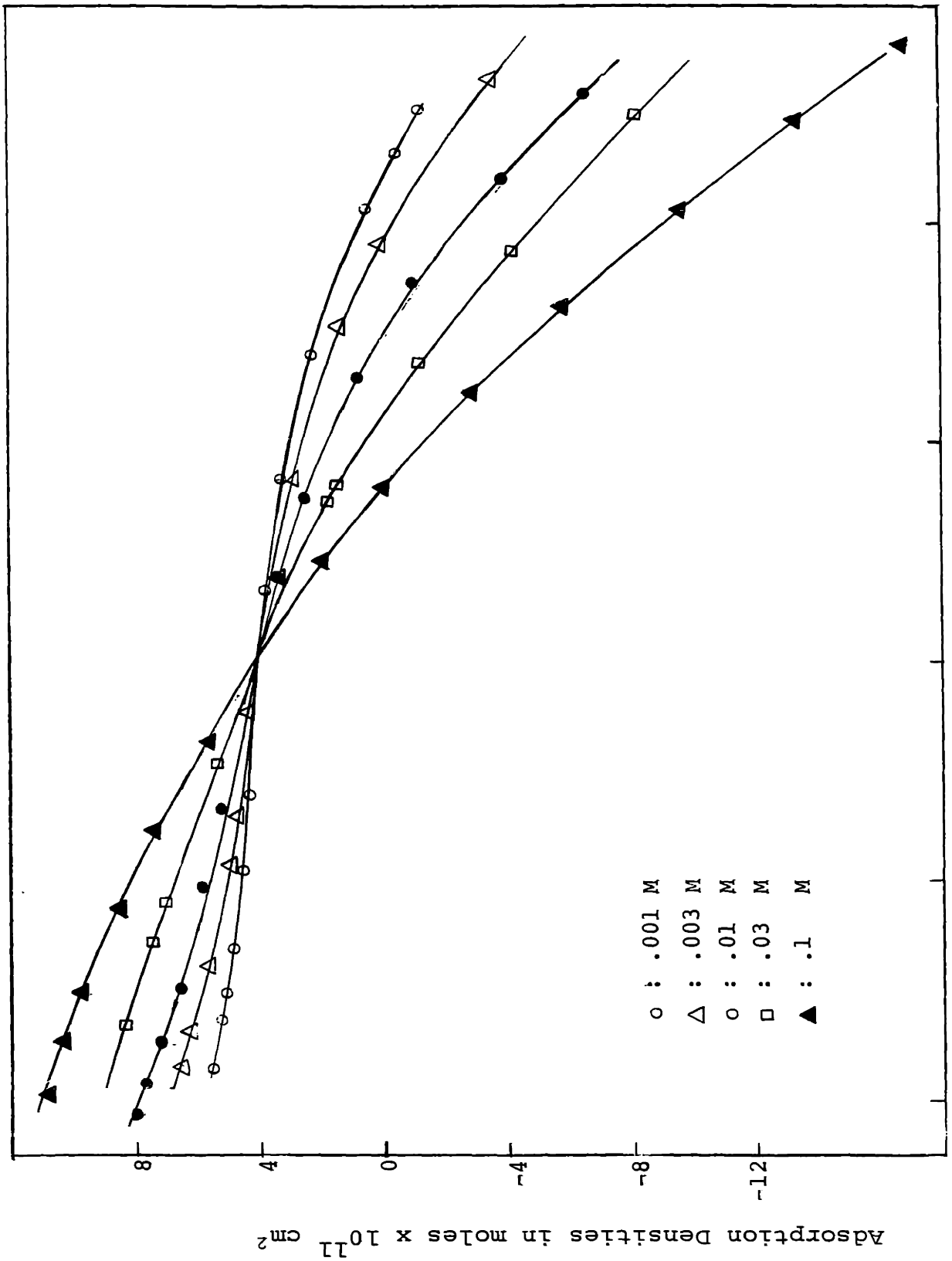

FIGURE 11. ADSORPTION ISOTHERMS ON RUTILE IN PRESENCE OF NaI AT 25°C.

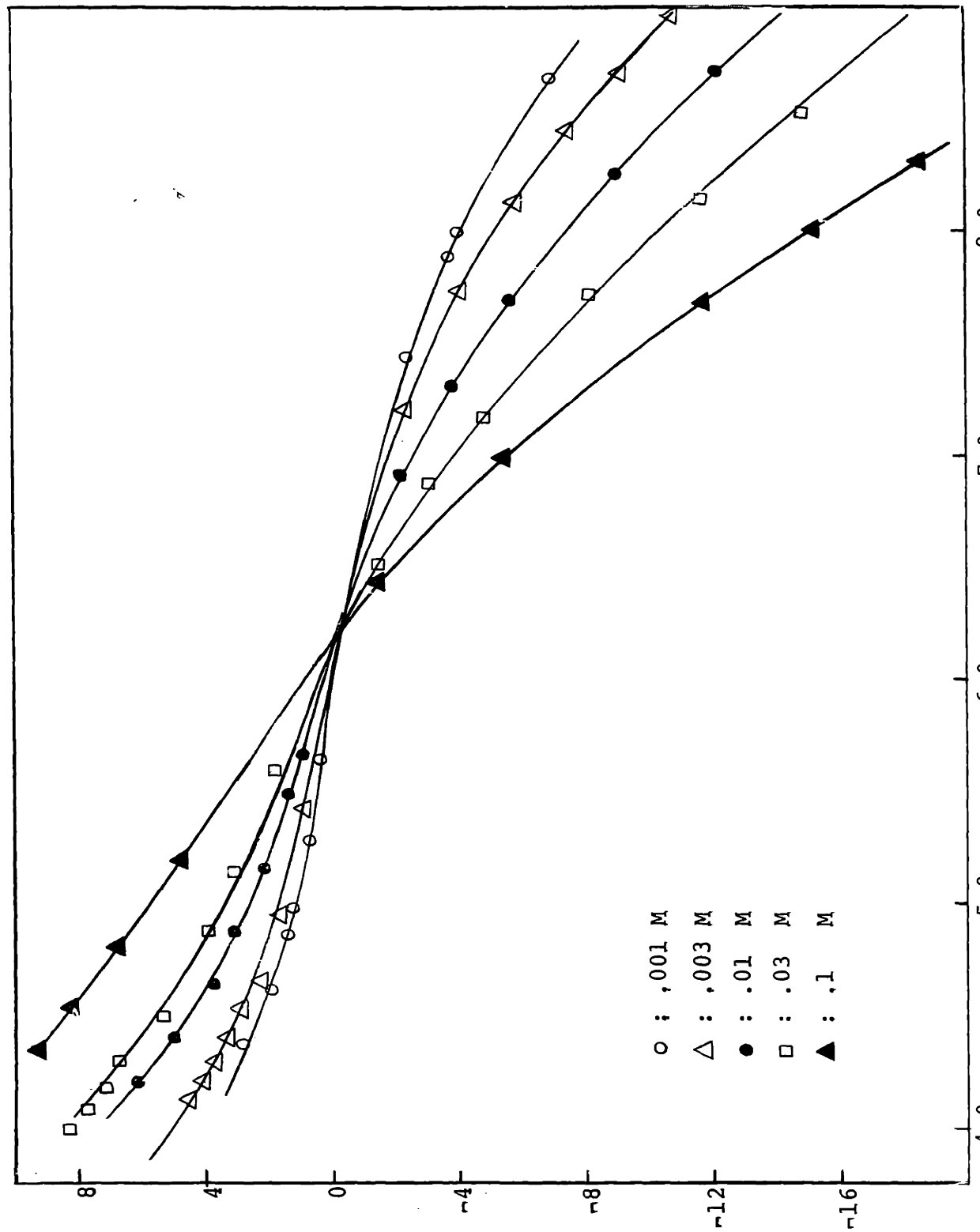

FIGURE 12. ADSORPTION ISOTHERMS ON RUTILE IN PRESENCE OF $LiNO_3$ AT 25°C.

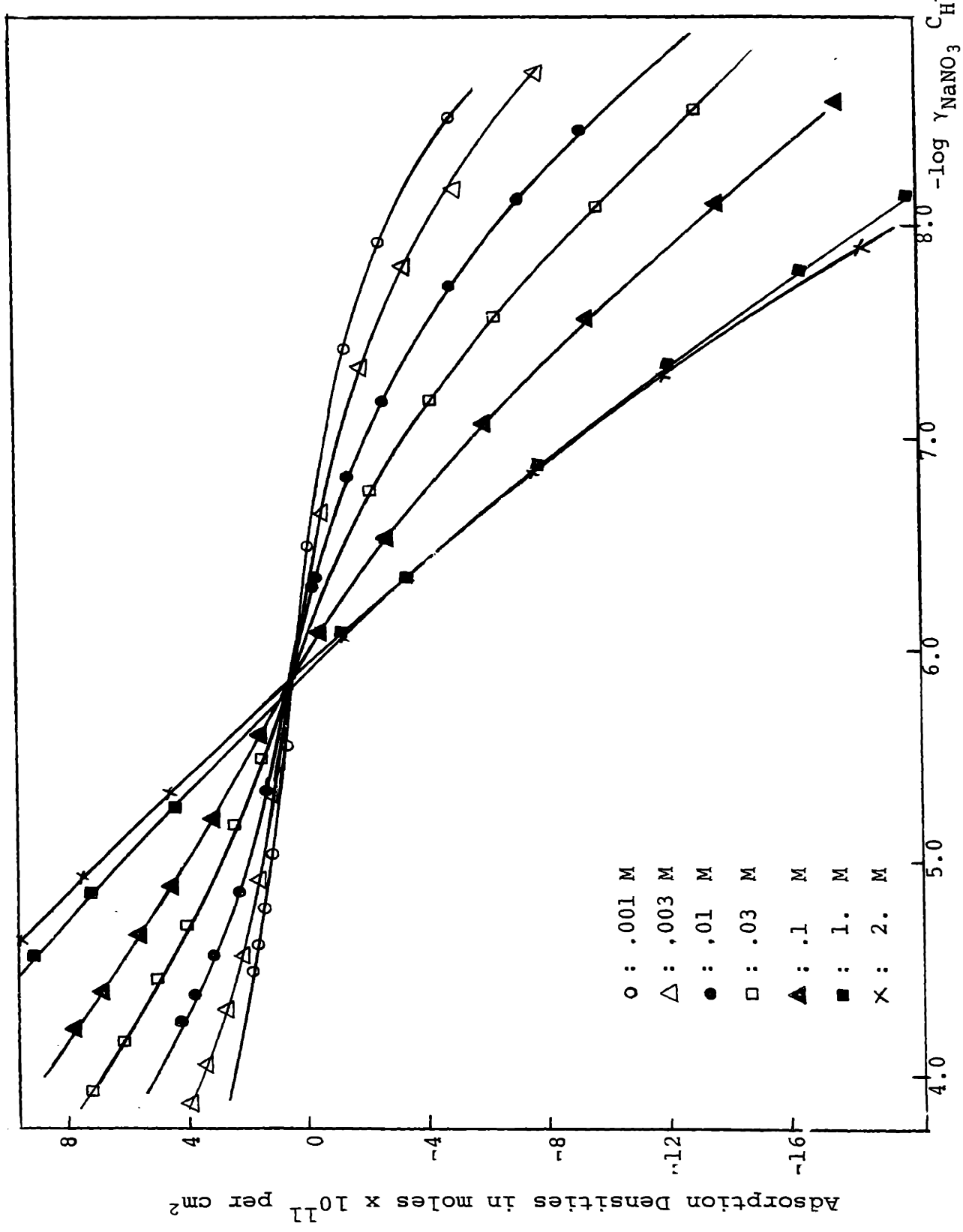

FIGURE 13. ADSORPTION ISOTHERMS ON RUTILE IN PRESENCE OF $NaNO_3$ AT 25°C.

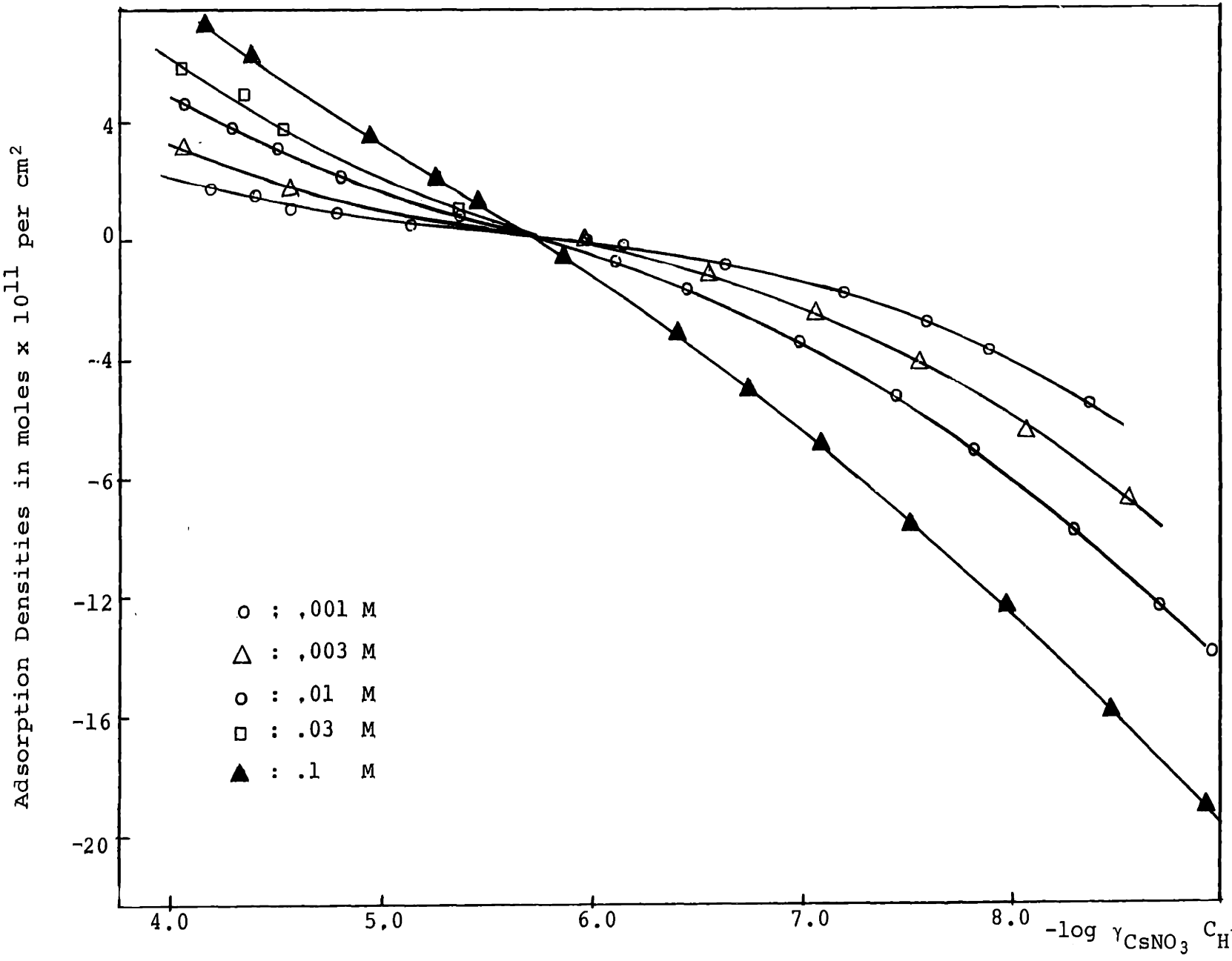

FIGURE 14. ADSORPTION ISOTHERMS ON RUTILE IN PRESENCE OF $CsNO_3$ AT 25°C.

the order Cs<Na<Li, while few variations are noticed on the positive side even when anions are varied.

4. Effect of Temperature on Fast Isotherms

With the magnitude of adsorption of hydrogen and hydroxyl ions and the effect of foreign ions now well characterized, titrations were made at elevated temperatures. Sodium chloride was used throughout these experiments, the reason being that it was found to give the most reproducible isotherms and offers the lowest junction potential at the reference electrode.

Lack of data in the literature on the variation in γ_{NaCl} with temperature required preliminary determinations of the activity coefficients for different temperatures. Appendix 2 describes the procedure and lists the obtained values. Another problem was met. While evaporation can be neglected at room temperature under the experimental conditions, it cannot be ignored at 95°C nor probably at 75°C either. For that reason, it was not possible to flow nitrogen in the cell and renew continuously an atmosphere free of carbon dioxide. In general, titrations were run faster and the cell kept closed in as much as possible. Experimentation with water indicated that CO_2 could not change adsorption values by more than 5 μmoles in all, an error of about 1 μcoul./cm^2 in this case.

Figures 15 to 17 give the resulting isotherms for the temperatures 50°C, 75°C and 95°C. Reference should be made to Figure 10 for the isotherms at 25°C. The figures show that the zpc shifts to lower pH values with increasing

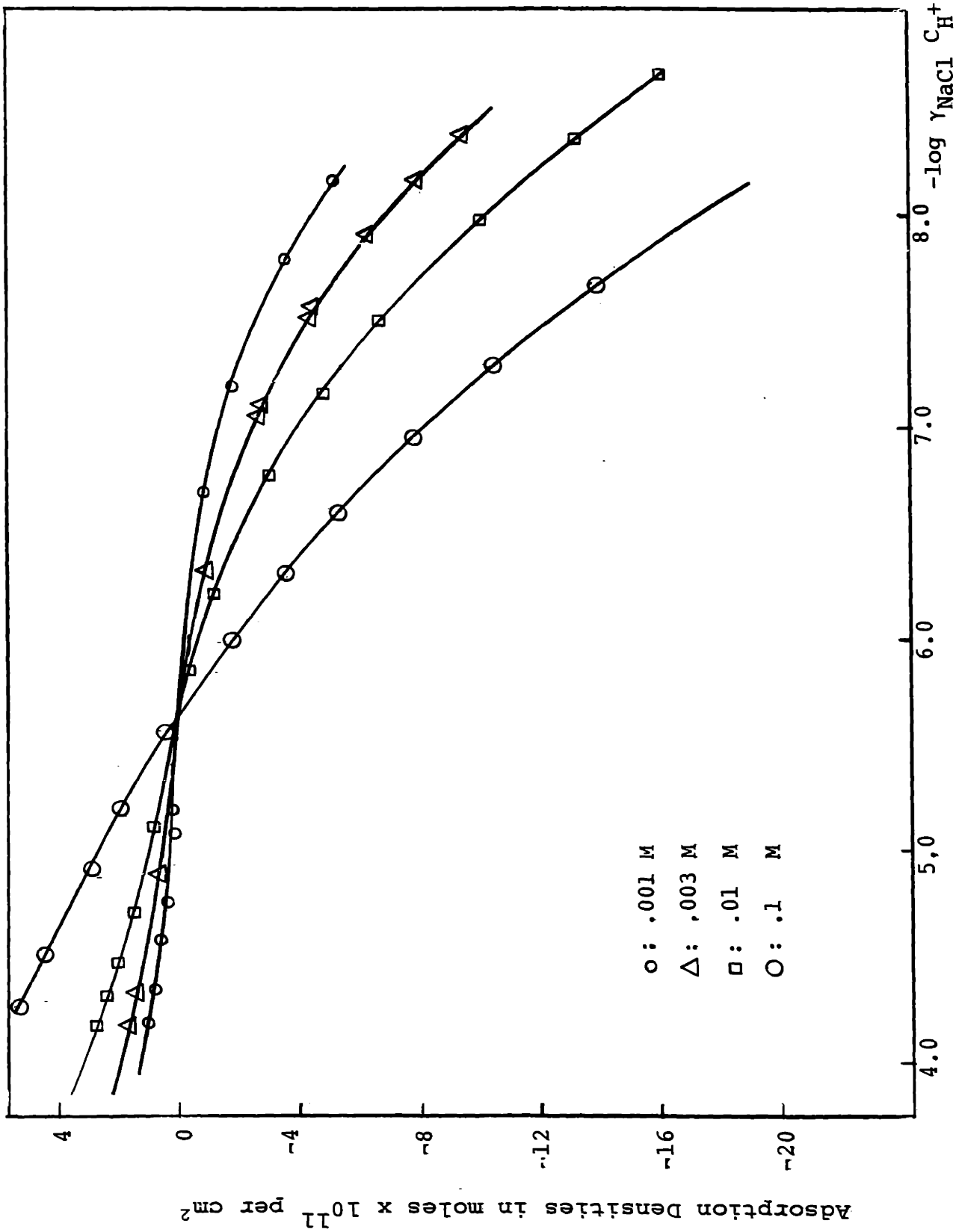

FIGURE 15. ADSORPTION ISOTHERMS ON RUTILE IN PRESENCE OF NaCl AT 50°C.

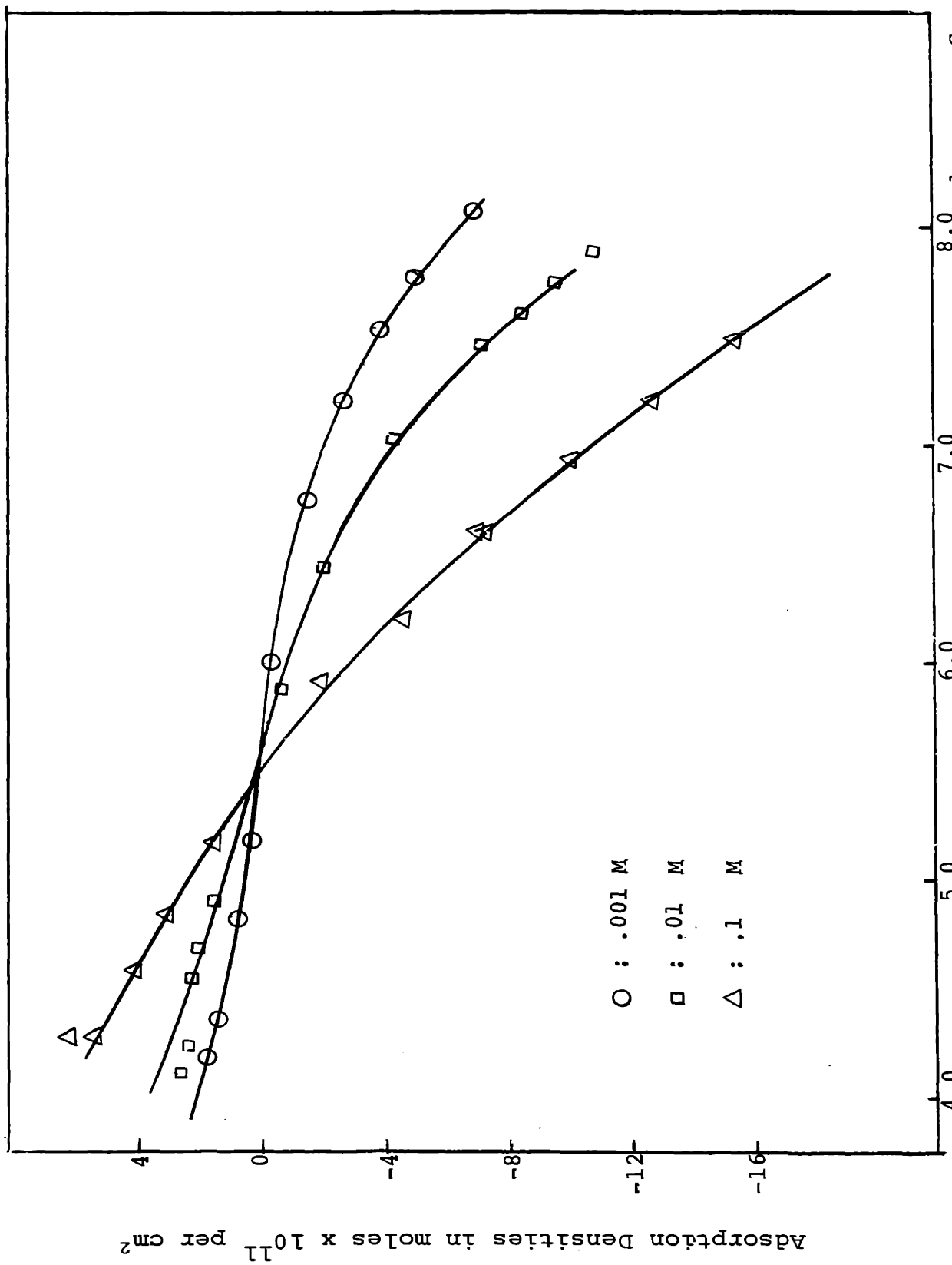

FIGURE 16. ADSORPTION ISOTHERMS ON RUTILE IN PRESENCE OF NaCl AT 75°C.

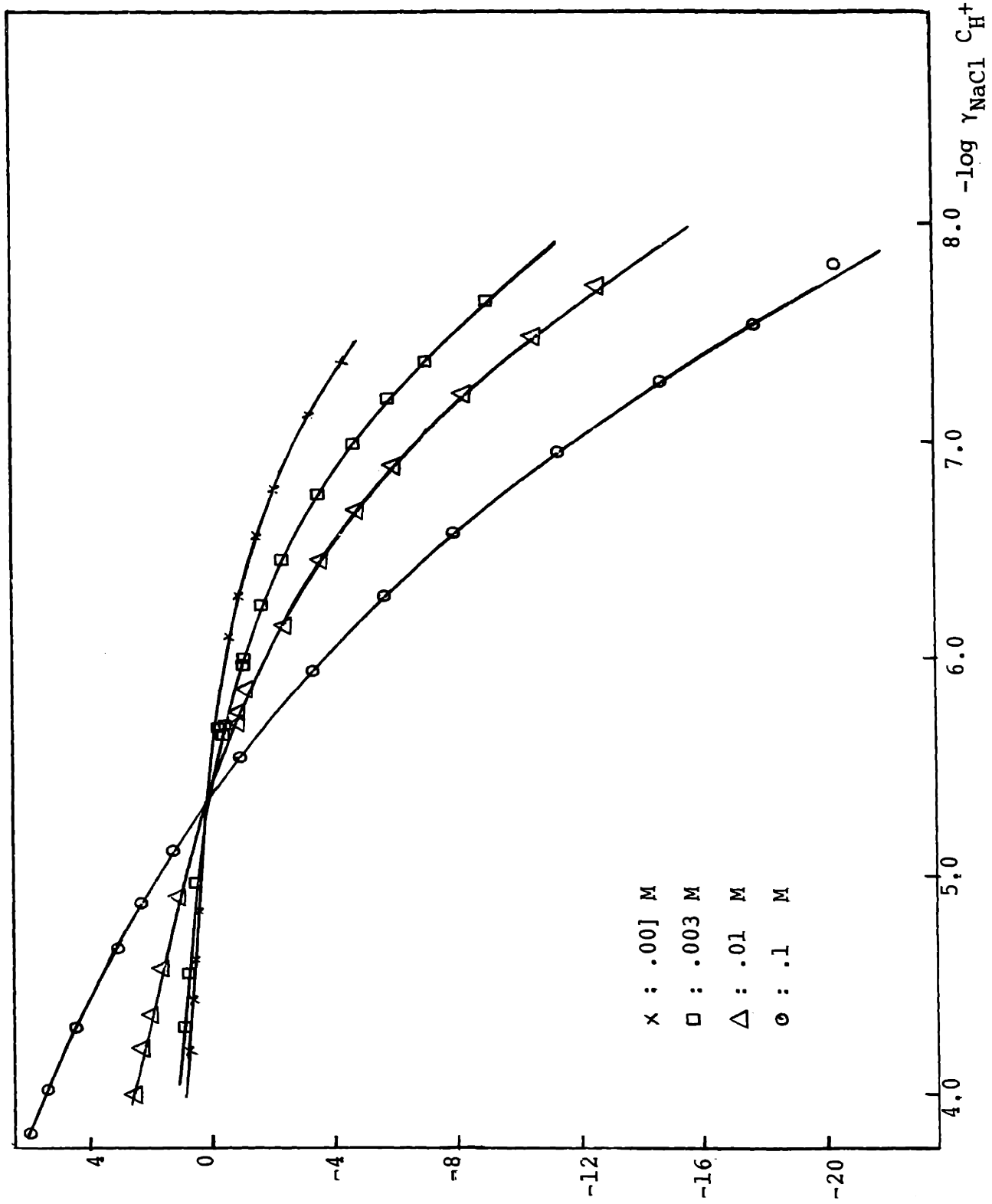

FIGURE 17. ADSORPTION ISOTHERMS ON RUTILE IN PRESENCE OF NaCl AT 95°C.

temperatures much in the same way as the point of neutrality of water. Adsorption is found to increase with temperature at fixed pH change away from the zpc, particularly so when the surface is negatively charged.

5. Influence of the Method of Preparation

Titanium dioxide exists in two crystalline allotropic forms, anatase and rutile. A review of the crystal structure can be found in Appendix 5. A description of the methods of preparation has been given under Materials. Adsorption isotherms for the rutile modification in the presence of sodium chloride are given in Figure 10. A similar set of isotherms is given in Figure 18 which pertains to the anatase form.

The crystalline form of TiO_2 does not seem to affect the intersection of isotherms in any way since a pH of 5.9 for the zpc is again found for anatase. However, it will be observed that while magnitudes of adsorption at the 0.1M concentration of salt are similar for both materials, at lower ionic strength the isotherms obtained with anatase are noticeably steeper than those obtained with rutile.

6. Influence of Heat Treatment

So far all experiments were done on a fully hydrated oxide which has never come in contact with a gaseous phase. In the following experiments, controlled dehydration was obtained by prolonged evaucation at various temperatures. The vacuum was maintained at 10^{-3} mm of mercury with a Hyvac

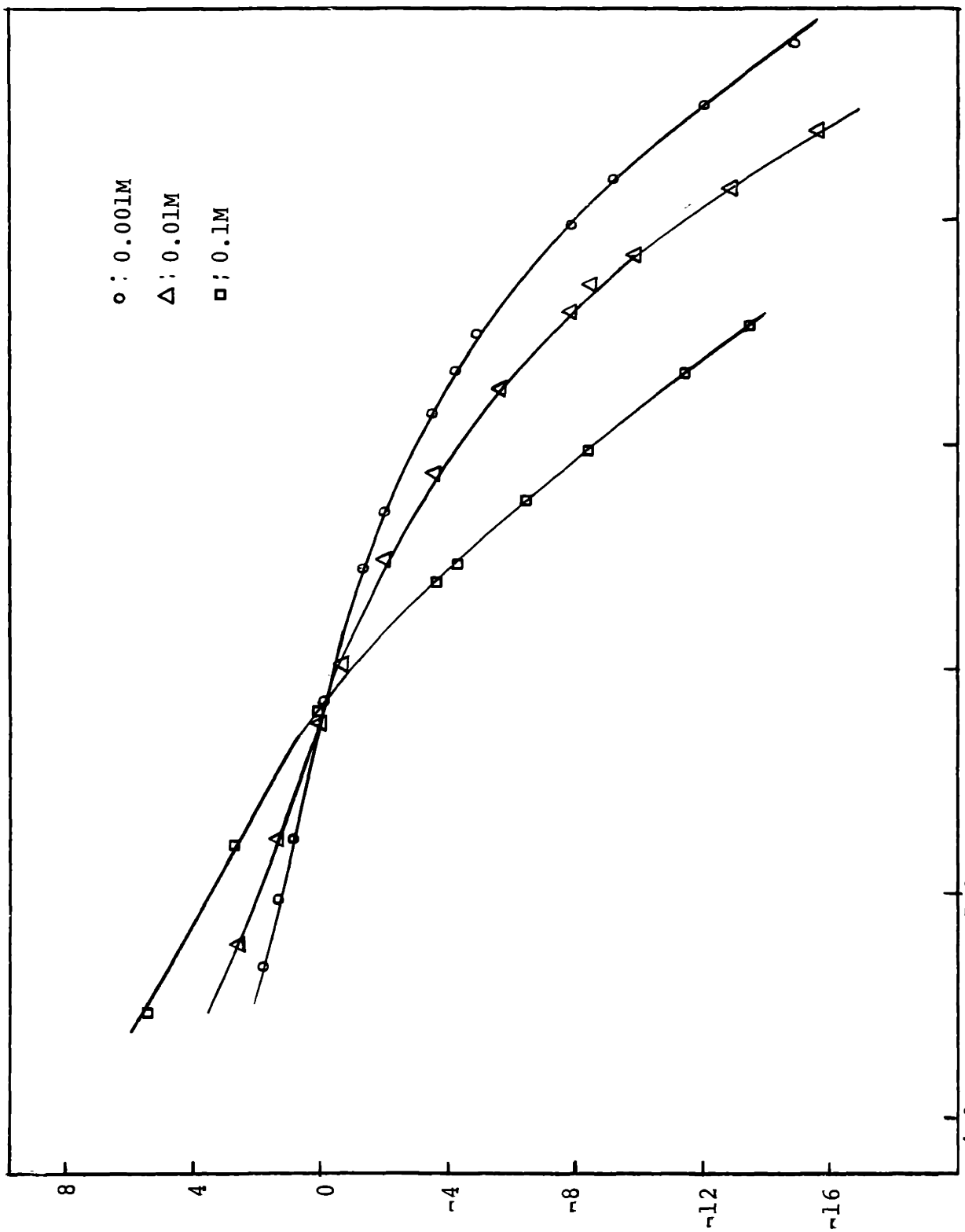

FIGURE 18. ADSORPTION ISOTHERMS ON ANATASE IN PRESENCE OF NaCl AT 25°C.

mechanical pump. Evacuations were done at various temperatures, 25°C, 200°C, 400°C and 500°C. Upon evacuation, the sample is contacted with water for 24 hours before the titration. Samples are kept aside to determine the new surface area (usually around 12 M^2 per gram).

Titrations are performed at 25°C. Materials evacuated at temperatures below 500°C were used in titrations with sodium chloride and typical isotherms are given in Figure 19. A set of fast isotherms run on the precipitate evacuated at 500°C is given in Figure 7. Perchlorate was used here and it can be safely assumed that its behavior is not different from that of chloride as was reported in the previous section. Isotherms obtained on the precipitates evacuated at 25°C and 200°C are deleted as they are similar to isotherms obtained on hydrated oxide.

High temperature evacuation presents the added difficulty of the chemical reduction of the interface[31,32] particularly favored in the presence of surface organic contaminants. For that reason, no attempts were made to evacuate at higher temperatures. Instead, heat-treatments at 800°C were performed either in air or under a nitrogen-water vapor atmosphere. Since there was no observed differences in the behavior of the materials submitted to these two atmospheres during treatments, only isotherms obtained on material treated under nitrogen and water are given. The titration procedure is the same as in all other experiments. The typical set of isotherms are given in Figure 20.

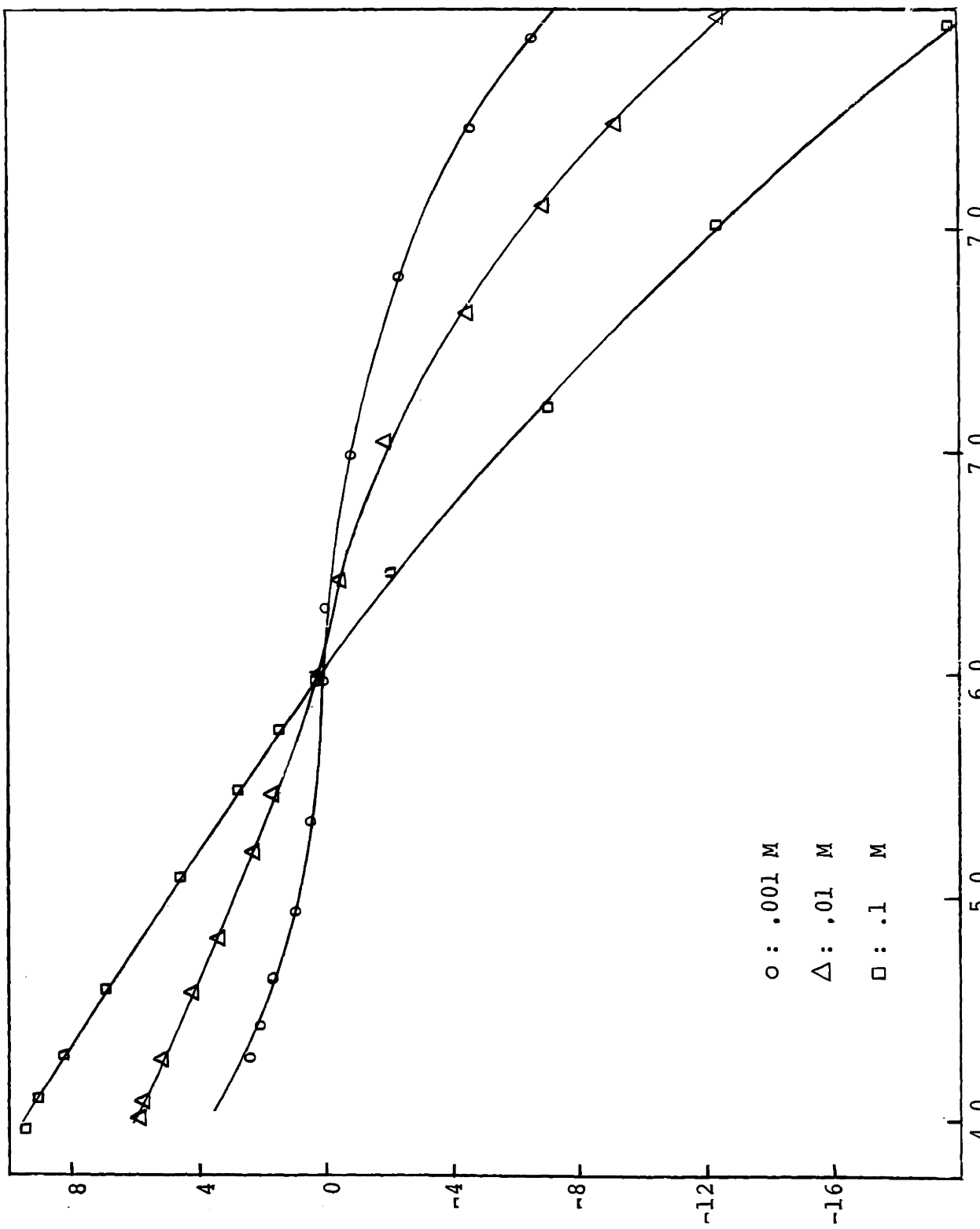

FIGURE 19. ADSORPTION ISOTHERMS ON RUTILE EVACUATED AT 425°C IN PRESENCE OF NaCl AT 25°C.

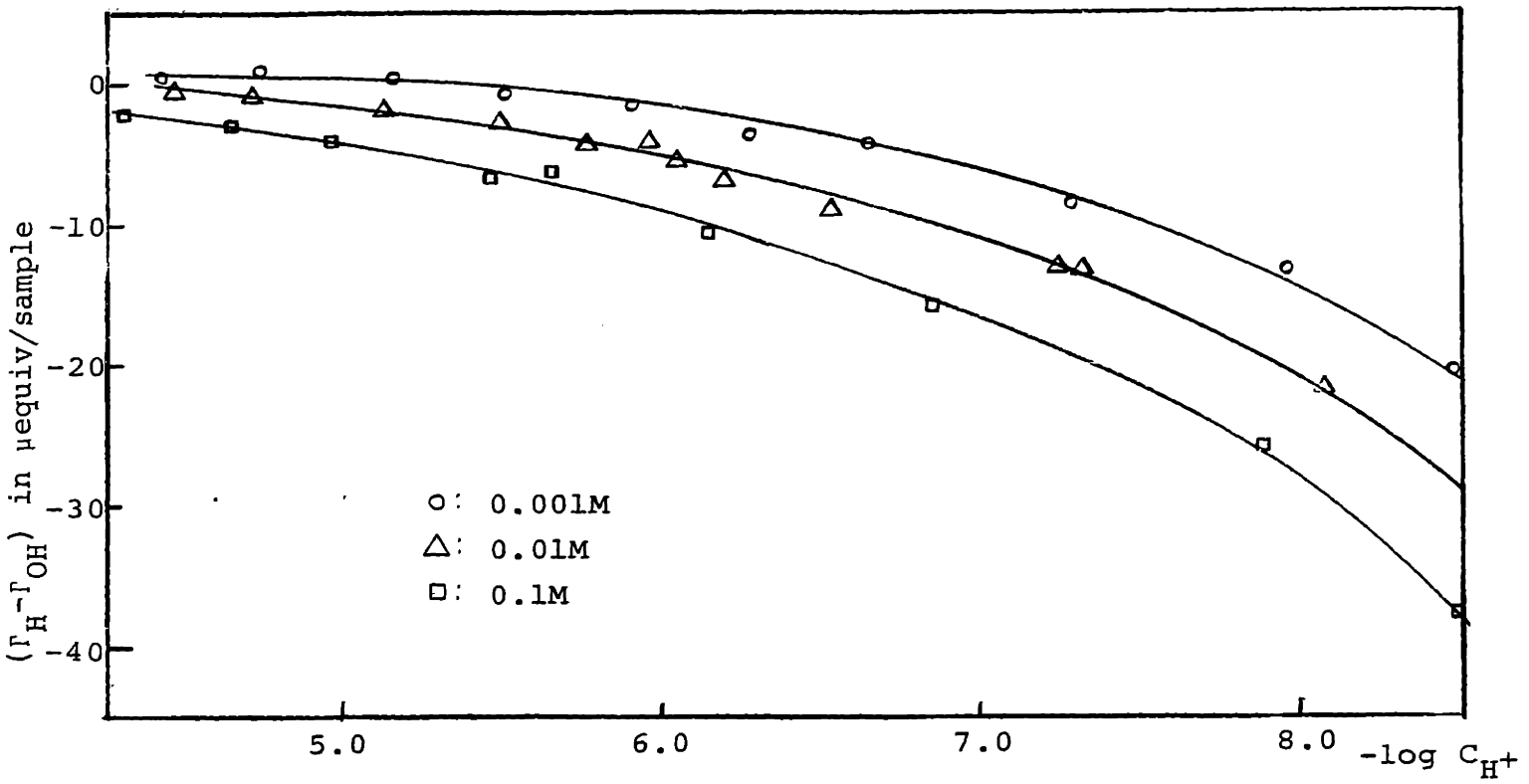

FIGURE 20. ADSORPTION ISOTHERMS ON RUTILE FIRED AT 800°C IN PRESENCE OF NaCl AT 25°C.

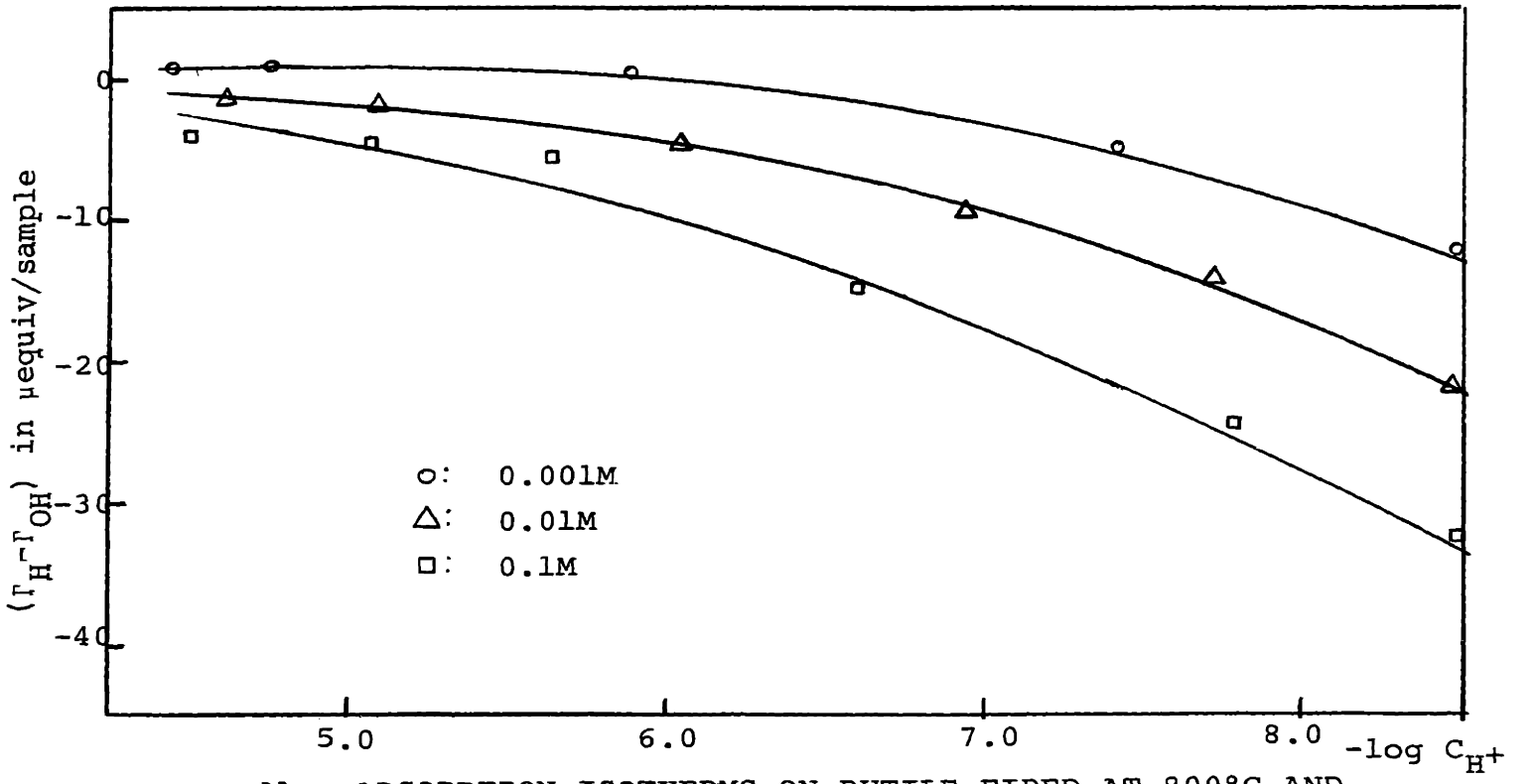

FIGURE 21. ADSORPTION ISOTHERMS ON RUTILE FIRED AT 800°C AND AGED IN WATER FOR 150 DAYS IN PRESENCE OF NaCl AT 25°C.

When the isotherms given in Figure 20 were completed, the solid was decanted in the vicinity of the zpc in order to wash the salt away. The precipitate was left in water at an ionic strength below 10^{-4}M for a period of 150 days, whereupon new isotherms were obtained on the precipitate. They are given in Figure 21. The data for these two sets of isotherms are given as adsorption per sample and no attempt was made to reduce them to absolute adsorption. The weight of the precipitate was 1.1 grams of rutile with a specific surface of 9.78 M^2 per gram.

Evacuation at temperatures below 500°C is found to have no effect on the surface behavior. Neither the intersection of isotherms nor the magnitude of adsorption is affected. A slight shift of the zpc appears at temperatures above 500°C though the magnitude of the displacement is not very well reproducible. It is only at temperatures as high as 800°C that the intersection is displaced to very acid values (pH of 3 to 3.5) where it is not experimentally measurable. Aging the surface in water does not recover the original properties of the hydrated material as indicated by Figure 21.

7. Tracer Exchange with Interfaces of Rutile and Hematite

A sample of rutile was equilibrated in tritiated water at 129°C for three weeks. The sample (about 1.2 grams) was centrifuged and transferred to an evacuator for 24 hours.

When dried, the sample is directly transferred to the desorption cell. A plot of amount of tritium desorbed versus time is given in Figure 22 where the amount of tritium is expressed as an equivalent amount of water on the solid.

Prior to this experiment, some other samples had been contacted with tritiated water at room temperature for various lengths of time (up to six months). Upon evacuation for 20 to 26 hours, the desorption curve was found to be identical in shape to that shown in Figure 22, but the amount of tritium desorbed varied by as much as 100%. Such a desorption curve is indicative of the fact that whatever tritium is left on the surface after evacuation, is exchanged instantaneously with the solution.

This effect of evacuation was then studied in more detail. A large sample was evacuated and portions of it was removed after 19, 28, 44 and 67 hours. Again a step-wise desorption was observed but the amount left on the solid was not constant. A curve relating the amount of tritium left on the solid to the time of evacuation is given in Figure 23. The open circles in this figure represent results obtained by this technique.

Due to the possibility of introducing water from the atmosphere in the specimen while sampling it, independent experiments were performed to check the reproducibility and accuracy of the previous results. This is important because introduction of water during sampling would initiate exchange between the surface and this excess water which would then be

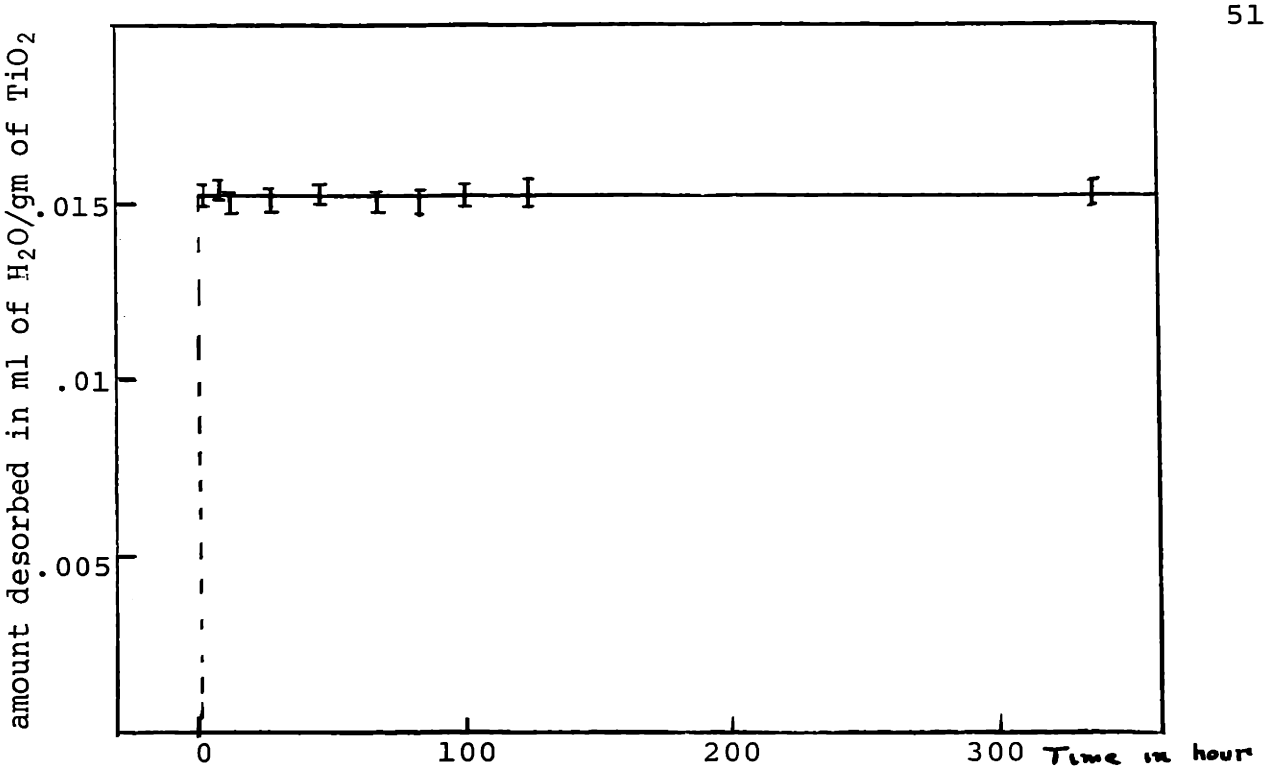

FIGURE 22. EXCHANGE OF TRITIUM BETWEEN RESIDUAL TAGGED WATER ON RUTILE AND PURE WATER. (Evacuation Time of 23 Hours.)

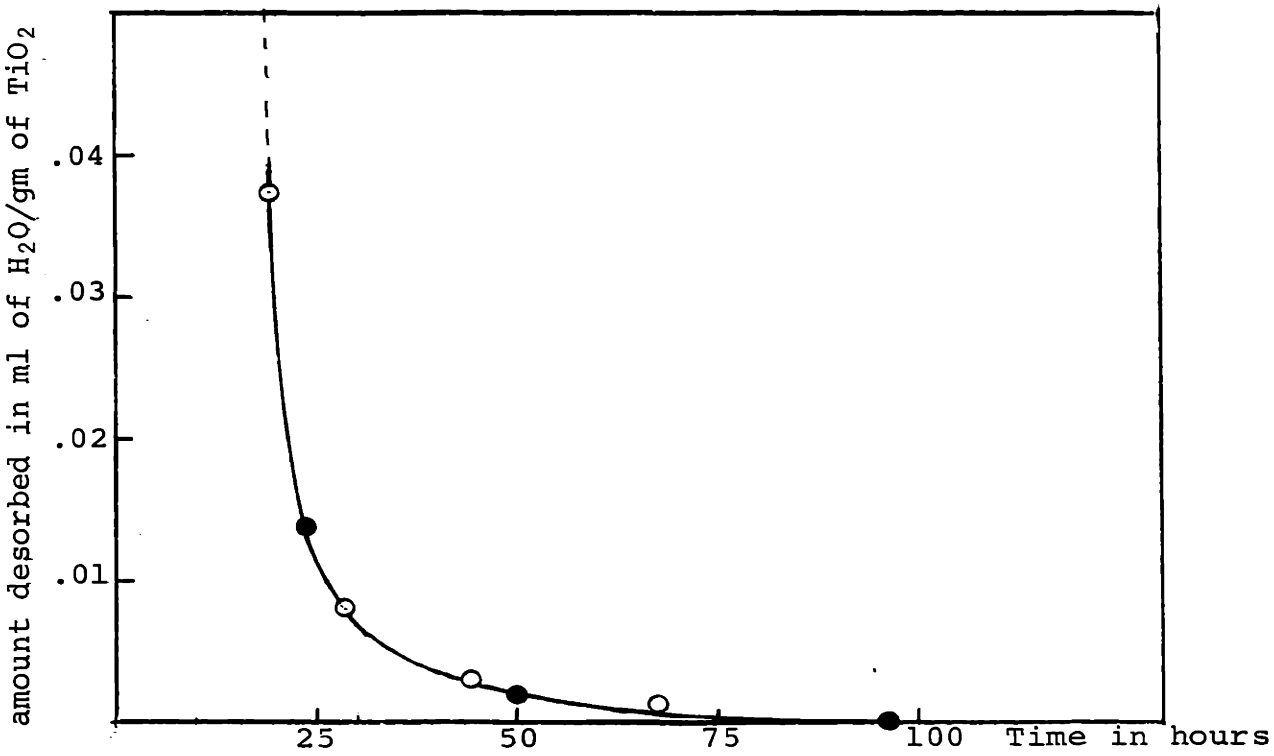

FIGURE 23. RESIDUAL LABILE WATER ON RUTILE AS A FUNCTION OF EVACUATION TIME.

removed on further evacuation. To avoid contact with the atmosphere, samples were introduced wet in the evacuator. When ready for desorption, they were frozen to liquid nitrogen temperature before exposure to atmosphere and transferred to the desorption cell. The results, indicated by filled circles, are also included in Figure 23.

This extra precaution proved not to modify the results in any way. The obtained results fall on essentially the same curve. The immediate conclusion to be drawn is that evacuation at room temperature can remove all of the excess water which has been tagged. If there is more water attached to the surface, tritium cannot exchange with it and the hydrogen is said to be non-labile.

Similar experiments were performed on a hematite powder supplied by Onoda[18]. The samples were tritiated at 129°C for one month. The evacuation procedure was always followed by freezing before transfer to the exchange cells. Desorption curves are given for two independent experiments (about 2 grams of hematite per sample) in Figure 24. Curve a describes desorption at room temperature (24°C $\pm$ 0.5) and Curve b at 95°C.

Without going into any detailed explanation, it is obvious from Figure 24 that evacuation at room temperature, even for extended periods of time, will not remove the tagged water. When the oxide is contacted with water again, this surface water is found to be extremely labile. Such a fast exchange

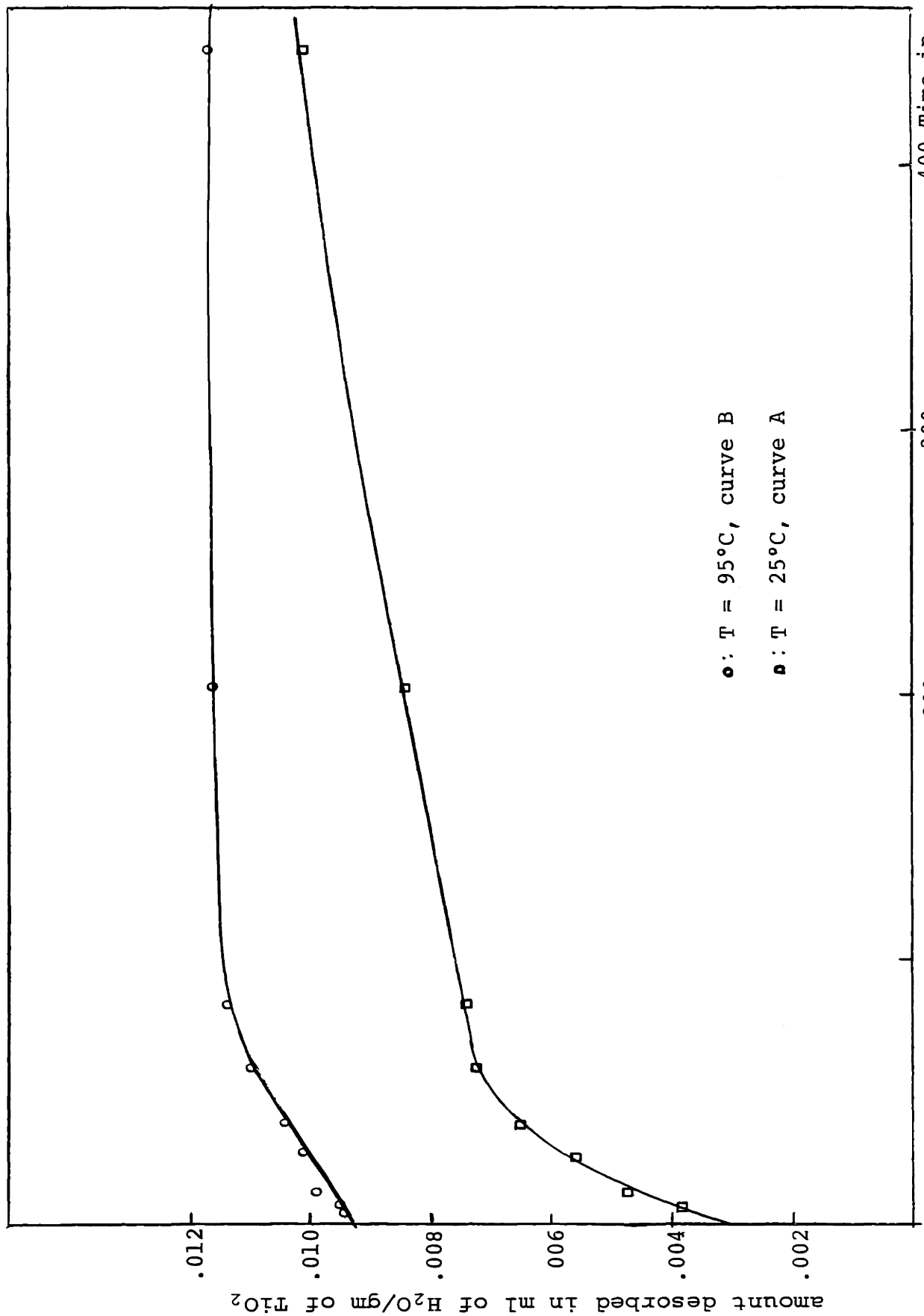

FIGURE 24. EXCHANGE OF TRITIUM BETWEEN RESIDUAL TAGGED WATER ON HEMATITE AND PURE WATER (100 Hours of Evacuation) at 25°C AND 95°C.

which involves more or less water depending on the temperature is followed by a slow exchange which can take as much as 600 hours to come to completion. The rate of exchange increases rapidly with temperature.

N.B. It should be noted that data points in the vicinity of the zpc for most sets of isotherms have been omitted, for sake of clarity.

V. DISCUSSION OF RESULTS

1. The Fast Adsorption Isotherm

There is little doubt that for all oxides studied, at least two mechanisms account for the abstraction of hydrogen ions from solution. Blok[19] observed them on zinc oxide, Onoda and de Bruyn[6] on hematite, Korpi[17] on alumina, and these solids are by no means identical. The solubility of zincite may be quite high while it is negligible for hematite. It is, furthermore, not known how the porosity of these various materials and how the amount of surface contamination vary. Finally, even the degree of hydration can vary among these oxides. Strictly speaking, only a change in pH of the aqueous suspension of these oxides with time has been studied. It is not clear at this stage whether one model can describe the behavior of all oxides. The questions may be asked, can such a phenomenon be described uniquely by dissolution of the oxides, or a diffusion of ions through the pores, or simply a diffusion through the lattice? These suggestions seem hardly likely since the oxides have quite different properties. Each oxide must be analyzed individually.

A. Possible Explanations of the Slow Step

A detailed interpretation of kinetic curves of the type shown in Figure 2 amounts to a near impossible task. The times involved in reaching equilibrium are so large that it becomes unlikely that some unknown contaminant will not be introduced in the system. Such a slow adsorption was followed

for over five months in a rutile-sodium chloride aqueous suspension. It tapered off but the system never came to equilibrium.

One obvious cause of the slow step could be leakage of CO_2 from the atmosphere into the cell and its absorption in the solution. Even though purified nitrogen is flowed through the cell, the calomel electrode must be removed after each measurement to prevent chloride contamination and the cell must also be opened to introduce the burets. Complete elimination of CO_2 from the cell is difficult. In fact, a blank cell kept at a pH of 9.5 will show pH changes due to CO_2 resulting in some 30 μequivalents of hydrogen ion to be introduced in the cell within 200 hours and, still, that applies to an ideal case where the cell is rarely opened for measurements.

It is, however, unlikely that CO_2 absorption could explain completely the observed slow step. In Figure 4, which describes the displacement of isotherms with conditioning in presence of sodium chloride, one will observe a displacement of the isotherm at pH 5.0 of some 10 μmoles of acid in a cell containing 330 cc of solution (or about 30 μmoles per liter of solution). Simple thermodynamic analysis will show that absorption of CO_2 cannot introduce this amount of HCO_3^- in the cell. Figure 25 shows the thermodynamic relationship between partial pressure of CO_2 in atmospheres against total CO_2 concentration in solution, represented by the heavy line. The dashed lines represent respectively the amount of HCO_3^- and H_2CO_3 as a function of

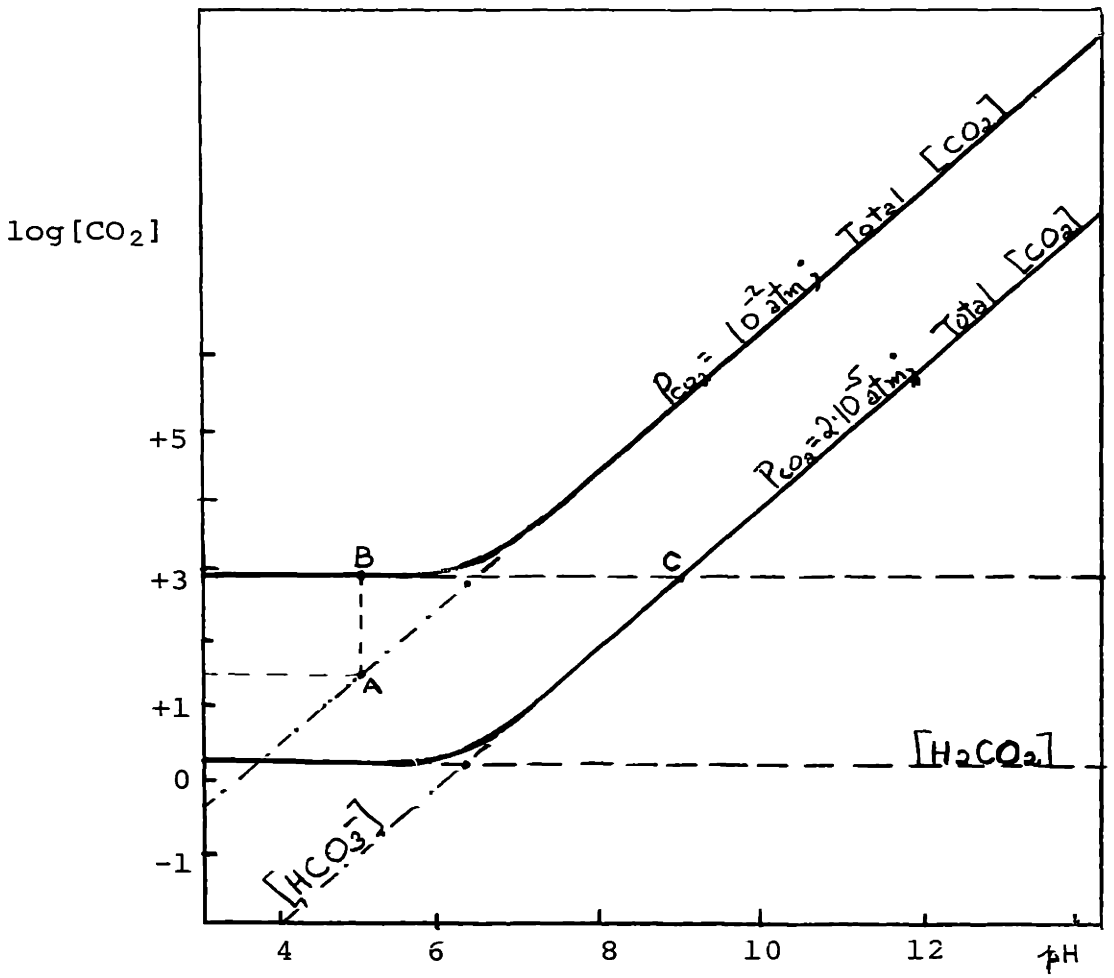

FIGURE 25. EQUILIBRIUM CONCENTRATION OF CO_2 IN WATER AT 25°C.

pH which, when added together, give the total CO_2 concentration in solution. The curve was obtained from the summation of two reactions,

$$CO_2\ (g) \rightleftharpoons CO_2\ (aq) \qquad K_1 = 0.03438$$

$$CO_2\ (aq) + H_2O \rightleftharpoons HCO_3^-\ (aq) \qquad K_2 = 4.45 \times 10^{-7}$$

and

$$(CO_2)_{total} = [H_2CO_3] + [HCO_3^-]$$

where [] is concentration in moles per liter. The equilibrium constants were determined by Harned and Davies[30].

Figure 25 shows that 30 μmoles per liter of HCO_3^- at pH 5 (point A) implies an equilibrium vapor pressure of 10^{-2} atmosphere of CO_2 and a corresponding 900 μmoles per liter of H_2CO_3 in solution (point B) (whether or not this CO_2 is in equilibrium with the atmosphere of the cell). At pH 9 (point C) this 930 μmoles per liter of CO_2 is found to be entirely dissociated, since point "C" lies on another curve where $[CO_2]$ is identical with $[HCO_3^-]$. It should be understood here that we are considering a case where the pH is brought instantaneously from pH 5 to pH 9 (as in a fast isotherm) so that the solution has no time to equilibrate with the gaseous atmosphere and the total CO_2 stays constant; only its distribution between the dissociated species HCO_3^- and the undissociated H_2CO_3 is affected by changes in pH. One would then expect in the cell itself a spacing between the two isotherm at pH 9 of some 300 μmoles per 330 cc of solution and not 30 as can be seen in Figure 4. It is concluded that CO_2 cannot account for all of the effect.

But CO_2 is not the only contaminant. Dissolution of pyrex in alkaline solutions could generate the same type of behavior. Dissolution of quartz to H_4SiO_4 and to $H_3SiO_4^-$ has been studied[41-43]. A value of $10^{-9.8}$ has been given for the reaction, consistent of:

$$H_4SiO_4 \rightleftharpoons H^+ + H_3SiO_4^-$$

while the reaction

$$SiO_2\ (s) + H_2O \rightarrow H_4SiO_4$$

is given an equilibrium constant equal to 1.8×10^{-4}. Hence, at pH 9.0, a concentration of 2.8×10^{-5} moles/liter of $H_3SiO_4^-$ is possible in solution. This is low, but pyrex, a sodium boro-silicate glass, should have a much higher solubility.

Finally, while silica and CO_2 would affect the acid concentration in solution, the precipitate itself can be contaminated. A suspension stirred for weeks will inevitably grind teflon stirring bars. Furthermore, as the cell is frequently opened, organic contamination from the atmosphere itself might be unavoidable; specific adsorption of contaminants is always a possibility.

B. Conditions for Obtaining Fast Isotherms

From the above discussion, it becomes clear that a correct interpretation of the slow step on oxides involves first an evaluation of the respective contributions of CO_2 and silica to the total pH change. For that reason, while

the slow step in adsorption was measured, the material was at times centrifuged and the supernatant solution analyzed for CO_2. A hydrogen consuming reaction (reaction of CO_2 or SiO_2 with water) will, upon titration of the solution, show up in an increased amount of acid and base required to scan between two reference pH's, say 4.5 and 9.5. Using this criterion, it was generally found that CO_2 absorption could be kept below 20% of the total observed slow adsorption in the cell. This was true, however, only if maximum care were taken.

The experimental information shown in Figures 1 and 2 indicates that it is possible to adjust rapidly pH and keep it constant for over three hours. This property is utilized in determining the fast isotherm, that is, if a titration is rapidly run on a precipitate conditioned at any pH away from the zpc, it should be reversible. This clearly does not exclude the possibility that the shape of the obtained fast isotherm would differ from that of another isotherm obtained on the same material prior to conditioning, or that isotherms are not reproducible.

Fast isotherms are normally obtained on rutile which was allowed to age in pure water in the vicinity of the expected zpc at pH 6. The first isotherm on Figure 4 represents such an isotherm that has been measured in both directions and found to be completely reversible (within 0.5 μmole per sample). The same observation would also have held for the first isotherm of Figure 3. This reversibility must be

be emphasized here as it represents a major experimental improvement for oxides. It was such a fast isotherm that enabled Onoda[18] to improve the past results on hematite considerably. Waiting too long between the various points of an isotherm introduces a slow kinetic phenomenon which complicates the interpretation and leads to a considerable scattering of the data.

The excellent reversibility does not always hold and Figure 6 illustrates this point. Following basic conditioning, the first isotherm is followed by another one, II, which is considerably less steep even though the oxide was not allowed to wait in between the two experiments. In Figure 3, isotherms 2 and 3 and isotherms 5 and 6 also show this flattening behavior when the precipitate is cycled from a basic to an acid pH.

The results shown in Figure 3 stress a further point. With reference to fast isotherms 1, 2 and 5, the slopes of these curves at any pH show a marked increase in going from 1 to 5. The same is true of Figure 4 but to a smaller extent. In contrast with the above observation, Figure 5 shows a nearly parallel displacement of isotherms at 0.1M of NaCl. This latter observation was also made by Onoda and de Bruyn on hematite.

We can now drawn some important conclusions. First, conditioning at basic pH leads to increases in the slope of the isotherms and particularly so at lower ionic strengths.

Treatments in acid solutions, as reported under Results, have no effect on a material that was aged at the pH of the zpc. Secondly, conditioning leads to an unstable system which is not in equilibrium with the solution. That may not be obvious but we shall show that it is truly the case. This conclusion may be justified on the basis of the irreversibility of isotherms after basic conditioning. A reversible fast isotherm would indicate a system which is in equilibrium and does not find any driving force to disrupt this situation. This would apply to isotherms obtained on a material aged at the zpc as we noted. Upon conditioning the oxide, we find a new fast isotherm which is steeper but we also find that cycling the precipitate between basic and acid pH's, even rapidly, tend to bring the isotherm back to the original one. There is a driving force now acting to change the shape of the isotherm and that is what permits us to conclude that the system is now in unstable equilibrium.

A last point must be made concerning Figure 3. It refers to the new intersection of isotherms obtained when, after conditioning on the basic side, ionic strength is changed (curves 6, 7 and 8). Isotherms 6 and 7 for 10^{-2}M and 10^{-1}M concentrations now intersect on the very acid side (close to pH 4). The one molar isotherm (curve 8) shows the same behavior, though the direction of travel here would tend to flatten the isotherm and reduce the effect of ionic strength on adsorption.

It is not possible at this stage to ascertain beyond doubt

the nature of the slow step. It seems reasonable to infer that (1) it involves a reaction of the surface with the solution, (2) it shifts intersections of isotherms to more acid values, indicating a possible lowering of the zpc, (3) at lower ionic strength, it increases the slope of the isotherm which is a measure of the differential capacity of the double layer. Since this preliminary discussion intends to set conditions under which more reliable isotherms would be obtained on oxides, it can be concluded that (1) isotherms should be determined rapidly to avoid any slow kinetic phenomenon and measure only the immediate interaction surface-solution, (2) the surface should be washed free of any contaminating salts to minimize the effects of previous history. We will assume that the kinetics of adsorption is characterized by two steps; one which is fast and in virtual equilibrium and a second, the rate limiting step, which is prevented from interfering in the fast isotherm.

2. The Electrical Double-Layer at the Rutile Interface

A. Thermodynamic Treatment of Interfaces

For systems such as silver iodide and silver sulfide, the potential-determining role of silver, for instance, is easily understood[11,12]. This potential-determing action of the silver ion which is common to both the solid and the solution is simply written as follows:

$$\mu_{Ag^+}^{-solid} = \mu_{Ag^+}^{-solution} \qquad (6)$$

where

$$\bar{\mu}_i = \mu_{i+}\,(T, \bar{P} = 0, C_1, \ldots, C_\gamma) - \frac{E^2}{8\pi}\left[\frac{\partial \varepsilon}{\partial C_{i+}}\right]_{T\ (C)} + z_{i+} F \phi \qquad (7)$$

$\bar{\mu}_i$ = electrochemical potential of the ith ion

μ_i = chemical potential of the ion in the same ionic surrounding, but without electrical field

$\bar{P}$ = polarization of medium per unit volume

E = the magnitude of the macroscopic potential field, $\bar{E}$

C = concentration in number of ions per unit volume

ε = dielectric constant of the medium

ϕ = macroscopic electrical potential, where $\bar{E} = -\nabla\phi$

z_i = the charge on the ion

e = electronic charge

F = the Faraday constant

Equation (7) is the more general form of the expression for the electrochemical potential as derived by Prigogine, Mazur and Defay[39], when the dielectric constant of the medium is affected by the electric field. For these heteroionic solids, the chemical potential is not changed by the few adsorbed potential-determining ions and changes in electrochemical potential of the ions in the crystal are accounted for by changes in electrostatic potentials (ϕ) only.

This reasoning is not as straightforward when applied to an oxide such as rutile. First, the potential-determining dependence of $O^=$ ions in oxide systems is not a direct

relationship as that of equation (1) but must be related to the chemical potential of OH^- in solution as in the following equation:

$$\mu_{O^=}^{-oxide} = \mu_{O^=}^{-solution} = 2\mu_{OH^-}^{solution} - \mu_{H_2O}^{solution}$$

Secondly, the low solubility of rutile does not allow enough ions in solution to account for the observed changes in surface charge with pH; the surface charge can only come through adsorption of hydrogen and hydroxyl ions, if the small amount of $O^=$ ions in solution is also ignored.

But adsorption of OH^- on the surface is not directly equivalent to adding $O^=$ ions to the crystal surface. An hydroxyl ion on the surface must be in equilibrium with both the oxygen ion and a water molecule. In other words, the hydroxyl must be adsorbed on a phase where water is already present and has a constant chemical potential equal to that in the solution. In such a case, we submit that the interface can be treated as a hydrated phase in equilibrium with the solution and that hydrogen and hydroxyl ions are directly potential-determining for the system.

Such a postulate is supported also by some experimental observations. Surfaces of oxides have always been thought to be hydroxylated[33-38,6]. In fact, the surface is probably much more complex. On hematite, for instance, the interface has been described as a succession of layers such as: anhydrous oxide, hydrous oxide[9], hydroxylation layer[36,37], strongly

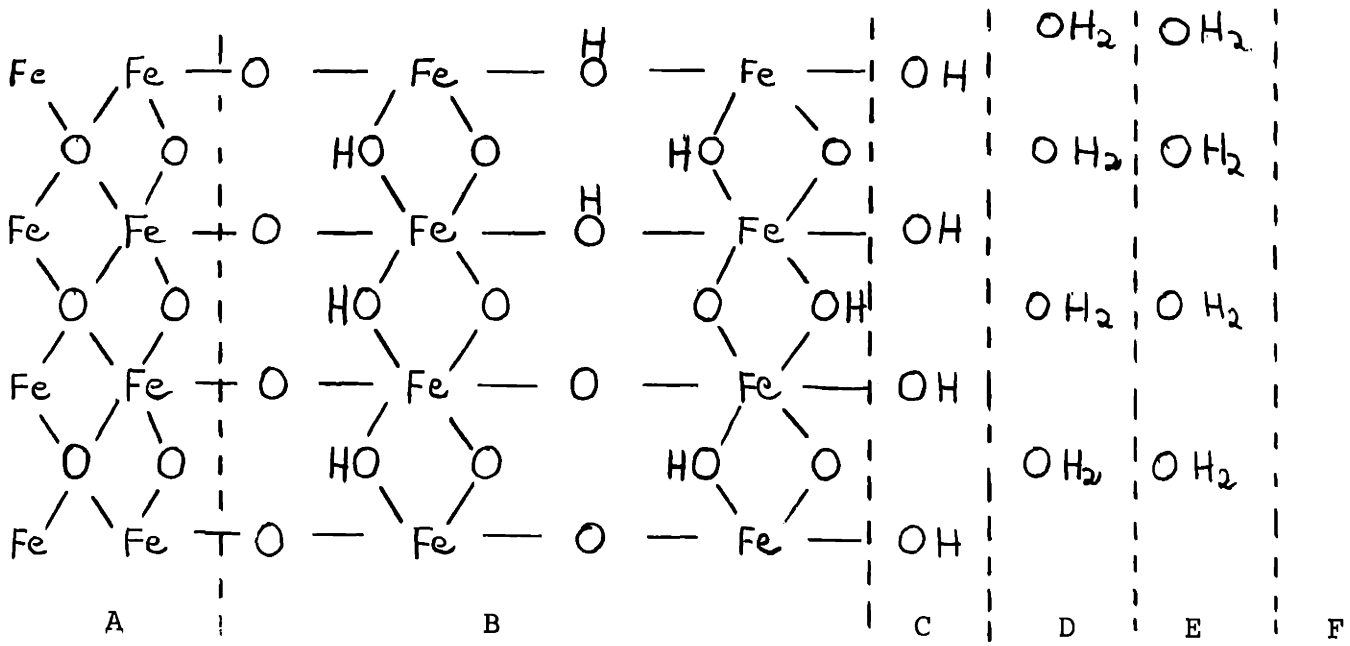

A: Anhydrous Hematite

B: Hydrous Oxide

C: Hydroxylation Layer

D: Strongly Hydrogen-Bonded Water

E: Weakly Hydrogen-Bonded Water

F: Solution

FIGURE 26. SCHEMATIC DESCRIPTION OF A PROPOSED MODEL OF THE HEMATITE INTERFACE.

hydrogen bonded water[38], physically adsorbed water and finally, the aqueous solution. A general illustration of this model is given in Figure 26.

If the surface is found to equilibrate rapidly with the solution, the reaction is presumed to involve only the water in contact with the solution, whether it is the hydroxyl groups or the physically adsorbed layers. Equilibrium is then always assumed between the surface and the solution.

The existence of some form of hydrated surface phase on rutile has been clearly established. Yates[33] and Parfitt[34] have identified its nature by means of infrared spectroscopy, while Jurinak[38] has determined the amount of water adsorbed on the surface. For a rutile crystal in contact with an aqueous solution, the relation

$$\bar{\mu}^{\text{surface}}_{H^+} = \bar{\mu}^{\text{solution}}_{H^+}$$

describes the equilibrium between H^+ in the solution and in the hydrated surface phase.

For the purpose of this discussion, we shall ignore the changes in dielectric constant of water and, therefore, with reference to equation (7), we write

$$\bar{\mu}_{H^+} = \mu_{H^+} + F\,\phi \,. \qquad (8)$$

Under normal conditions, water is weakly dissociated and the chemical potential of the hydrogen ion in pure water depends

on its concentration in solution. The same reasoning, if applied to the adsorbed water phase, would make $\mu_{H^+}^{surface}$ a function of the surface concentration and the following equation,

$$\bar{\mu}_{H^+}^{surface} = K_{H^+} + z\ F\ \phi^{surface} \qquad (9)$$

where $\mu_{H^+}^{surface}$ is assumed constant, would not hold.

Such a relationship was successfully applied to the silver iodide[10] crystal where the atoms of the lattice are in a nearly pure ionic state and adding a few more ions does not change their chemical potential. It is obvious, however, that if the surface water on oxides is in a molecular state, weakly dissociated, bringing hydrogen ions to the surface will greatly affect their chemical potential $\left(\mu_{H^+}^{surface} \neq K_{H^+}\right)$. Equation (9) would not apply were it not for the fact that water molecules are known to dissociate on the surface of an activated oxide. The hydroxyl groups are fixed on the surface[33-38] and, because of the strong metal-oxygen bond, the proton is more free to dissociate than in pure water. If the charging of the interface does not involve the hydroxylation layer (C, Figure 26) but the adjacent layer of strongly hydrogen-bonded water, a similar reasoning will show that a strong crystal field effect results in a more ionic character for the water phase.

We may now write,

$$K_{H^+} + F\ \phi^{surface} = \mu_{H^+}^{solution} + z\ e\ \phi^{solution} \qquad (10)$$

or

$$K_{H^+} + F\ (\chi+\psi) \quad = \quad \mu_{H^+}^{solution} \tag{11}$$

where the potential difference between the surface phase and the solution has been divided into a contribution of the spacial distribution of ionic charges, ψ, and, χ, the contribution of water dipoles and other atomic interactions. The χ potential will be assumed constant and will be combined with the constant K_{H^+} to give

$$K \quad + \quad e\ \psi = \mu_{H^+}^{solution} \quad . \tag{12}$$

At the zpc, in the absence of specific adsorption, $\psi = 0$ and at room temperature,

$$\frac{1}{F}\ d\mu_{H^+}^{solution} \quad = \quad d\psi \quad = \quad -59.19\ dpH \quad . \tag{13}$$

Values for $F\ (\Gamma_{H^+} - \Gamma_{OH^-})$, determined experimentally and defined as σ, can be obtained as a function of pH. Equation (13) is integrated between the pH of the zpc and any other pH, σ can now be plotted against ψ. An analogy can then be established with the mercury system where σ is assumed to give a two-dimensional smeared-out charge and $E - E_0$, the ψ potential at the surface, where E_0 is the potential difference across the electrodes at the zpc.

B. ZPC and Specific Adsorption

We have now described how fast isotherms can be obtained in order to allow only an instantaneous equilibrium between the surface and the solution. We have also discussed the potential-determining role of hydrogen and the subsequent electrochemical model of the interface. If one considers a system where no specific adsorption can occur, one can predict from diffuse double layer theory the shape of the isotherms obtained at low ionic strength.

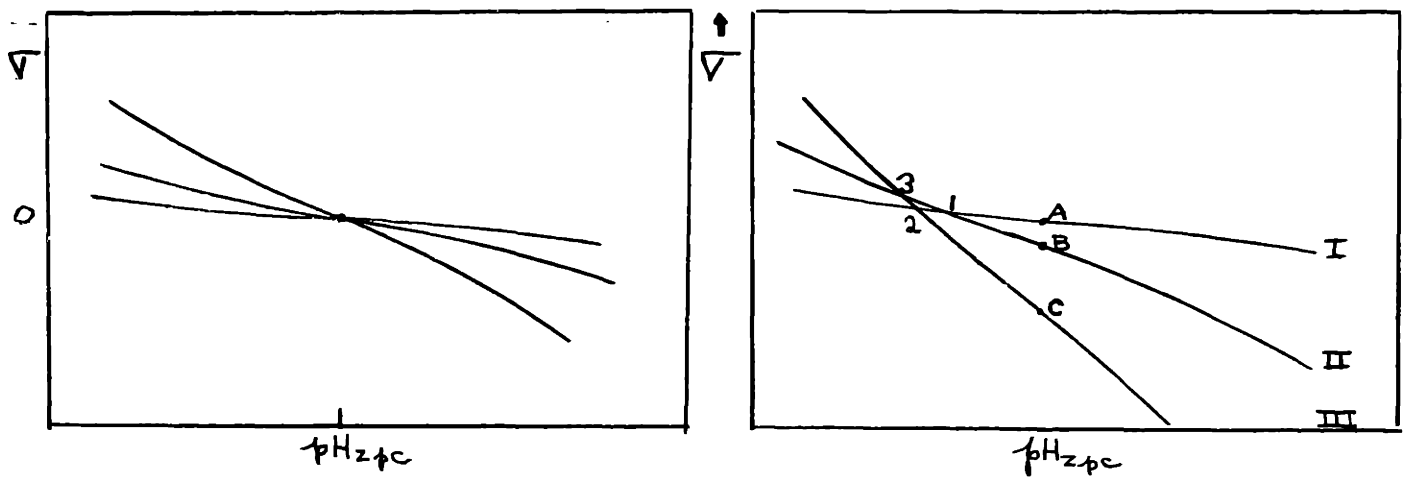

FIGURE 27. SCHEMATIC ILLUSTRATION OF ADSORPTION ISOTHERMS.
A. Without Specific Adsorption
B. With Specific Adsorption

more at the original zpc and that they do not have a common intersection point. Such a behavior is normally obtained with mercury in the presence of specifically adsorbed ions and was well illustrated by Grahame and Soderberg[44]. It is not possible to comment on the position of the inflexion point from their measurements as they were obtained at too high ionic strengths. Recent work by Payne[45] has shown a displacement of the minimum capacity due to the diffuse layer in presence of specific adsorption of NO_3^- ions. Accepting Payne's results, we would presume that the inflexion point in the presence of specifically adsorbed cations would be displaced to more acid pH's.

In view of the above discussion, it will now be clear why it is not so obvious that the isotherms of Figure 7 intersect at the zpc. Figure 27b shows that specific adsorption would drastically displace the general region of the intersection point. But because the downward displacement of isotherms with specific adsorption is coupled with increased steepness of the isotherms, all isotherms could tend again to intercept in the same region. Experimental inaccuracies, as may be seen in Figure 7, are such that the intercept is usually defined only by the steepest isotherms. In other words, in spite of specific adsorption, isotherms could still appear to intercept in the vicinity of their inflexion points. There are, however, some arguments in favor of defining the intersection point of Figure 7 as the zpc. This intersection

occurs practically always at pH 6 for hydrated materials, implying, therefore, that all ions would tend to be specifically adsorbed in the same way, a most unlikely situation.

The above ambiguity can be resolved in an easy way. In Figure 7, the results of the pH drift experiments in the 0.01M solution of perchlorate clearly show that the pH at which Γ_{H^+} equals Γ_{OH^-} is within experimental error equal to the pH of the intersection of isotherms. In as much as one can be sure that all excess acid was removed from the precipitate before it is introduced in the various cells, the pH of the zpc is equal to the pH of the intersection of isotherms and is located at pH of 5.78 $\pm$ 0.04. The difference in the value obtained here and the value of 5.90 given in Figure 8, also in presence of sodium perchlorate, is attributed to the surface treatment prior to the actual titration. This effect will be analyzed in detail later on.

In view of all the above arguments, we will conclude that there is enough evidence to state that specific adsorption of any kind can be neglected at the zpc. The pH of the zpc is, therefore, also the point where ψ is zero; where there is no ionic double layer in solution.

C. Double Layer Theory and Its Applications

It was stressed under Results that reproducibility of adsorption has not been too satisfactory. Because the magnitude of adsorption is generally reproducible only to within 10%, the shape of the isotherms and their intersection are not too well established. This irreproducibility of the system is not

an experimental error as such, since isotherms are reversible under fixed conditions. The existence of the slow step which has been shown to modify drastically the isotherms at constant ionic strength is felt to play a major role in this non-reproducibility from sample to sample of the same batch. An interaction solid-solution exists that has not been controlled yet.

(i) Adsorption in the Presence of Sodium Nitrate.

Experimental Capacity Curves. Before we can attempt to compare specific effects of salts, it would be desirable to analyze results with a given salt. Figure 13 gives some typical isotherms obtained in the presence of sodium nitrate.

The potential-determining role of hydrogen has already been postulated. We will now postulate further that $F \cdot (\Gamma_H - \Gamma_{OH})$, an experimental quantity defined as σ, is located on the surface as a smeared-out two-dimensional charge with the counter charge lying on the solution side of the interface. The differential capacity of the double layer at a reversible interface is defined as:

$$\left(\frac{\partial \sigma}{\partial \psi}\right)_{\mu_{salt}} = C \qquad (14)$$

where $d\psi$ is defined by equation (13).

Figure 28 shows a plot of differential capacity versus ψ for the isotherms shown in Figure 13 with $NaNO_3$ as indifferent electrolyte. The capacities were obtained according to equation (14) by graphical differention. It should be noted that such a procedure tends to amplify any experimental error

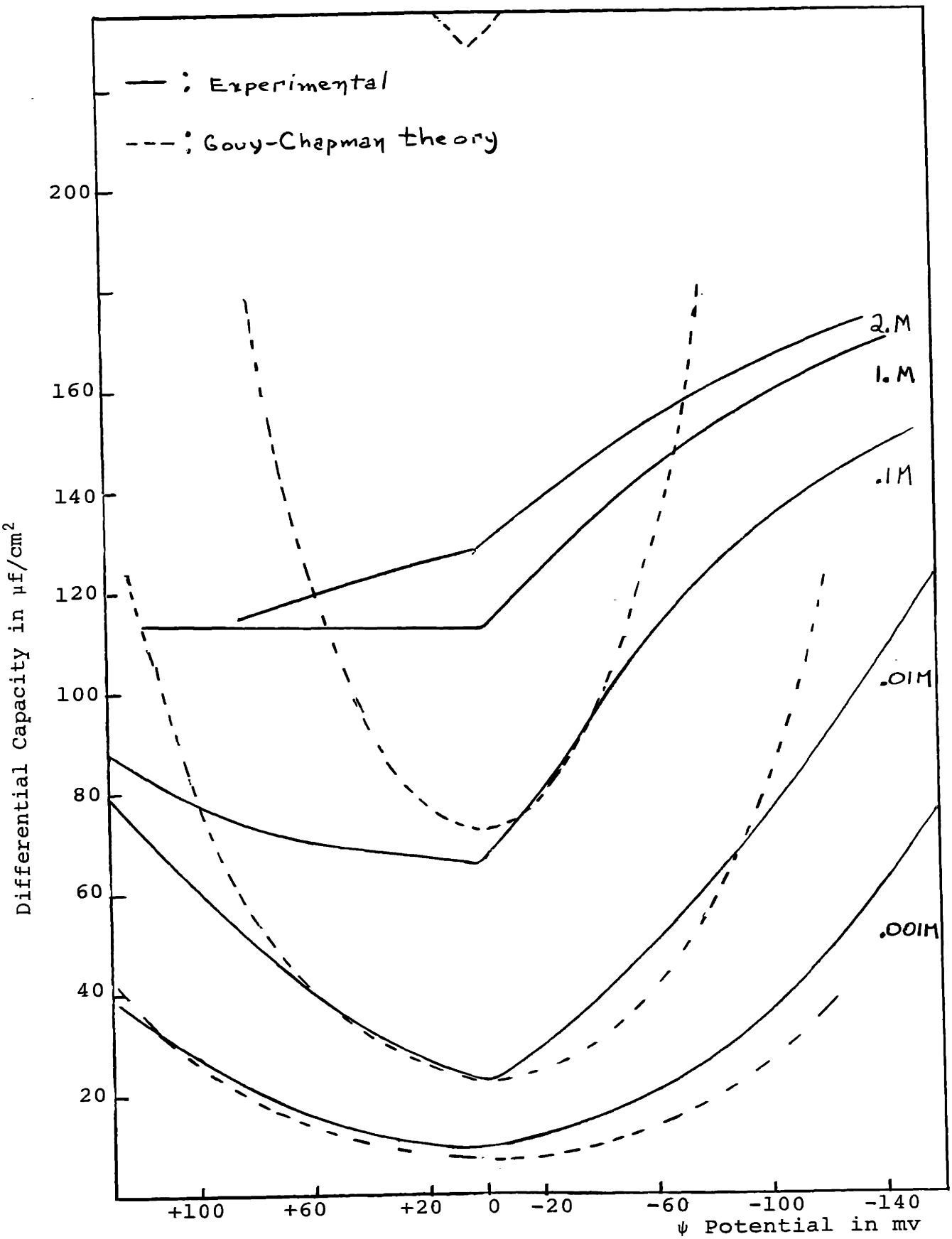

FIGURE 28. DIFFERENTIAL CAPACITY CURVE FOR THE RUTILE INTERFACE IN PRESENCE OF $NaNO_3$ AT 25°C.

and for that reason is less accurate than direct capacity measurements.

In Figure 29, the capacity is plotted against $\sigma(=F\Gamma_{\pm})$. Figure 30 compares capacities observed on rutile with similar data reported for the mercury/sodium fluoride[20], silver-iodide/sodium perchlorate[11], and silver sulfide/sodium nitrate[12]. Except for the minimum capacity at 0.001M, there is little similarity between the rutile system and all the others. Also, a rapid look at Figure 28 discloses an asymmetry of the capacity curves with increased capacities on the negative side. The opposite is observed for the other systems in Figure 30.

Double-Layer Theory. If the Gouy-Chapman theory of the double layer at the plane interface is applied to the system, values for C against ψ are calculated and plotted in Figure 28 (as a dashed line). It is apparent at first sight that a surprisingly good fit is obtained at 0.001M and more than acceptable agreement at 0.01M. It is possible to improve this fit by taking into account the effect of particle size on double layer theory. The assumption of plane interfaces is nevertheless made because of the inaccuracy of the data at low ionic strength when expressed in the form of differential capacity and we will now show the error thus introduced. The minimum capacity in solutions of ionic strength, 0.001M, as determined from data given in Figures 8 to 14 is found to range between 6 $\mu f/cm^2$ and 11 $\mu f/cm^2$, with an average value of 9 $\mu f/cm^2$. Planar diffuse layer theory predicts a minimum of 7 $\mu f/cm^2$.

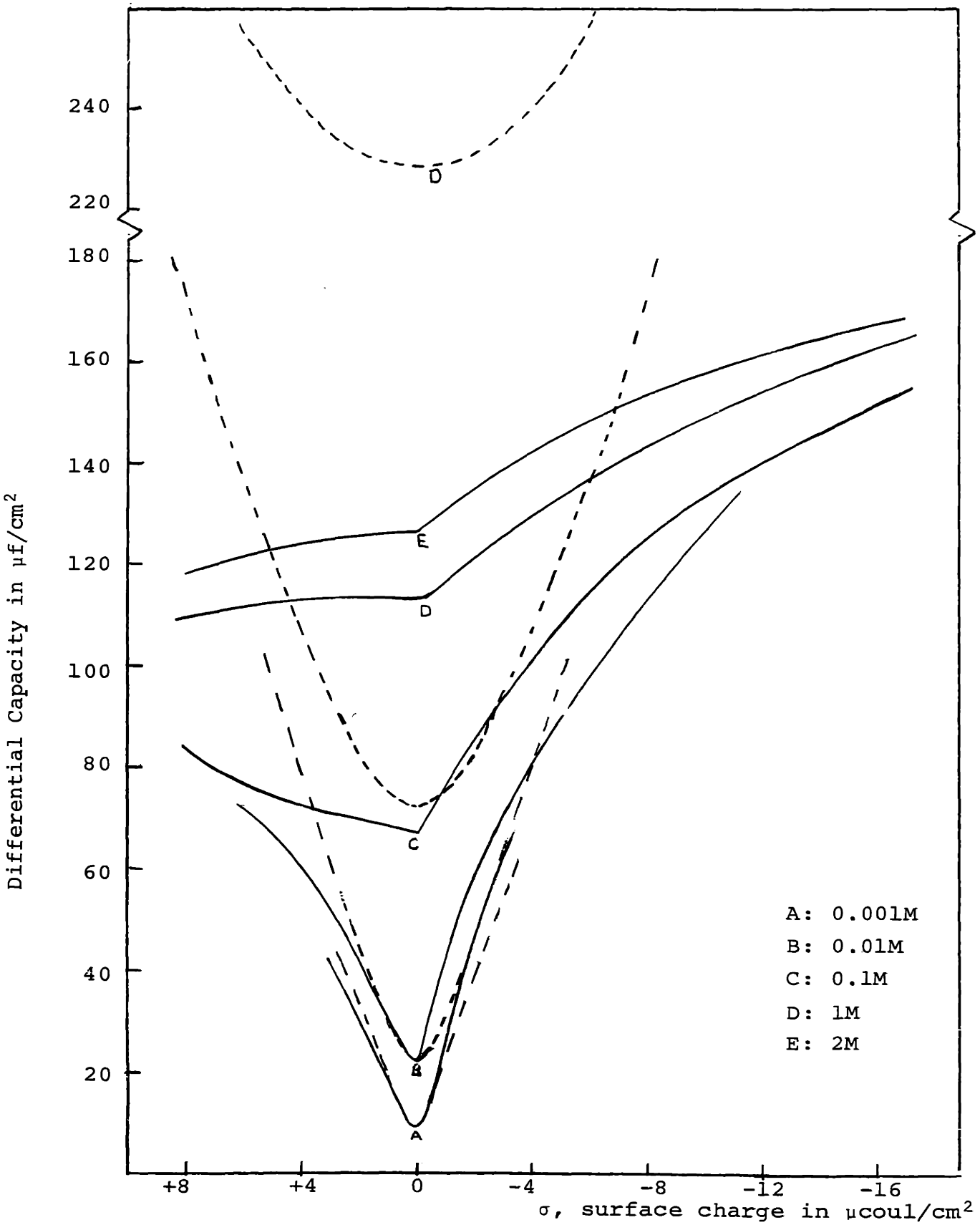

FIGURE 29. DIFFERENTIAL CAPACITY CURVE OF FIGURE 28 REPLOTTED AGAINST SURFACE CHARGE.

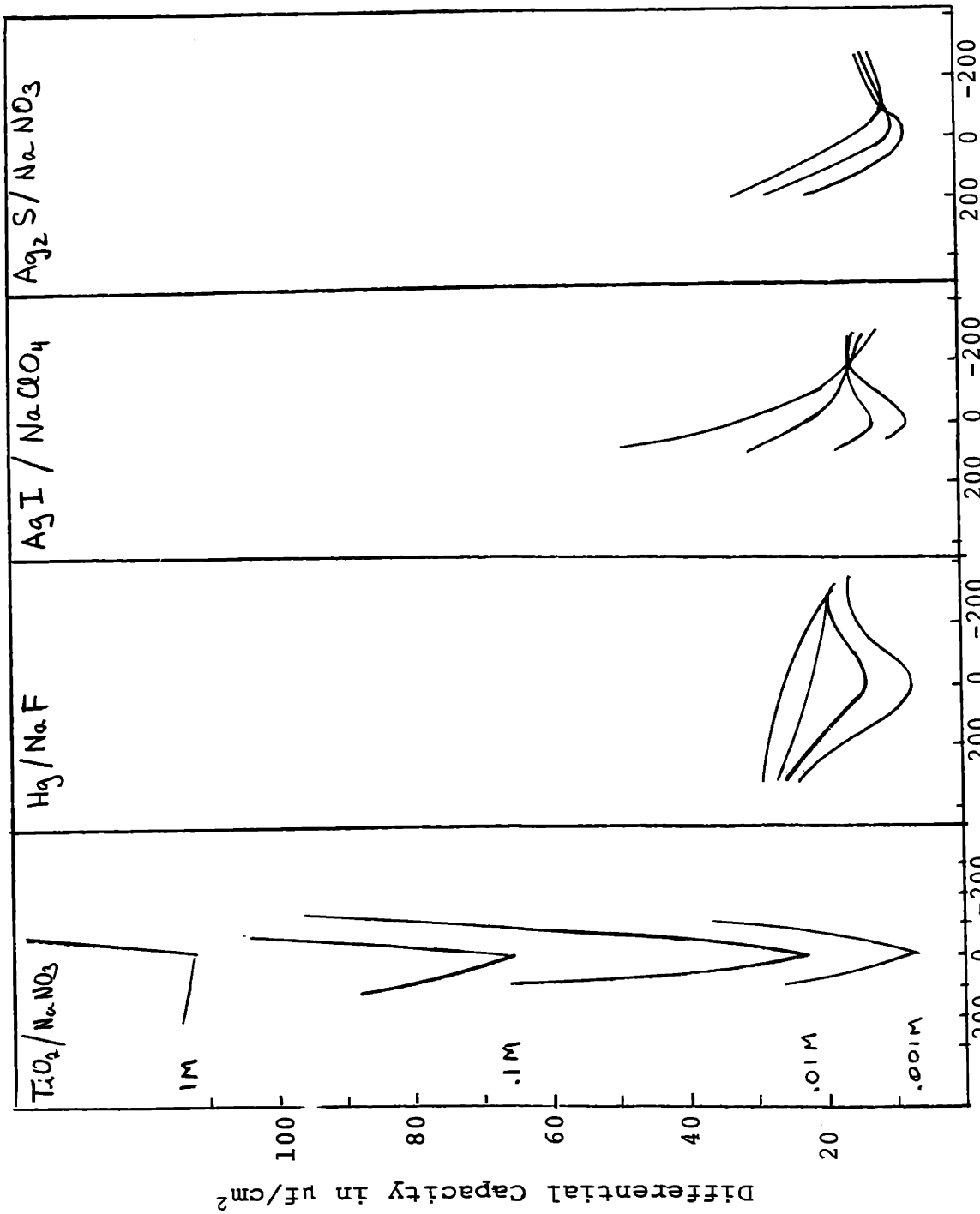

FIGURE 30. COMPARISON OF DIFFERENTIAL CAPACITIES REPORTED FOR VARIOUS INTERFACIAL SYSTEMS.

If we assume the rutile particles to be spherical in shape, then the error introduced by assuming a planar interface may be evaluated by referring to the work of Loeb, Overbeek and Wiersema[46]. For uni-univalent electrolytes and double layer potentials of 25 mv, the errors are tabulated in Table 1. In this table

$$\sigma\ (q^\circ) \;=\; K\ I\ (q^\circ)$$

where K is determined by temperature, dielectric constant of the medium and the ionic strength and, for uni-univalent electrolytes,

$$q^\circ \;=\; \kappa\ a$$

where κ is the well-known[47] reciprocal Debye-Hückel length and a is the particle radius.

TABLE 1

q°	0.5	1	2	5	10	20	∞
$I(q^\circ)$	3.02	2.03	1.53	1.24	1.14	1.10	1.04

Now for a given specific surface of 43 M^2 per gr, an average radius (a) of 1.62×10^{-6} cm is obtained and q° is then equal to 1.62 at 10^{-3}M ($1/\kappa = 10^{-6}$ cm).

From Table 1, it follows that the error introduced in σ by using a value of ∞ for q° instead of 1.62 is of the

order of 65% (I (1.62)/I (∞) = 1.65). The error in capacity will be of the same order at the zpc (somewhat smaller since we have approximated the curve σ vs. ψ as a straight line around the zpc). Instead of 7 μf/cm^2 predicted by diffuse layer at the zpc, a value of 11 μf/cm^2 is indicated. Because of the scatter in the data, and because already at 10^{-2}M the error would only be 25%, as q° is now equal to 3.0, it is felt that such a correction can be neglected for the sake of simplicity.

Before we go any further in refining our quantitative analysis of the experimental capacity curves, it is important to note briefly the assumptions made in the Gouy-Chapman theory. Ions are treated as point charges and will approach the surface within an infinitely small distance. The diffuse layer is uniquely controlled by potential and ionic strength while changes of dielectric constant in solution as well as electrostriction are neglected effects in a first approximation.

The original model proved to be very poor in predicting results on mercury. Stern[49] modified the theory by adding an inner capacitor or a plane of closest approach for ions. Adding this capacitor in series with the diffuse capacitor dramatically improved the agreement between theory and experimental results. In fact, Frumkin[48] showed that a better fit could be obtained if two planes of closest approach were assumed; one on the negative side of the zpc* and another on

*that branch of the curve for which σ < 0.

the positive side, depending whether the counter charge is positive or negative. Finally, Grahame[20] showed that the best possible agreement was obtained by making the inner capacity a continuous function of the total surface charge. Using Stern's analogy we can say that

$$C_i = \frac{\varepsilon}{4\pi d} \tag{15}$$

where

C_i is the inner capacitance

ε is the dielectric constant of the medium

d is the distance from the surface to the plane of closest approach of counter ions.

The inner capacitor is introduced in series with the diffuse capacitor and the total capacitance is given by

$$\frac{1}{C} = \frac{1}{C_i} + \frac{1}{C_D} \tag{16}$$

where C_D is now related to the diffuse layer only and must be integrated from the plane of closest approach to infinity. The potential at this plane does not correspond any longer to the total potential difference across the interface. We can avoid the difficulty by always plotting capacity against total surface charge and make use of

$$C_D = \frac{zF}{RT}\left[\frac{R\ T\ \varepsilon\ C^S}{2\pi}\right]^{1/2} \cosh\left[\frac{zF\psi_D}{2\ RT}\right] \tag{17}$$

and

$$\sigma = 2 \left[\frac{R\ T\ \varepsilon\ C^S}{2\Pi}\right]^{1/2} \cosh\left[\frac{zF\psi_D}{2\ RT}\right] \qquad (18)$$

where C^S is the ionic strength, to eliminate ψ_D, the potential at the plane of closest approach. To calculate C_i, one simply assumes that C_i is a unique function of total charge and follows the method suggested by Parsons and Levie as outlined by Delahay[58]; $1/C$ is plotted against $1/C_D$ for various ionic strengths but constant charge, in which case a straight line should be obtained with an intercept equal to $1/C_i$. C_D is calculated in this fashion and given in Figure 29 as a function of σ (dashed line).

In the above derivation, specific adsorption is entirely neglected. However, equation (18) will hold only for a case where q_i, the fraction of the total charge due to specific adsorption, is zero. In applying equation 16 for series capacitors to the case where no specific adsorption occurs, it is obvious that introducing a value for C_i can only lower the total measured capacity. However, when specifically adsorbed ions are introduced in the system, there is a specific force between the ions and the surface which, added to the electrostatic attraction just described, tends to increase adsorption and, in the same fashion, the total capacitance. If, for one reason or another, C_i is too large and can be neglected in front of C_D, specific adsorption will increase the total observed capacitance above the minimum

predicted by $1/C_D$. Trying to apply equation (16) to such a case will yield a negative C_i . If, on the other hand, C_i , due to the inner capacitor, is low enough so as to be comparable with C_D , adding a specifically adsorbed ion to the system may raise the total capacity without taking it to values greater than the calculated C_D (calculation based on no specific adsorption, it should be remembered). In such a case, a positive C_i is calculated which may seem reasonable though it is still completely meaningless; it simply indicates the presence of an inner capacitor which must be smaller than the calculated one. The decrease in observed capacitance cannot be treated by series capacitors as Sluyters[50] pointed out, whenever specific adsorption takes place.

Applications to Capacity Curves. Referring to Figure 29 where C_D has been calculated for a case of no specific adsorption, it will be noticed that the experimental capacities at low ionic strengths lie above those predicted by diffuse double-layer theory. This is particularly the case for the negative branches of these curves. From our discussion, we will now conclude to the presence of specific adsorption of sodium on the negative rutile surface. From our discussion of specific adsorption at the zpc (section B), we can safely assume that specific adsorption on rutile is not strong and we will, therefore, go on calculating C_i whenever possible, that is, whenever C is smaller than C_D . We follow the method outlined above. Figure 31 shows such results for various ionic strengths where C_i is plotted against σ. No attempts

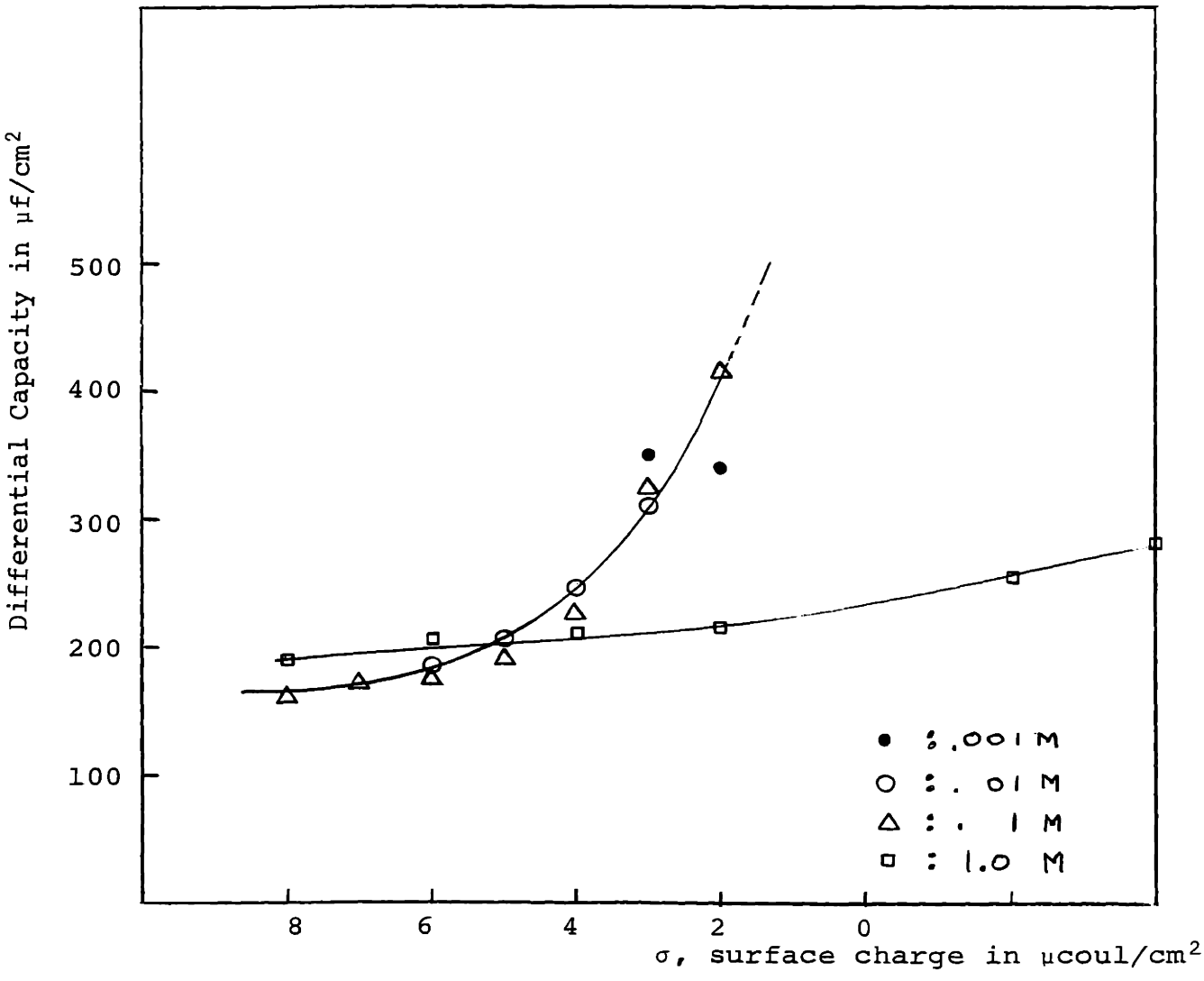

FIGURE 31. CALCULATED VALUES OF INNER HELMHOLTZ CAPACITY FOR THE RUTILE-$NaNO_3$ SOLUTION INTERFACE.

are made to calculate inner capacities corresponding to negative charges except for the 1M concentration. At that concentration, the effect of the inner capacitor is seen to greatly lower the total capacity below that predicted by diffuse layer and an order of magnitude for C_i can then be made available.

Without going into a detailed analysis of the variation in inner capacitance with charge, it will be first observed that the value of the inner capacity at the zpc is considerably larger than that of the mercury interface. In a one molar solution we find 230 $\mu f/cm^2$ as opposed to 22 $\mu f/cm^2$. Such a conclusion could have been drawn directly from Figure 30 where the capacity curves for mercury are shown to lie at values below 30 $\mu f/cm^2$ while for the rutile interface capacities tend to follow more closely diffuse layer values. In other words, the inner capacitor on rutile is too high to affect noticeably the total capacity due to essentially the diffuse layer.

Since we find little specific adsorption around the zpc, we can look more closely at the magnitude of this inner capacity defined as $\epsilon/4\pi d$. It is clear that ϵ can vary between 7 for dielectrically saturated water to 70. If ϵ is assumed to be 7 at the mercury interface because of dipole orientation at the surface, it can hardly be expected to be different at an oxide interface. Water is not chemically bonded on mercury while it is on rutile[51,52,33]. There is also on rutile a very strong hydrogen bond between the hydroxyls of the surface and the water molecule. This electrostatic bond

leads one to expect a low dielectric constant due to dielectric saturation when molecules are all oriented and, by the same token, to a lower inner capacitor. The solution must, therefore, lie with the plane of closest approach "d".

At the zpc itself, there can be two radii of closest approach, that of the anion and that of the cation. It is the longest distance of approach which defines the inner capacitor at the zpc as it gives lower C_i and makes a more important contribution to the total capacity. On mercury, the hydrated sodium has an effective radius[53] of 4Å and will control the inner capacity instead of chlorine, for example, with a radius of 2Å. However, on oxides there is some water of hydration in the plane of charge which can also be shared by sodium. The radius falls to 1Å and the anionic radius now controls the capacitor (see following diagram).

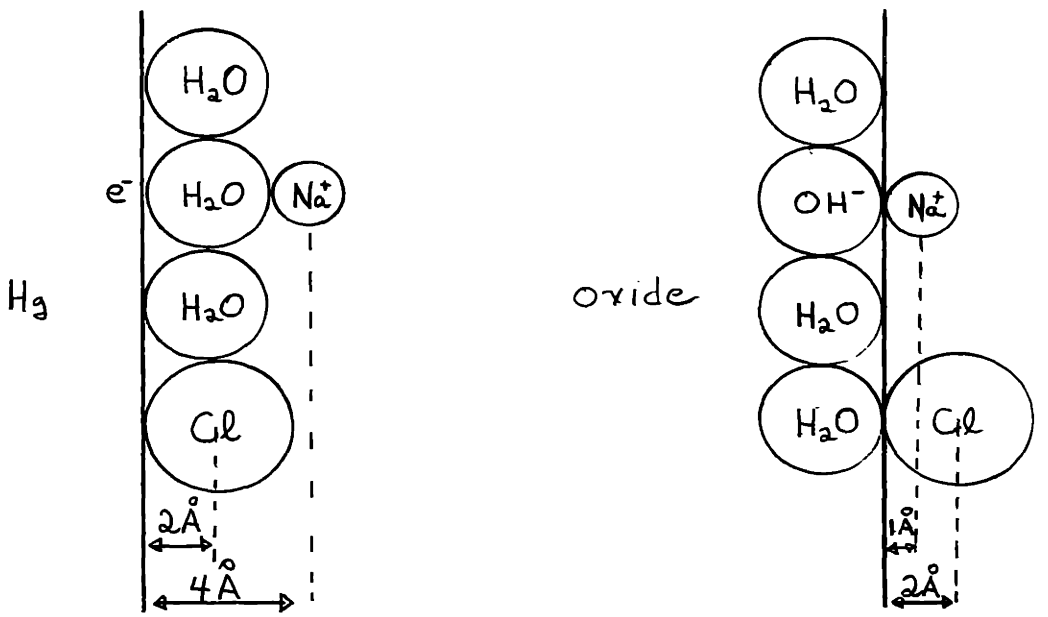

It is not easy to ascertain the exact dimension of a nitrate ion as it is not symmetrical and can be polarized, with its negative pole very close to the surface. Since adsorption isotherms show no differences between chlorine and nitrate, we will assume them to have the same effective radius of 2Å. It will, therefore, appear that the capacity of the inner region at the zpc could at least be twice that of the comparable capacity on mercury since the effective d is now 2Å instead of 4Å. But 44 $\mu f/cm^2$ is still too small in particular when it is compared with values greater than 500 $\mu f/cm^2$ obtained at the zpc and lower ionic strengths.

A larger value of the inner Helmholtz capacity can be achieved simply by allowing counterions in solution to penetrate the plane of surface charge. This can be achieved in two different ways. Work by de Boer[54] on the determination of surface areas of colloid materials by the BET technique showed that microporosity, while undetected by the normal BET equation in the linear range, can still be present. Recent work on rutile[4] previously heat-treated in air has corroborated this assumption. Hence, it could be suggested that the surface charge would lie on an average plane with bumps and dips. Counterions would to some extent lower their energy by filling micropores, thus lowering the effective distance between their center of charge and the average plane of charge.

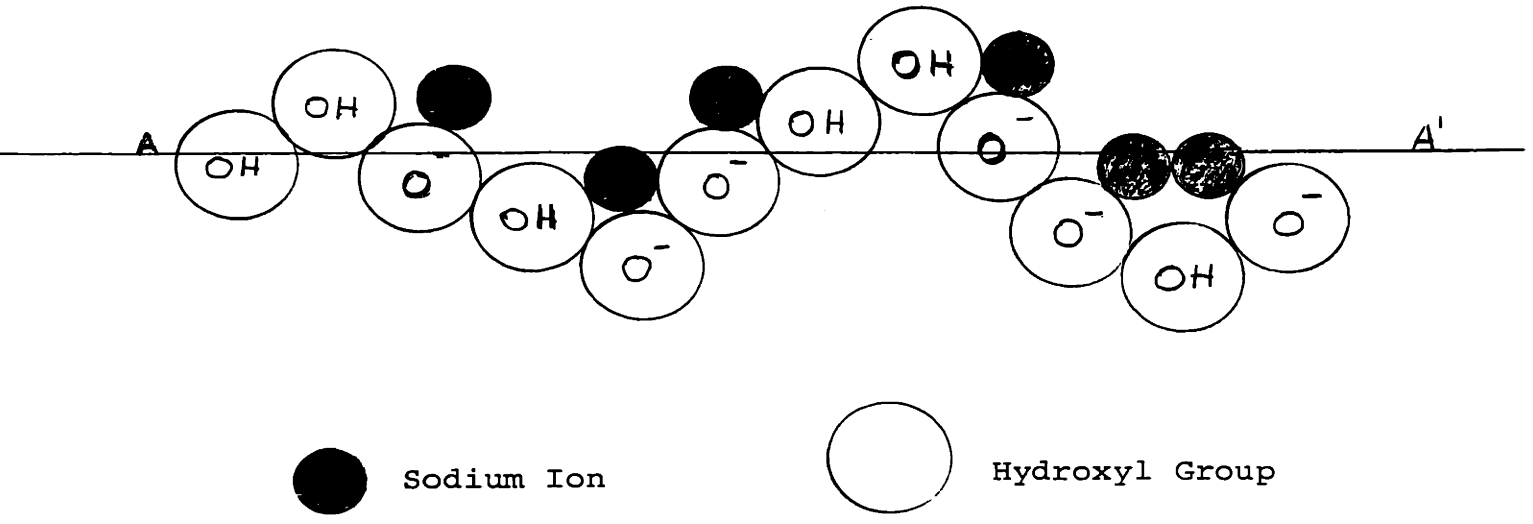

AA': average plane of surface charge

Representation of a Negatively charged Rough Surface.

There are objections to such a model though it is not possible to completely eliminate it. First, no changes in surface areas upon evacuation at temperatures up to 150°C were ever observed. Liberating some micropores by evacuation of water would increase the measured surface area. Higher temperatures of evacuation required to remove strongly held water and create micropores simply results in sintering and a final lowering of the surface area. For that reason, we have never observed any large amount of porosity. Secondly, Parfitt[4] suggests that such porosity is probably occupied

by some strongly bonded molecular water and will leave little place for a nitrate ion, for instance.

A second model will now be proposed for the rutile-solution interface. It was suggested in the past[5] that rather than looking at the dissociation of surface hydroxyls as the charging reaction, it might be proper to consider the complex, M-OH-OH_2, as the potential-determining radical. It would be the strongly bonded water with its characteristic dissociation constant (influenced by the crystal field) which would control the surface charge. By the same token, this layer of hydration, probably more loosely held in place than the hydroxyls themselves, would be mobile enough to allow counterions to penetrate into its plane, at least to some extent. The model is illustrated in Figure 32 for a negative surface charge. A (110) surface is exposed to the solution while the crystal is cleaved at right angles to show a ($\bar{1}$00) plane. The surface is shown to be fully hydroxylated and these hydroxyls are said not to participate in the creation of surface charges. A second layer of strongly bonded water is allowed to dissociate and transfer protons in and out of solution. Counterions can squeeze themselves into this layer to some depth and will use the surrounding water molecules in their first layer of hydration. This is equivalent to saying that the center of charge of these counterions can come infinitely close to the plane of smeared-out surface charge.

In view of the above model of the interface, the behavior of the inner capacitor can be better understood.

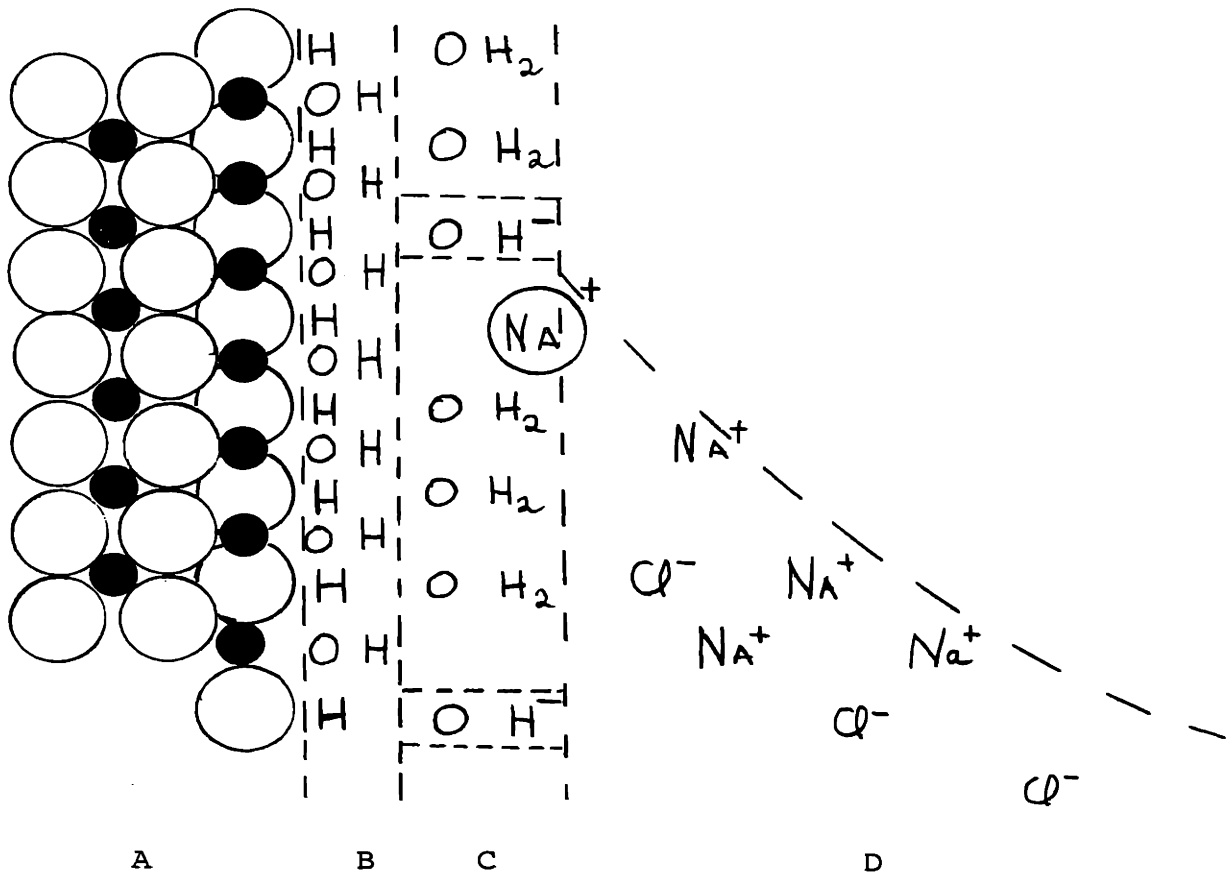

A: Rutile (110) Anhydrous

B: Surface Hydroxylation

C: Sorbed Water, Plane of Surface Charge (where adsorption of potential-determining ions occurs)

D: Solution, Diffuse Layer.

FIGURE 32. SCHEMATIC REPRESENTATION OF THE RUTILE INTERFACE.

It is still, however, impossible to interpret inner capacities in the presence of specific adsorption and inner capacities for the negative segment of the polarization curves cannot be calculated. In terms of our model, it can be said that the smaller an ion is, the better it will penetrate this hydrated layer and also the higher will the inner capacity be. This would apply, for instance, to cations with their relatively smaller radii. Another effect is also introduced on the negative side of these capacity curves; a change in dielectric constant of the medium. Because of the electrostatic nature of the hydrogen bond, water molecules tend to orient their dipoles in order to have the negative parts facing the surface, as opposed to their behavior on the mercury interface[52]. With increased negative charges on the surface, repulsion of the physically adsorbed water will occur and the water will gradually randomize its dipoles; an increase in dielectric constant takes place which results also in an increase in the value of the inner capacity. Finally, there is the observed specific adsorption which also tends to increase the inner capacity. All of these effects act together and cannot be dissociated. The only way to approximate a value of the inner capacity might consit in going to extemely concentrated solutions of salt (5M) and measuring total capacity.

The results of Figure 31 are more encouraging at positive charges. At ionic strengths below 1.0M, the inner capacities are surprisingly independent of charges. It is

even permissible to presume that an experimental error would explain the discrepancy at 1M for values of σ above 5 $\mu coul/cm^2$; the error is about 15%. In line with Grahame's view, it can be concluded that the inner capacitance is a unique function of total charge on the surface.

In order to arrive at Figure 31, a highly debatable assumption was made. No specific adsorption even for fairly high positive charges was postulated. What can probably save the treatment is the lack of tendency of the titanium ion to complex with chloride ions and even less with oxyanions[55,28]. Recent work[45] on mercury with NO_3^- had indicated fairly strong specific adsorption of NO_3^- anions on mercury. It is possible that similar behavior is avoided on rutile because of a shielding effect due to hydration. In fact, Kargin[56] in line with other workers found little or no sorption of inorganic neutral salts.

The general behavior of the internal capacitor with increasing positive charge is surprising. It is lowered by increasing positive charges on the surface and since specific adsorption tends to raise total capacitance, the observed effect must be truly due to the inner capacitor itself. This behavior points to a defect in the original assumption where we had assumed that counterions could penetrate the charged layer in an infinite number. Obviously, this cannot be. The counterions have finite sizes and at low charges can fit in the surface as required by diffuse layer theory. As the

charge increases, those counterions cannot accommodate themselves on the surface and are gradually expelled until they are at their distance of closest approach, in other words, the inner capacitor decreases with charge. Also, it was recently recalled in a most rigorous treatment by Hurwitz, Sanfield and Steichen-Sanfelt[57] that ionic sizes could not be neglected for charges above 10 $\mu coul/cm^2$ and the correction could become extremely important at a concentration of one molar. Hence, we expect in a one molar solution a more rapid crowding of counterions at the interface and consequently, a lower inner capacitor as we can observe in Figure 31. Hence, with increasing ionic strengths, the diffuse layer is compressed at the interface and the inner capacity becomes also dependent on the ionic strength at low charges. It is interesting to see that it gradually tends towards the same limit as that reached by the inner capacity at lower ionic strengths but higher charges. It shows that the same mechanism applies to both cases, a crowding out phenomenon.

It ought to be said here that we have decidedly ignored any possible deficiencies in our postulate of constant chemical potential for the hydrogen ion at the surface. This obviously would bear greatly on adsorption densities and on calculated inner capacities.

(ii) Influence of Various Electrolytes. The role of different ions in the double layer can now be understood somewhat better. From the data in Figures 8 to 12 and in

Figure 14, for various univalent inorganic electrolytes, capacity curves are calculated and the results are plotted in Figure 33.

While the intersection of isotherms often varies, it is found that in calculating capacities the minimum is nearly identical at the same pH for all salts and ionic strengths. The sodium perchlorate titration in Figure 8 shows, for instance, a displacement at 10^{-1}M which can easily be explained by a non-detected variation in the junction potential of the reference electrodes or other surface contamination of the glass electrode. When calculating differential capacities for that particular curve the minimum again corresponds to the pH of intersection of the other isotherms.

The specific influence on adsorption of various counter-ions is barely visible at low ionic strength where diffuse double layer theory represents a good approximation. In general, adsorption is larger at negative potentials with sodium and lithium salts than it is at positive potentials, while capacity curves for cesium nitrate are nearly symmetrical around the zpc. To illustrate specific effects of ions, capacity curves at 0.1M for these salts are superimposed in Figure 34. Figures 34a illustrates the effects of cations while Figures 34b, the effects of anions.

As can be seen, anions show very little specific effect; the negative arms of the capacity curves coincide within experimental error, as expected, since the cation in the counter charge, sodium, is common to all electrolytes.

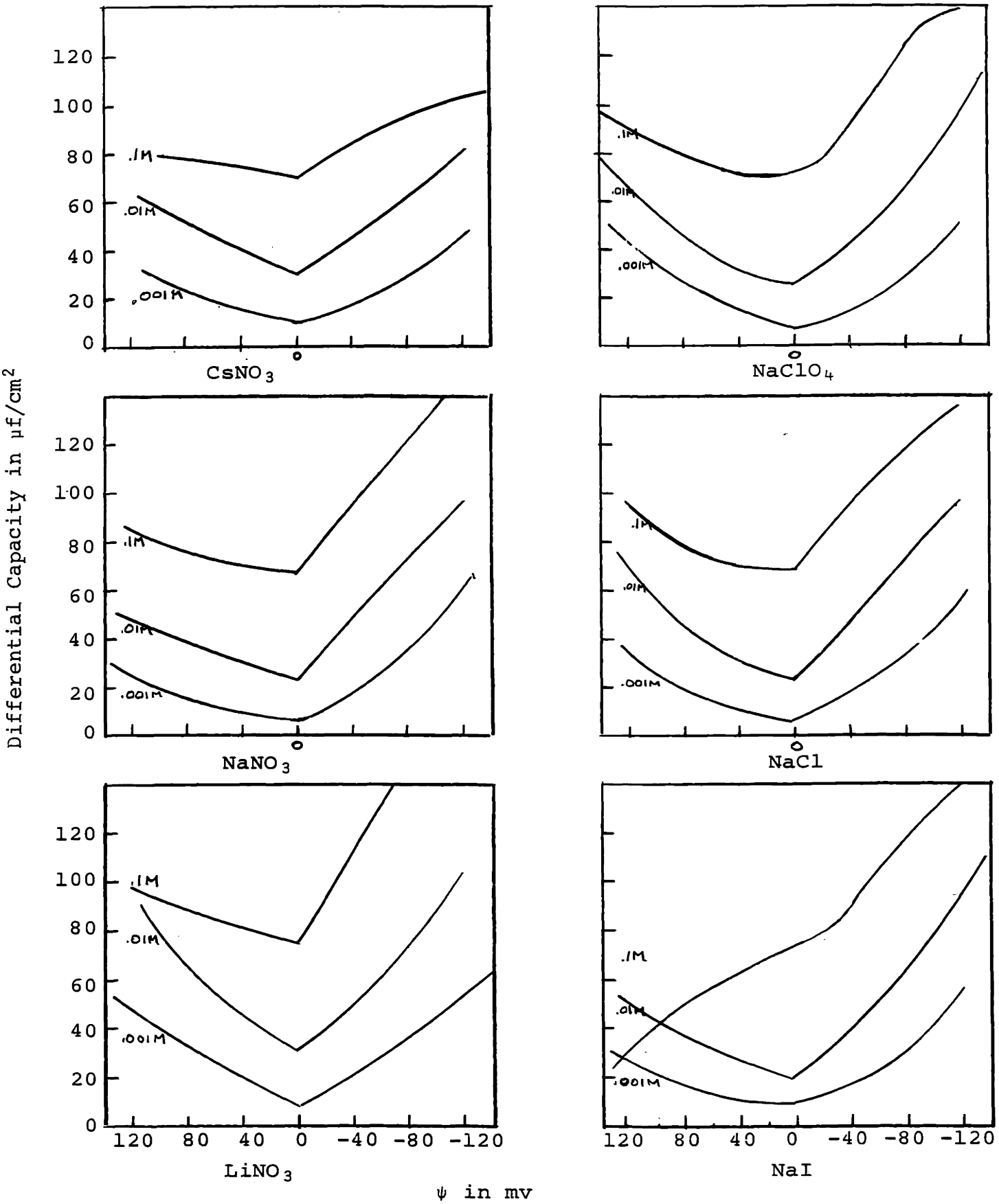

FIGURE 33. DIFFERENTIAL CAPACITY OF THE RUTILE-SOLUTION INTERFACE FOR VARIOUS SALTS.

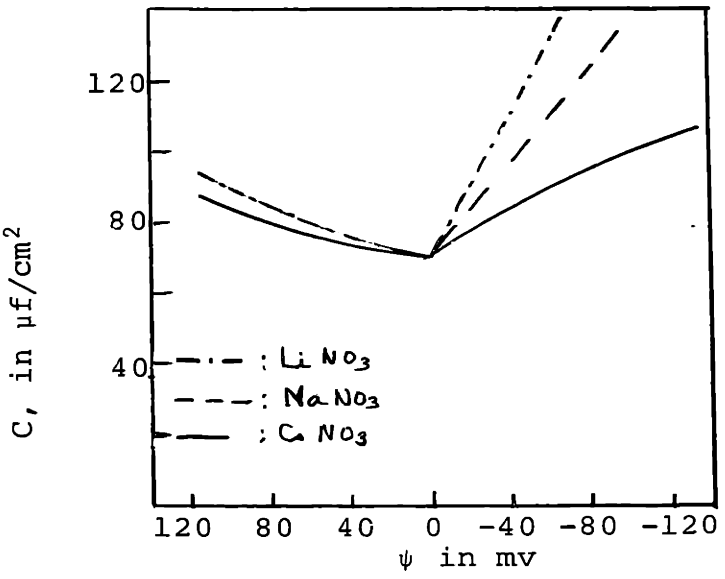

Figure 34a. Superposition of 0.1M Differential Capacity Curves for the Nitrate Salts.

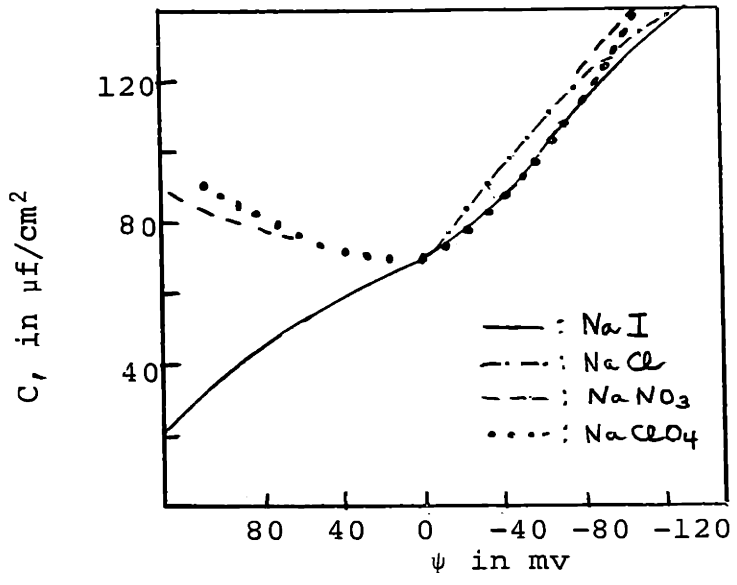

Figure 34b. Superposition of 0.1M Differential Capacity Curves for the Sodium Salts.

FIGURE 34. SUPERPOSITION OF 0.1M CAPACITY CURVES.

On the positive arm of the capacity curves, only iodine presents some interesting features. Despite the fact that the iodide curve is probably slightly exaggerated on this particular set of data, the effect is nevertheless real and shows one of the best examples of asymmetry in capacitance that can be found in a reversible interfacial system. The behavior here is entirely reversed from that of mercury and silver iodide; the sodium is now specifically adsorbed while the iodine is simply crowded out of the plane of charge. In view of our discussion of the inner capacitor at the interface of rutile, one would expect that as ions become bulkier and do not hydrate readily they find little space in the hydrated layer of the oxide and that at high charges and high ionic strengths the inner capacitor would decrease quite fast. As iodine is more spherical than other bulky oxyanions, it cannot as easily provide the polar group which would penetrate the surface layer. For that reason, it is probably kept outside the surface layer and one experimentally finds a decrease in total capacity.

The effect of cationic specificity is also reversed from what is considered usual. On mercury, the cesium with zero[51] affinity for water of hydration comes close to the surface and is specifically adsorbed. On rutile, cesium (1.70Å) is bulkier than sodium and finds, therefore, less place inside the interface. However, it is of the same size as chloride which we also find can penetrate the lattice. One, therefore, expects cesium to behave similarly to anions. The interesting

symmetry of the capacity curves obtained in the presence of cesium nitrate implies if one assumes no specific adsorption of NO_3^- that the same holds for Cs^+. Since we have shown that negative inner capacities, as in the case for sodium nitrate isotherms, must be explained in terms of specific adsorption, it is, therefore, not entirely by the difference in sizes that the specific cationic effect can be explained.

We now come to the explanation of specific adsorption on rutile. While Conway and Bockris[51,51b] have advocated decreases in tendency to hydrate, to explain the tendency for ions to be bound to the interface of mercury, it is argued that the reverse holds for the rutile interface and probably for all hydrated oxides. The reverse order is experimentally obvious in Figure 34a where capacities are higher at negative polarization of the interface for the most strongly hydrated cation, lithium, and decrease with decreasing hydration in going to sodium and finally to cesium. This can also be justified on the basis of the model.

The interface can be looked upon as a water phase ordered in some ice-like structure with little thermal motion. In solution, when water molecules hydrate a cation, there is a net loss of translational degrees of freedom. This loss comes about as the individual translations of the water molecules are limited to the translation of a single complex. There is a net decrease in total entropy compensated by the binding energy and some smaller increases in vibration entropy. This

hydration of the cation can be best achieved inside the hydrated surface layer. In this ice-like phase, water molecules have already no translational freedom and they will not loose any significant entropy in binding with the sodium ion. It is clear that a net loss in free energy is achieved by specifically adsorbing cations since for a constant energy gain due to hydration there is a smaller loss in entropy when hydration occurs at the interface. It is also clear that a constant energy gain has been assumed in having the cation hydrate at the interface instead of in the solution. At the zpc, from our discussion of the electrostatic bond in the water phase of the surface, it appears that bringing sodium ions at the interface would increase the electrostatic energy in contradiction with our postulate of constant energy of hydration. It is probably for that reason that cations do not adsorb at the zpc but require instead a net negative surface charge to be favorably attracted by the interface. If this reasoning is correct, specific adsorption would increase with hydration tendencies. This is exactly what is observed, specificity in adsorption increases in going from cesium to lithium. For the same reason, non-hydrated ions must force their way through a hydrated layer before they can strongly feel the crystal field effect and they will be less specifically adsorbed. For that reason, anions show little specificity outside a dimensional effect, as in the case of iodide. The same hold for cesium.

If it is recalled that no slow step could ever be

detected on the positive side of the interface, it supports the idea that the slow step takes place because of an interaction ion-surface and it can happen only with ions that have a tendency to bind with the interface; that is, the hydrated cations.

(iii) Influence of Temperature. Four sets of isotherms at 25°C, 50°C, 75°C and 95°C are given in Figures 10, 15, 16 and 17. At the time of these experiments, the system was not fully understood and these experiments were intended to study changes in specific adsorption with temperature. Two interesting observations were made; a displacement of the zpc and a small change in adsorption.

The lowering of the zpc is tabulated below against temperature and against the dissociation constant for water.

Temperature	zpc	pKw
25°C	pH 6.00	14.00
50°C	5.67	13.27
75°C	5.50	12.67
95°C	5.35	12.24

The displacement in zpc with temperature is not readily predictable. From the table, it appears that the pH is displaced in the same direction as pKw; the point of water neutrality goes from pH 7 at 25°C to pH 6.12 at 95°C, a shift of 0.88 pH units. At the same time the zpc or point of surface neutrality is shifted by 0.65 pH units. From this difference it might be intuitively concluded that the specific affinity

of the surface for hydrogen and hydroxyl ions has somewhat varied with temperature; if the affinity was constant, the zpc would always correspond to the same ratio of potential-determining ions in solution and would shift with the dissociation constant of water. A tentative thermodynamic analysis might go beyond this intuitive reasoning.

First, we consider the reactions at the interface

$$H^+ \ (L) \rightleftharpoons H^+ \ (i) \tag{19}$$

$$OH^- \ (L) \rightleftharpoons OH^- \ (i) \tag{20}$$

where "L" stands for liquid phase and "i" for interfacial phase. We consider equation (19) and write,

$$\bar{\mu}_{H+} \ (L) = \bar{\mu}_{H-} \ (i) \tag{6}$$

With the help of the already derived equations (6), (8) and (11) and introducing the constant χ potential into the standard chemical potential of the ion on the surface, as this is simply equivalent to defining another standard state, we write

$$\mu^{\circ\prime}_{H^+} + F\psi = \mu^{\circ}_{H+} \ (L) + RT\ell na_{H+} \ (L) \tag{21}$$

An activity of unity is implied for the surface ion since we postulate that its chemical potential is constant. The same holds true for equation (20), and,

$$\mu^{\circ\prime}_{OH-} \ (i) - F\psi = \mu^{\circ}_{H+} \ (L) + RT\ell na_{OH-} \ (L) \tag{22}$$

At the zpc, where $\psi = 0$, we write,

$$\left[\mu^{\circ 1}_{H^+}\ (i) - \mu^{\circ}_{H^+}\ (L)\right] - \left[\mu^{\circ 1}_{OH^-}\ (i) - \mu^{\circ}_{OH^-}\ (L)\right]$$

$$= + RT\ \ell n \frac{a_{H^+}(L)}{a_{OH^-}(L)} \qquad (23)$$

or

$$\left[\Delta\mu^{\circ}_{H^+} - \Delta\mu^{\circ}_{OH^-}\right] = \frac{-RT}{2.3}\ (pH - pOH)_{zpc} \qquad (24)$$

Making use of the integrated Gibbs-Helmholtz equation, we write

$$\frac{R}{2.3}\ (pH - pOH)_{zpc} = -\left[\Delta H^{\circ}_{H^+} - \Delta H^{\circ}_{OH^-}\right] 1/T + K\ . \qquad (25)$$

In Figure 35, $(pH - pOH)_{zpc}$ at different temperatures is plotted against 1/T and the slope is determined by connecting the two end points because at these temperatures, at least three independent measurements of the zpc were made. A value of 625 calories per mole for the enthalpy difference in the adsorption of H^+ and OH^- is then obtained.

But we would like to predict the temperature dependence of the zpc and obtain $\left[\Delta H^{\circ}_{H^+} - \Delta H^{\circ}_{OH^-}\right]$ directly. This may be done in the following way. On introducing the value for $(pH - pOH)_{zpc}$ in equation (24) at room temperature, a value of +520 calories per mole is obtained for $\left[\Delta\mu^{\circ}_{H^+} - \Delta\mu^{\circ}_{OH^-}\right]$ corresponding to a value of $(pH - pOH)_{zpc}$ equal to 2.0. It might be suggested that, in the transfer of ions to the surface, the change in entropy is

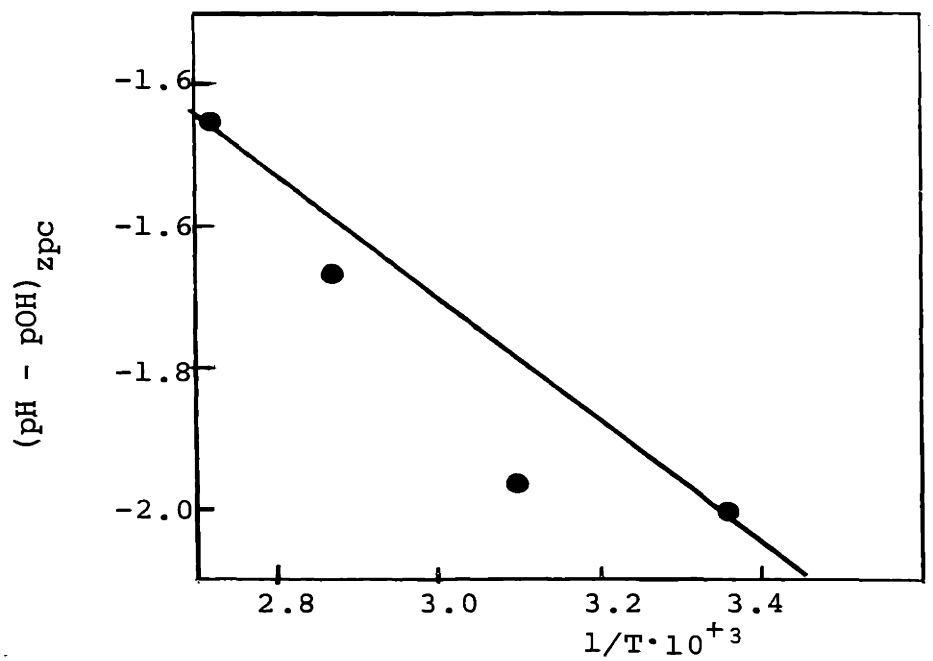

FIGURE 35. INFLUENCE OF TEMPERATURE IN THE ZPC OF RUTILE.

almost identical for various ions; changes in entropy involve a loss of translational degrees of freedom with a minor compensation in vibrational entropy. For that reason, one would expect the enthalpy change to follow closely the chemical potential changes. We find 625 calories for the enthalpy difference as opposed to +520 calories for the chemical potential changes. The difference of 105 calories is indeed quite small and we might like to assume the same of all oxides and presume that values for $\Delta(\Delta\mu^\circ)$ obtained from the determination of the pH of the zpc could be used as a rough approximation to predict the dependence of the pH of the zpc on temperature, as describedby equation (25). The difference of 105 cal cannot be assumed significant because of the experimental error (~0.1 pH unit) and it may, therefore, be concluded that the entropy change is zero or very small.

The fact that for rutile ($\Delta\mu^\circ_{H^+} - \Delta\mu^\circ_{OH^-}$) is such a small quantity might point to the existence of a water phase on the solid which behaves very similarly to liquid water. However, this cannot be proved from our thermodynamic reasoning as we deal with differences in $\Delta\mu^\circ$'s and not $\Delta\mu^\circ$'s themselves. We will now study the temperature effect on adsorption.

A direct comparison of changes in adsorption with pH at different temperatures may lead to wrong conclusions. The relationship between pH and potential at the surfaces follows, at least in theory, the Nernst equation (13). Any changes in temperature will modify the Nernst slope and to be consistent, one has to plot adsorption densities against potential.

This was done on Figure 36 where all the adsorption results at different temperatures are combined in one graph with a common intersection point. The data is considered quite accurate but still the scatter makes comparisons difficult. On the negative side where specific adsorption is reported, the effect of temperature is negligible within experimental error. It might be reasoned that the forces binding the ions are strong enough not to allow the effects of slight temperature changes to be felt. It could also point to the inapplicability of the Nernst equation to oxides though from what follows, this seems unlikely.

On the positive side, one may report what seems a definite trend towards lower adsorption with temperature, especially at 95°C. It is reasoned here that since there is no specific force holding the counterions at the interface, increases in thermal agitation show the effect predicted by double-layer theory and support the assumption of applicability of the Nernst law to the potential at the interface. At 0.01M, an increase in adsorption of some 20% is observed between 95°C and 25°C, while diffuse double layer would roughly predict also an increase of 20% at low potentials (below 50 mv) because of the $(1/T)^{1/2}$ dependence of σ (Equation (19)).

More accuracy will be needed if a strict application of the theory is desired but our rough approximation may be a clue to the applicability of the Nernst equation and would confirm the potential-determining role of hydrogen.

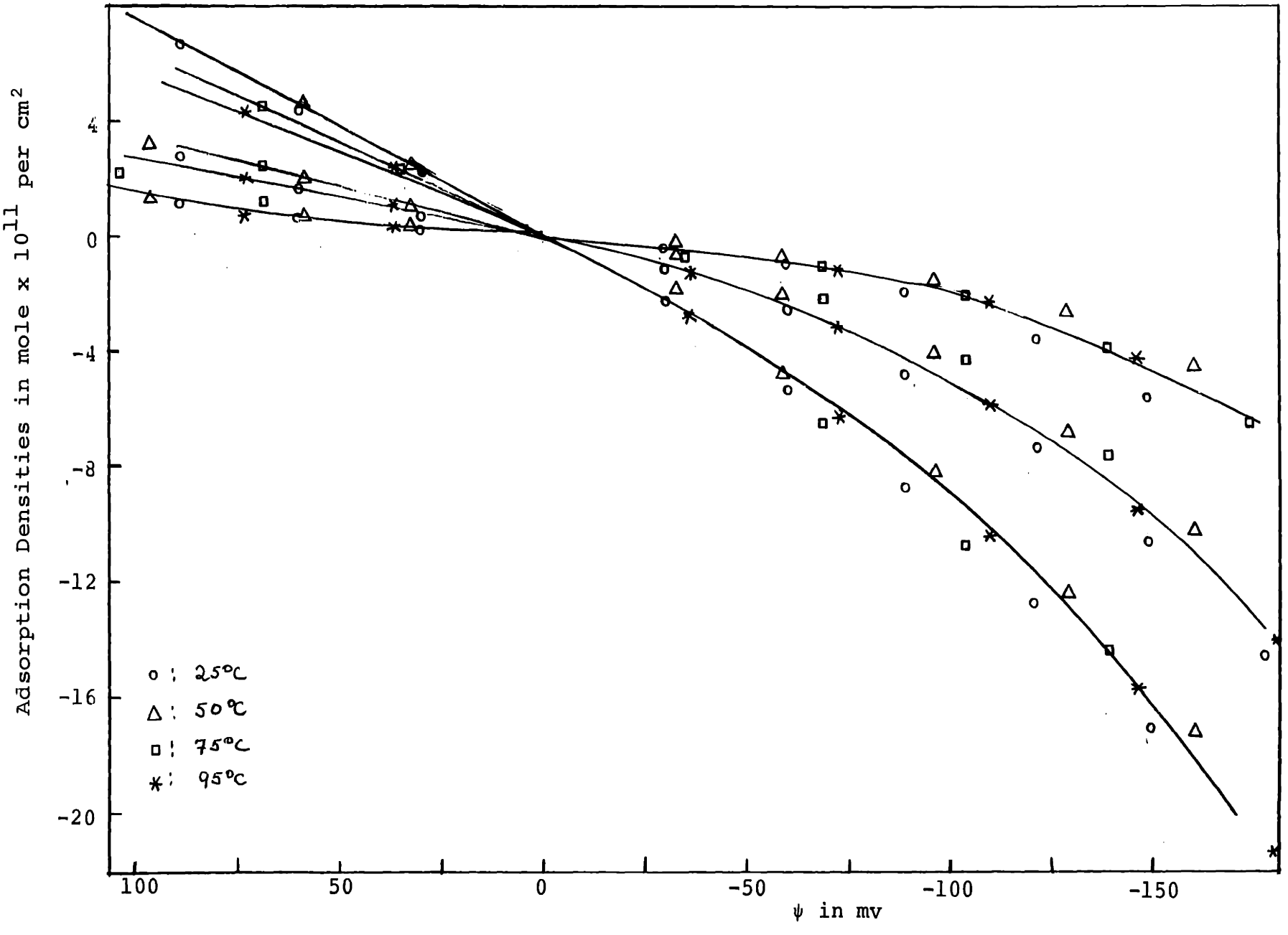

FIGURE 36. ADSORPTION ISOTHERMS ON RUTILE IN PRESENCE OF NaCl AT VARIOUS TEMPERATURES PLOTTED AGAINST ψ.

(iv) Influence of the Past History of the Surface. Methods of Preparation. It was pointed out earlier (page 6) that the ionic environment during preparation has an important effect on the crystal structure of TiO_2. Work by Rao[59] has related the transformation temperature of anatase to rutile to the presence of sulfate impurities in the lattice.

While precipitation of anatase in the presence of sulfate ions is no proof of ionic contamination of the lattice, the increase in transformation temperature from anatase to rutile is a clue to such contamination. Salamitou[32] indicated a transformation temperature of 700°C for anatase precipitated from a sulfate solution. This, according to Rao, would indicate sulfate contamination. No such studies were undertaken on our precipitate.

Blok[19] has shown that the nature of the mother solution was of a major importance in determining the zpc of ZnO. Comparison of Figure 18 and Figure 10 indicates no such effect on titania. The pH of the zpc has not shifted and the only difference between the two systems would consist in an increase in adsorption at constant pH and low ionic strength on the anatase interface. Adsorption densities may also be inaccurate because of errors in surface area determination. In this particular case, the very high value of 125 M^2 per gram could be somewhat in error.

This high area does not, however, explain everything. It will be noted that, if adsorption is too high at low ionic strength, it is, however, of a normal magnitude at 0.1M. Hence,

it is the relative spacing of isotherms which is to be explained, not the higher adsorption. Another possible explanation could be in the size of the particles. We discussed in the application of double-layer theory to isotherms obtained in presence of sodium nitrate the effect of particle size on the diffuse double-layer (see page 79). A surface area of 125 M^2 per gram is equivalent to an average radius of 60Å per particle or an equivalent q° of 0.5 to be introduced in equation (15) for a 0.001M concentration of salt in solution. The ratio 3.02/1.04 for the function I (0.05)/I (∞) would indicate in this case an increase of 300% in the minimum capacity over the value of 7 $\mu f/cm^2$ obtained for a planar interface, the predicted minimum capacity being now 21 $\mu f/cm^2$. The minimum capacity observed in the 0.001M concentration is approximately 23 $\mu f/cm^2$. It is, therefore, possible to explain the high adsorption at low ionic strength simply by introducing the concept of sphericity of the particles. This is, however, a maximum correction since we did not have electronmicrographs of the anatase precipitate to evaluate the particle shape and the correction could be somewhat too large.

Though it may not seem necessary after the preceding discussion, a third correction will also be offered. For a particle with a radius of 60Å, calculation of the predicted double-layer capacity for the 0.1 molar solution ($1/K = 10^{-5}$ cm) requires a 20% increase from the 72 $\mu f/cm^2$ calculated for a planar interface. The new corrected value comes to 86 $\mu f/cm^2$.

Double-layer theory predicts minima of 21, 44 and 86 $\mu f/cm^2$ at $10^{-3}M$, $10^{-2}M$ and $10^{-1}M$. By comparison with the experimentally observed minima of 23, 36 and 74 $\mu f/cm^2$, this shows an exaggerated correction factor at high ionic strength. If we increase the effective value of q° so as to lower the 0.1M minimum capacity, there remains the problem of the too low minimum for the 0.001 molar solution. Our discussion of the effect of conditioning on the fast isotherm has shown that any treatment of the interface at basic pH's lead to higher adsorption at 0.001M. This effect could play a role here since the precipitate was washed in ammonia before the titration. Because the surface does not readily recover from a conditioning at basic pH's, it is felt that part of the increased adsorption at low ionic strength is attributed to the past history of the surface.

By adding together all the effects due to errors in surface area, small particle sizes and past surface conditioning, it is possible to explain the type of adsorption densities obtained with anatase. It is felt that such variations in adsorption is not due to the different crystalline structure but to the other factors mentioned above.

Influence of Heat Treatment on the Rutile Interface.

Adsorption isotherms obtained on material evacuated at temperatures varying between 25°C and 425°C (Figure 19) for 20 hours are identical. In fact, this observation suggests that it would be worthwhile always to submit the surface to this treatment before diagnostic surface studies are made.

There is a possibility that foreign ions are released from the surface during the treatment, giving a better reproducible surface. This is specifically applicable to rutile because of indications of instantaneous rehydration.

A slight effect is felt for evacuations at 525°C; the zpc is lowered to pH 5.85 as shown in Figure 7. It was found, however, that the variation was not readily reproducible; a kinetic phenomenon is involved during evacuation which could form the object of a study by itself.

Evacuation at temperatures exceeding 425°C introduces complications. Already at 525°C reduction of the oxide can become a problem on an incompletely cleaned surface. Chessick and Hollabaugh[60] in a study of water adsorption on hematite report a modification of surface properties if the solid is not heat-treated in oxygen. Recent work by Parfitt[34] involving infrared spectroscopical studies on rutile, corroborates the observation of Chessick and Hollabaugh. To control reduction, heat-treatment at elevated temperatures was done both in air and a mixture of nitrogen and water vapor. There were no observed differences due to the ambient atmosphere and the data given applies to specimens heated in a nitrogen and water atmosphere.

As can be seen in Figure 20, the zpc has been drastically displaced to a value below pH 4. Johanssen and Buchanan[2] already noticed a decrease of zpc to a pH of 4.7 upon firing in air at 1000°C for two hours. More drastic treatments[5] at

975°C in a 10% hydrogen mixture with argon for two hours raised the zpc to 7.4. There seems to be two phenomena involved. Reduction under hydrogen atmosphere raises the zpc while simple dehydration will lower it. Parks[5] has suggested the following semitheoretical relation for predicting the zpc.

$$zpc = A - B\,(z/R - D\Delta F) \qquad (26)$$

A = constant
B = constant
D = constant
z = ionic charge of the lattice cation
R = $2\,r_o + r_+$ where r_o = ionic radius of oxygen
r_+ = ionic radius of lattice cation
ΔF = non-coulombic contributions to the hydrogen ion binding energy.

It is seen that reduction of the metal ion (decrease in z) increases the zpc. The effect of hydration is included in A where the radio of hydroxyl to non-hydroxyl oxygens appears. Evaluation of A is, however, mostly empirical and there is yet no satisfactory explanation for the effect of hydration on the zpc. Intuitively, it would seem reasonable to assume that removal of hydroxyl groups increases the repulsion between the cation and hydrogen and, if rehydration is not completely reversible because of surface reordering, the zpc will have shifted to lower pH values.

The material used for the titration given in Figure 20 was left in water after the supporting electrolyte had been washed away. Three months later, a titration was performed

on the material and it was impossible to observe any change from the previous isotherms (Figure 21). Some important conclusions may be drawn which will eventually contribute towards the overall understanding of the nature of the rutile interface. Only high temperature treatments can irreversibly remove water of hydration, we shall call it, water of hydroxylation. Furthermore, once removed, the surface does not rehydrate readily. This fact is corroborated by other workers[1,2,4] who report a lower zpc for rutile and never find a tendency for it to drift back to the hydrated value.

This supports the idea of very strongly bonded hydroxyls resulting in irreversibility whenever they are removed.

3. The Structure of Oxide Interfaces

A. Nature of Adsorbed Water on Rutile and Hematite

We have not yet attempted any explanation of the slow adsorption step on oxides. However, when the slow step was first observed on rutile, its characteristics had definite analogies with parallel results obtained on the hematite interface. There were also differences and a quantitative analysis of the type suggested by Onoda and de Bruyn[16] was not directly permissible. In fact, the data on the slow step in rutile would much better fit the experimental observations by Blok[19] on zincite as regards the reversibility of the isotherms, the magnitude of pH drift with time and the times necessary to reach equilibrium.

Onoda and de Bruyn proposed that the slow step represents the diffusion of protons in an out of the oxide lattice. It was rightly pointed out by the authors that hydrated layers of oxide are required as a source or sink of protons in the lattice. Furthermore, the diffusion coefficient of hydrogen must be compatible with theory. It is with this model in mind that tracer studies of the hydrogen distribution at the interface of rutile and hematite were undertaken. The nature of the interface would influence the rate of desorption of tritium from the surface of oxides. It must be said here that even in the absence of tracer exchange studies with hydrated surface of rutile some information would still be available on the rutile-water vapor interface. The accumulated knowledge about the nature of the oxide surface has been obtained from two distinct experimental approaches; tracer exchange studies and water adsorption studies (including infrared analysis).

(i) Quantitative Analysis of the Water at the Interface.

Water adsorbed at the interface of an anhydrous oxide is found firstly to dissociate on the surface into chemically adsorbed hydroxyls which in turn bind a second layer of strongly hydrogen-bonded water. This distinction is, however, somewhat difficult to establish experimentally and resistance to evacuation often serves as the criterion for deciding between the two types. In water adsorption studies for instance, Jurinak[38] used evacuation at 10^{-3} mm Hg and room temperature for 20 hours, Yates[33] evacuation down to 10^{-5}

microns, others[36,61,34] used similar criteria. However, Kipling and Peakall[35] showed the error introduced when applying evacuation resistance as the diagnostic criterion for rutile and other oxides. While studies by Blyholder[36] and Gregg[61] tend to agree with the above criterion as applied to hematite, Peakall suggests that 20 hours evacuation on titania is insufficient to remove physically adsorbed water; it will be achieved only after some 70 hours or more of evacuation.

Infrared spectroscopy can shed further light on the problems of defining chemisorbed water. Whenever the vibrational frequency of the OH group of all adsorbed water molecules can be detected without the presence of the bending frequency of the undissociated water molecule, the water molecule is said to be chemically adsorbed. That is, as Yates[33] points out, provided the bonding of the water does not displace the bending frequency beyond the frequency range under study. Infrared analyses by Yates and by Parfitt[34] on rutile are in essential agreement. For 20 hour evacuations at 150°C, they showed that some of the molecular water was removed but not all. At lower temperatures, none at all was removed. It might be suggested here, in view of Peakall's results, that longer evacuation time could modify the conclusions of Parfitt and Yates. When evacuating at temperatures above 300°C, all molecular water is removed and some of the hydroxyls start coming off. Parfitt further refines the picture by showing that hydrogen bonding takes place between hydroxyl groups. Similar work with

hematite[36,60] indicates the same mechanism except for the fact that the molecular water is much more loosely bonded.

From this discussion, it may be concluded that adsorbed water would form a hydroxylated layer at the interface. To this layer would be attached some strongly hydrogen-bonded molecular water. Evacuation at room temperature for 20 hours is sufficient to remove the molecular water on hematite while it is not expected for rutile. Moderate temperatures of evacuation (below 350°C) remove hydroxyl groups from the hematite surface while it takes drastic treatments (450°C) to do the same on rutile. When water adsorption studies of Jurinak[38] (Fe_2O_3 and TiO_2), Chessick[12] (Fe_2O_3) and Gregg[61] (TiO_2), are interpreted in terms of the above model, it is found that water of hydroxylation forms one monolayer, with each hydroxyl group occupying 15.4Å^2, while the molecular water occupies 23.5Å^2; that is, one molecule of water adheres to two hydroxyl groups. It is not known whether precipitated rutile would also contain some water in the lattice.

(ii) Lability of Surface Protons. The next question to be answered is related to the lability of the protons on surfaces of oxides. From a purely theoretical point of view, it can be said that tritium would exchange rapidly with protons on oxides. Rutile illustrates this point. Because of the strong titanium-oxygen bond, the proton on the surface is certainly less tightly held by comparison with that in water. The resonance time of a water molecule is about 10^{-13} sec[62];

hence, exchange of hydrogen between hydroxyl groups of free molecules is very rapid. It can be imagined that the rate of exchange on the surface would also be rapid. The presence of free electron pairs in the hydroxyls favors the associative exchange[63] which has a very low activation energy, hence a fast exchange rate. Such an exchange is described by the following scheme:

$$H:O:H + T:O:T \rightarrow \begin{matrix} & H & \\ & | & \\ O:T:O:T & & \end{matrix} \rightarrow TOH + TOH$$

However, the assumption that rates of exchange at the surface and in the solution are similar needs to be scrutinized more closely. The hydroxyl group is strongly bonded to the surface in a tight monomolecular layer which offers some steric hindrance to the necessary associative hydrogen exchange. A strong dipole orientation of the hydroxyls on the surface could also repel any incoming proton and slow down the exchange, as implied by the electrostatic nature of the hydrogen bond to the adjacent water molecule[62]. It is quite possible that in such a case, exchange would have to proceed through a dissociative mechanism of the type described below.

$$(O:H) + T:O:T \rightarrow (O:) + T + H + :OT \rightarrow (O:T) + H:O:T$$

This mechanism is much slower because of the high energy of activation involved.

Exchange studies with radioactive tracers have been performed on the surface of oxides. Kiselev[64], who pioneered the application of infrared spectroscopy to oxide catalysts, has also studied the exchange of deuteriated water with surfaces of silica and silica-alumina. The exchange when performed at 250°C is rapid and this technique was, therefore, used to analyze quantitatively the presence of hydroxyl groups on those catalysts. Aldeman and Emmett[65] went to lower temperatures on the same catalysts and found complete exchange within three hours at 110°C. One of their interesting conclusions was that isotope effects were insignificant. Finally, Yates and Parfitt could, at 250°C, exchange deuterium with the hydroxyl groups on rutile and follow the displacement of the frequencies in the OD bond. In fact, at those high temperatures, even surface oxygens are labile[66].

The only clue to the effect that exchange of deuterium could be slower on rutile comes from Parfitt's work, where 12 hours at 250°C may be necessary for an exchange which never goes to completion anyway. Furthermore, contacting a surface with D_2O vapor at room temperature did not seem to give any exchange that would lower the frequency of the hydroxyl groups. Insufficient experimental data did not, however, warrant in his opinion any conclusion. Similar conclusions could not be drawn from Blyholder and Richardson's studies of the hematite interface.

In conclusion, it would seem that evacuation at room temperature cannot remove hydroxyl groups on rutile. Exchange

of deuterium either as a gas or as a water vapor proceeds to quite an extent at 250°C but is not complete. No definite experimental work has shown that deuterium would exchange at room temperature on the rutile interface. It should also be said that it is never possible to relate directly quantitative removal of water by evacuation to observable infrared spectrum modifications, as the two experiments are done independently and under conditions often different. This introduces an element of uncertainty in the interpretation of the results.

With the assumption of fast surface exchange, one can proceed to analyze desorption from a hydrated phase. Berthier[67] gives a complete treatment of the exchange of radioactive tracers between solids and solutions. His theoretical calculations are successfully applied by Feitknecht[68] to the desorption of tritium from a tritiated goethite and nickel hydroxide. In the systems of interest, rutile and hematite, we want to determine the existence and extent of hydrated layers inside the oxide lattice. As described under experimental work, the oxides are first tritiated by contacting them at 129°C for a month.

B. The Rutile Interface

(i) Tracer Exchange with Rutile. We will first discuss the results obtained on rutile. Figure 22 gives the typical desorption curve at room temperature after 24 hours of evacuation. Actually, no changes were observed when desorbing at 95°C. There is little need to describe the results. The

tritium-tagged water exchanged instantaneously with the solution. If we assume a cross sectional area of 15.4$\mathring{A}^2$ for surface hydroxyls and 23.5$\mathring{A}^2$ for the strongly bound water, two layers of water would give 0.015 ml H_2O/g of precipitate (specific area assumed equal to 50 M^2/g). Since 24 hours evacuation essentially leaves 0.0152 ml of water, there appears to be a good agreement with the prevailing opinion that evacuation at room temperature leaves essentially two layers of adsorbed water after 20 hours on rutile.

But had we prolonged evacuation, it is clear from Figure 23 that the amount left would have decreased to zero, where the zero point is determined by the limit of experimental accuracy, 5 μmolesof hydrogen. This is a surprising result. Either all surface hydroxyls are removed by room temperature evacuation or tritium never exchanged with the surface hydroxyls. The first statement is contrary to the conclusions of our discussion on chemisorption of water, the second possibly in contradiction with infrared studies of the lability of surface protons.

Figure 23 represents a well established observation reproducible under various experimental conditions. There is also little room for experimental error. The procedure is deceptively simple. After equilibration in very active tritiated water (1 mc per cc or 2.2×10^9 dpm while the average concentration in water at desorption is of the order of 2×10^4 dpm), the sample is placed still wet in an evacuator kept at a pressure

of 10^{-3} mm of mercury. When evacuation is completed, the sample still under vacuum is frozen at liquid nitrogen temperature to stop any further exchange with the atmosphere. It is brought to atmospheric pressure and immediately transferred to the effusion cell. Since vacuum was always maintained over the specimen before desorption and because there are no obvious causes of experimental error, the results leave only two choices; either hydroxyls are left intact after 100 hours of evacuation and, therefore, our results prove that they are non-labile, or they are removed by simple evacuation. Because infrared analysis of the rutile surface indicates that hydroxyls are especially tightly bonded and because the possibility of the non-lability of these hydroxyls has not been disproved to complete satisfaction, it is felt that the alternative of non-lability of protons at the rutile interface is a better warranted conclusion. Particularly so because the oxide is fully hydrated and should, therefore, bind its hydroxyls more strongly. It will be recalled that when discussing heat-treatment effects, evacuation at temperatures up to 425°C had no effect on the surface and only heat-treatments at 800°C lowered the zpc, such a lowering being interpreted as a loss of water of hydration. These conclusions were in general agreement with the work done by infrared analysis of the rutile interface, that is, water is tightly bonded to the surface. It is, therefore, felt that a combination of isotopic effects, low temperatures of exchange and non-lability of the hydrogen on the surface makes exchange at the interface too slow to be

observed. Such a conclusion has some very important implications with regard to the model of the interface proposed in Figure 32. If protons of the hydroxyl groups are non-labile, it is clear that the surface charge cannot be the result of a dissociation of the latter. The model is greatly strengthened by this added support which had already been suggested by the results of heat-treatments.

(ii) Interpretation of the Slow Step in Adsorption.

In the discussion of the kinetics of adsorption, the behavior of the surface was characterized well enough to permit the determination of reversible and fairly reproducible fast isotherms. No attempts were made to interpret the results for lack of sufficient information at the time. With all the experimental results on rutile now analyzed, we can attempt to understand the mechanism of slow adsorption at the rutile interface.

Some Past Interpretations of the Slow Step. Since rutile is not the only oxide to behave kinetically in the way showed, we first review some of the recent ideas on the subject of slow steps in adsorption. To interpret the slow process on hematite, Onoda and de Bruyn[16] divide the interface of hematite into four layers, anhydrous oxide, hydrated oxide, hydroxylated layer at the solid-solution interface and the adjacent solution, see Figure 26. According to these authors, the instantaneous adsorption of potential-determining ions occurs in the hydroxylated layer. A given pH (the pH of the zpc) fixes the point of zero excess charge on the surface;

away from the zpc, the surface charge creates a concentration gradient in the hydrated layers of the oxide and protons diffuse in or out depending on the sign of the charge. This is the proposed slow process. During this process, the surface charge is assumed to remain constant; it does this by taking or releasing protons to the solution. Now, changing the pH back to the zpc will again yield a zero charge on the surface, but because of mobility problems protons may be trapped inside leaving a net total charge on the solid. The pH of the zpc at the surface is not affected by conditioning, only the i.e.p. is displaced away from the zpc (where i.e.p. has been defined as the point of zero zeta potential).

To explain a similar slow step in adsorption on alumina, Korpi ignores the diffusion possibility but looks instead at the alumina interface as an ampholytoid, an interpretation that was also suggested by Albrethsen[13] for the hematite interface. This ampholytoid is characterized by some acid groups with a dissociation constant Ka and some basic groups with a dissociation constant Kb. These constants added to the dissociation constant of water Kw will determine the pH of the zpc. (Korpi uses the terminology IEPS.) The fast adsorption of potential-determining ions comes about through the dissociation of these ampholytic groups as a function of pH. The slow step in adsorption can then be explained by a slow exchange of counterions with the surface radicals of the same sign. The reaction interacts directly with the dissociation constants of

the surface so as to displace the zpc.

One could questions the applicability of this model to the fast isotherm on the basis that there is no expressed dependence of adsorption on ionic strength and that the effect is taken into account either through the dissociation constants themselves or through some helpful activity coefficients. Also, in writing equilibrium constants based on standard chemical potentials, the influence of electrostatic potential is ignored or simply fed into the activity coefficient as an exponential term. In fact, whenever a reaction is written between two phases kept at different electrostatic potentials, a strict application of thermodynamics to ions requires the use of electrochemical potentials and any resulting equilibrium constant includes both the standard chemical potentials and the electrostatic potential difference between the phases. However, the proposed model has the advantage of not requiring hydrated layers to operate and, furthermore, at the zpc where a constant potential is the only potential difference involved, there is no absolute need for using electrochemical potentials as we show in section V.2.C(iii), and Korpi's treatment would be valid.

Applications to Rutile. As regards the interpretation of the slow step on rutile via a diffusion mechanism, the results of tritium exchange with the same interface leave no uncertainty. The step-increase in effusion of tritium from the surface indicates that either the hydrogen is completely labile, hence

reacts instantaneously with solutions, or it is completely non-labile, hence there is no slow step of any short. Our experimental results though they do not identify, beyond doubt, the right alternative, at least indicate that diffusion of hydrogen into the lattice cannot explain the slow step.

It is certainly unsatisfactory to propose only negative answers to the problem, but coming up with a positive explanation to as complicated a phenomenon as the slow adsorption, on the basis of so little information, is also quite risky. We can only hope to clarify the conditions of the slow step and suggest some possible mechanism.

To do so, we must sum up all the past results on rutile and draw some of the consequences. It should be clear by now that the model of the interface has some support in the experimental results. Double-layer theory seems to apply reasonably well to the interface; magnitudes of adsorption, effects of temperature, influence of particle size, specific influences of counterions, all blend into a harmonious picture which is further corroborated by the effect of heat-treatment on the zpc and the non-lability of surface hydroxyls. For all those reasons we will accept, for the time being, this model as being a good representation of the interface. If we now recall the fact that the slow step in adsorption is uniquely observed for negative surface charges where sodium is specifically adsorbed, and if we recall the passivity of all anions because of the water shield on the surface, we are tempted to look into this property of the cations as the

possible explanation for the slow step. We are attracted by Korpi's interpretation of an ion exchange between the surface and the solution.

There is little evidence of ion exchange in general with the rutile interface. Zabrova and Egorov[69] did review most work on ion exchange with oxides but they do not report any results on the slow abstractive properties of oxides. In most of the reviewed work, there is often an ambiquity as to whether exchange really takes place or whether it is simply an accumulation of counterions in the diffuse double-layer; this is particularly apparent when exchange of cations is reported at basic pH's and exchange of anions at acid pH's[70,71]. Some specific adsorbability of ions is clearly illustrated for alumina[72,73], but none is reported on titania[56].

Hence, the only knowledge we have of any specific affinity of the titania for some cations comes from our results described in the analysis of the effects of electrolytes on the adsorption of potential-determining ions. In the proposed model, through a fast reaction, the hydrated cation first adsorbs in the molecular plane of charge (Figure 32, plane C). The cation, now much closer to the hydroxylated layer, could interact with those surface hydroxyls either to replace a hydrogen (ion exchange), which would at the same time release a hydrogen bond between the molecular water and a hydroxyl, or to complex with the hydroxyls (penetration into the hydroxylated layer) or both. Intro-

ducing positive charges in the lattice of the surface would repel positive charges on the surface or require a low solution pH to reach the zpc. In terms of an ion exchange treatment, this means a lowering in affinity of hydrogen for the surface or a lowering in Ka. It would result in a new intersection of isotherms at more acid pH's which is in agreement with experimental observation.

The slow rate of exchange would be explained by the high activation energy required to break the strong hydrogen bond or to insert the cation inside the hydroxylated layer. This explanation remains highly speculative and further experimentation will be required if the whole process of adsorption at the interface were to be understood.

C. The Hematite Interface

(i) Tracer Exchange. The case is quite different for the hematite system. Although the same experimental procedure as used for rutile was followed, the desorption of tritium is seen to follow quite a different pattern. There is a definite slow exchange which follows the initial step increase. Figure 24 gives such an effusion curve obtained after some 100 hours of evacuation.

The effect of varying the evacuation time on the tritiated hematite was not studied in as much depth as on rutile. In general, it was found that the amount left on the solid after 24 hours did not change very much with longer evacuation time. When it was found that 100 hours

was sufficient to remove all excess tagged water in rutile, a similar treatment was then followed for hematite. If we rely on accepted ideas, the physisorbed water is less tightly bonded on hematite than on rutile. One would have expected this time even less tritium left on the solid. It does not turn out that way. On Figure 24, curve A refers to room temperature desorption, while curve B describes desorption at 95°C.

If we look at the room temperature desorption, we can delineate three steps, a fast instantaneous equilibration, a medium fast exchange which takes some 60 hours followed by a very slow exchange. The total amount of water involved in the hydroxylated layer can be calculated. Using a surface area of 15.5 M^2 per gram obtained from krypton adsorption measurements and a value of 15.4$\mathring{A}^2$ as the parking area of hydroxyl groups on the hematite interface, we calculate 0.00291 ml of H_2O per gram as hydroxylation water. The agreement is almost too good to be true when compared with the fast surface exchange of tritium, 0.00292 ml/gram.

We can draw the immediate conclusion that the BET equation as applied to hematite gives an accurate determination of the magnitude of the surface which is in immediate contact with the solution. We, therefore, accept the proposition that evacuation has left on the surface essentially all hydroxyl groups and no more (as predicted from our previous discussion) and that these groups are labile.

The interpretation of the tail of the effusion

curve is certainly more difficult. Comparing curves A and B (Figure 24) reveals that the "medium fast" process is accelerated with temperature to the point of disappearance at 95°C. For that reason and also because high temperature experiments are somewhat more difficult to perform (due to evaporation of the water in the cell and the impossibility to stir while the sample is in the oven), it is not possible to analyze such a curve. Feitknecht reported that surface exchange could involve up to 4.5 layers at high temperatures before the reaction becomes diffusion-controlled. In our case, because of the small amount of water involved when the surface exchange becomes too large, it wipes out diffusional phenomenon and it becomes difficult to interpret the data quantitatively.

Berthier[67] derived the diffusion rate equation for the diffusion of tracers out of thin plates. Berthier's treatment will be applied to the diffusion of tritium out of a thin layer of hydroxide on the surface. His derivation yields as a final solution,

$$\frac{M_t}{M_\infty} = \frac{2}{\sqrt{\pi}} \left[\frac{D \cdot t}{\delta^2}\right]^{1/2} \qquad (27)$$

where

M_t = amount of tritium desorbed at time t
M_∞ = amount of tritium desorbed at t = ∞
D = diffusion coefficient in $cm^2/sec.$
t = time in seconds
δ = thickness of the exchanging layer in cm.

The equation fits well the results obtained on bulk particles of goethite[68] where the surface concentration is small with regard to total amount of tritium in the solid. In our case, it is not easily seen where exchange is diffusion controlled and where it stops being so. Since the long slow ascent of Figure 24 does fit reasonably well a $t^{1/2}$ dependence, when replotted as in Figure 37, the question is now: what value for δ and M_∞ should be introduced in the equation?

An approximate value is obtained in the following way. The total amount of water M_∞ is obtained by subtracting the amount of hydroxyl groups from the total exchange at 95°C (0.0118 - 0.00291= 0.0089 ml of H_2O in the solid). This water is assumed to exist in the lattice in the form of goethite according to the reaction

$$Fe_2O_3 + H_2O = 2\ FeOOH \quad . \qquad (28)$$

Thus the total amount of FeOOH is calculated. With a given density[74] of 4.28 and a surface area of 15.5 M^2, the depth of this layer is calculated to be 13.3Å.

From Figure 37, the slope (ml/g/$C^{1/2}$) is read and divided by 0.0089 to express the diffusing quantities as M_t/M_∞ . Replacing δ in equation (27) by the value of 13.3Å just calculated, D is calculated and is found to be equal to 2.4×10^{-21} cm^2/sec. On the same material Onoda could from his data evaluate a diffusion coefficient of 3.5×10^{-21} cm^2/sec. The agreement is good but one would have expected a lower

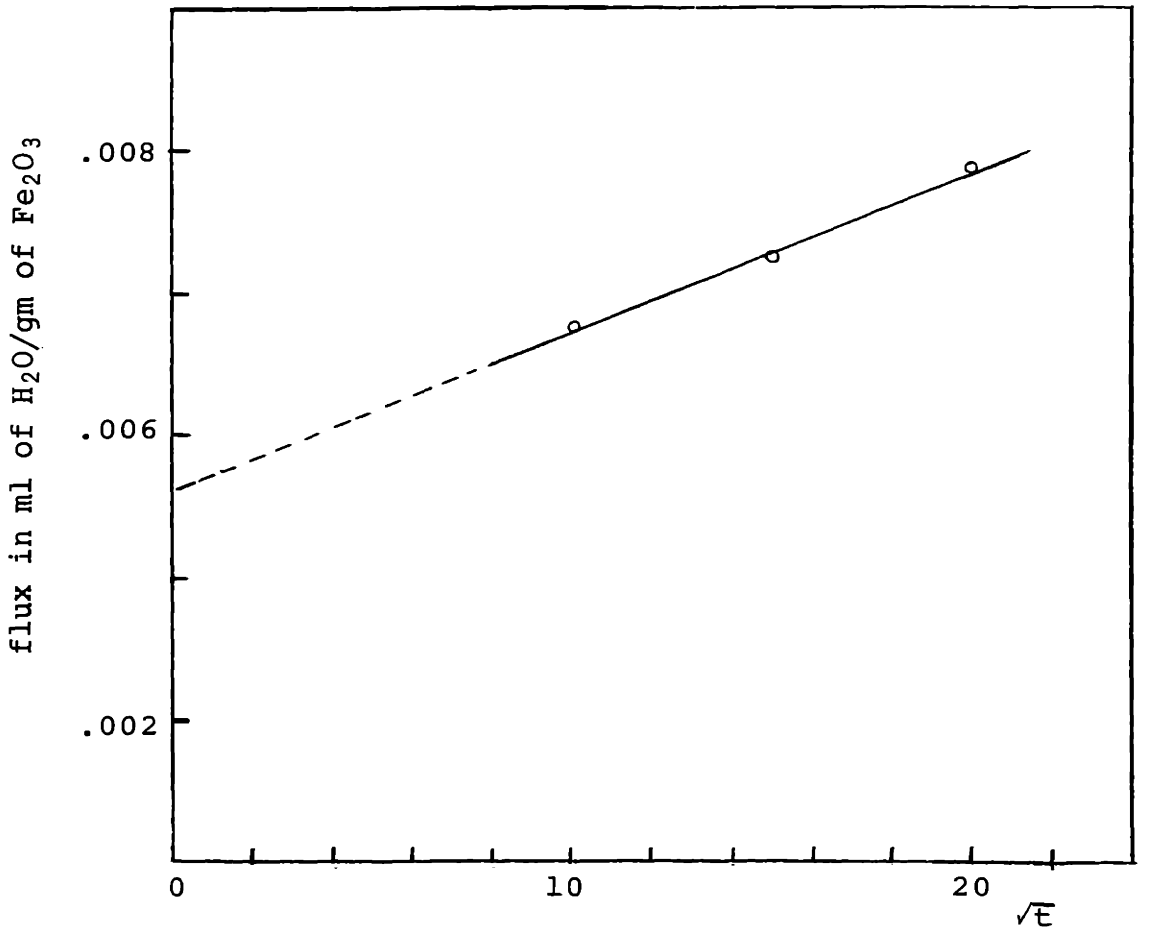

FIGURE 37. EFFUSION CURVE OF TRITIUM FROM THE HEMATITE INTERFACE (Curve 24) REPLOTTED AGAINST $\sqrt{t}$.

value for tritium simply because of the mass difference with hydrogen. However, it is always possible that, as Kiselev reports, isotope effects are negligible. As we have calculated a very consistent value for the amount of water of hydroxylation, we could conclude to a very small thermodynamic isotopic effect. The agreement between our diffusion coefficient and that of Onoda, though possibly accidental, could also indicate the absence of kinetic isotopic effects of any large magnitude.

(ii) Discussion of Proton Space Charge Theory. We can now conclude that the hypothesis of a proton space charge for hematite is not disproved by isotopic exchange of tritium with the lattice. Hydrated layers are reported to exist. A diffusion coefficient for tritium through these layers measured under conditions where no electrostatic field complicates the problem can be calculated and will be found in agreement with a value reported by Onoda, based on the analysis of the initial rate of adsorption. Our data does support his point of view.

One should probably qualify this statement. In Onoda's thesis, the displacement of isotherms is followed with time; one of the apparent unexplained discrepancies in his isotherms comes from the increase in steepness with conditioning on the basic side (see Figure 38). It is not difficult to imagine that dissolution of CO_2 in the cell would also cause the increasing slope of the fast isotherm with time while diffusion of protons, because of electrostatic repulsion, would flatten the isotherm, at least on the negative side. The

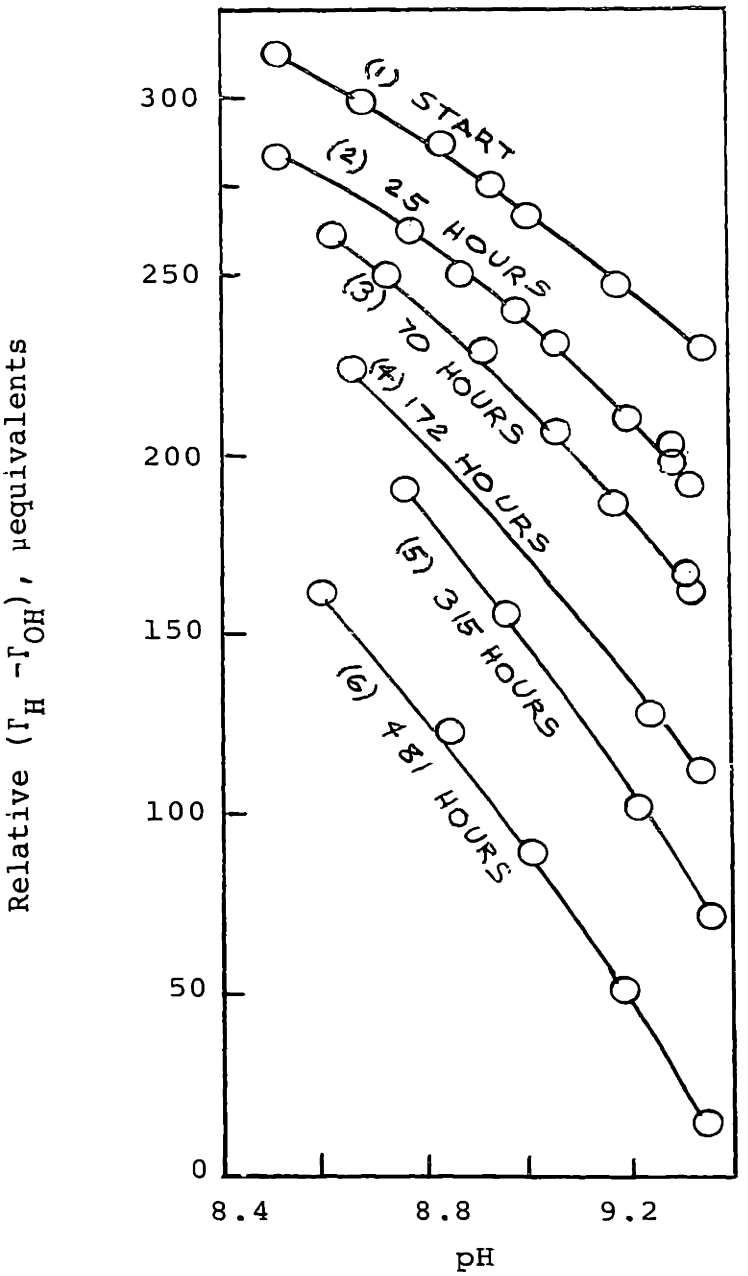

FIGURE 38. CONTINUOUS SHIFTS IN THE FAST ISOTHERMS OF HEMATITE DUE TO CONDITIONING AT CONSTANT pH VALUE OF 9.35 (from Onoda's thesis).

influence of CO_2 was to some extent controlled or at least evaluated in some independent work on hematite[75]. Again, it was confirmed that a slow step did exist on both sides of the zpc but it was found to be of a much smaller magnitude than reported in some of Onoda's experiments. It is felt that CO_2 does on certain occasions complicate the analysis, especially when experiments last for weeks.

However, there is no doubt that the hematite system does not reach instantaneous equilibrium with the solution. Upon changing pH, a slow drift involving as much as 20 to 30 mv will take place in the first 10 hours, and the same is not true of rutile or zincite where a maximum drift of 3 to 5 mv is observed each day upon changing the pH from the equilibrated zpc value. A mechanism has to be proposed for hematite and the proton space charge theory offers the best approach to this initial equilibration of the solid with the solution. But two strong arguments militate against using it as a sole explanation.

First, the amount of water in the solid is insufficient to warrant such conclusions. With a hydration depth of 13Å, one can imagine a stacking of 4 layers of water at the most. Then assuming that for a given surface charge the electrostatic field is not felt by the ions in the solid, a maximum of 4 times the surface charge can be accommodated in the solid. That is far from a "hundred times" value observed by Onoda.

Second, the magnitude of the diffusion coefficient

is too low. One can calculate a diffusional distance (δ) at which $C(\delta) = 0.001\ C^{surf}$ (76). It is equal to $4\sqrt{Dt}$ for diffusion into a semi-infinite plane. After 50 hours of equilibration time, δ equals 8Å. Integrating the concentration gradient over such a small distance will give at the most 1.5 times the charge on the surface. Again, the amount diffusing, according to calculation, disagrees with the magnitude of the observed shifts of isotherms obtained by Onoda.

It is felt that the proton space charge theory can be applied only to the first day of equilibration. Thereupon, other mechanisms that were reported for alumina, zincite or rutile take over and one cannot generalize the theory to all of the observed phenomenon.

(iii) Discussion of Some Assumptions. In view of the estimated short diffusion distances, one might question the validity of a diffusion equation derived for macroconcentration gradients and not molecular layers. Luckily, since the same mathematical approach is followed for both the initial rate calculations of Onoda and the tritium exchange, the error is self-consistent. The fact that our diffusion coefficient is one order of magnitude larger than those observed on goethite could be a clue to our error, though it could always be argued that the substrate is different from goethite and possibly more open. It would certainly be more correct to look at the diffusion as a jumping mechanism and to apply the model to a 5-layer-deep phase. Though the basic mathe-

matical expression turns out to be exactly the same,

$$J = -\nu \frac{dN}{dX}$$

where

ν = jumping frequency

N = number of atoms per unit area

X = distance into the lattice

J = flux in # per unit time and unit area.

It is the integration over the layers which is not continuous but stepwise and leads to a summation that is only approximated by the integration. This would not change the diffusional model for hematite but simply modify the method of calculation.

VI. CONCLUSIONS

Throughout the course of this discussion some partial conclusions were drawn as regards some properties of the interface. One's knowledge of a problem often comes from the accumulation of separate pieces of information which are found eventually to piece together and dovetail nicely.

For instance, our calculations of capacities in terms of a Gouy-Chapman treatment of the interface point to the existence of a plane of charge situated in an environment resembling the liquid rather than the solid in structure and composition. Such a model can then explain nicely the specific affinity of hydrated cations for an ice-like water phase at the surface. The model can also qualitatively predict the effect of charge on the inner capacitor and give an explanation for size effects with various counterions.

The measurement of the effect of temperature on the fast isotherm indicates the validity of the Nernst relationship as applied to the potential-determining role of H^+. Finally, particle size effects in going from a rutile precipitate to a much finer anatase again support the assumptions of the diffuse layer theory as applied to the system. Then there is the effect of heat-treatment on the zpc which emphasizes the strength of the bond between the oxide and the surface water. When this is related to the non-lability of protons at the interface, it can be concluded that the layer of hydration participating in the electrical charging of the

interface cannot be the hydroxylated layer and, therefore, is the adjacent layer of physically bonded water.

There is always the temptation to jump to conclusions and hastily make use of what John Stewart Mill[76] referred to as his fifth canon of scientific methodology: "Whatever phenomenon varies in any manner whenever another phenomenon varies in some particular manner is either a cause or an effect of that phenomenon, or is connected with it through some fact of causation". The careless application of his criterion in defense of theories is a case of wrong inductive reasoning.

It is with this reminder in mind that this model of the interface is offered as an explanation of the behavior of the rutile interface. As long as it is not known what causes the observed variations in the surface properties of rutile (as well as with many other oxides), it probably will not be possible to offer a better approximation.

By assuming a rather inert layer of hydroxylation, one can explain its non-lability and its resistance to rather severe vacuum treatment. By assuming the surface charge to lie in the adsorbed molecular plane of water, one can satisfy both its permeability to counterions and its affinity for hydrated cations and possibly also explain the effect of temperature on adsorption and location of zpc.

With the help of the model, it has been possible to predict the correct dependence of minimum capacities on the square root of ionic strength. That, in itself, would present

a considerable improvement over the ignorance one had previously of the mechanisms of adsorption.

VII. SUGGESTIONS FOR FURTHER WORK

Many questions have been raised in the course of this dissertation that received only sketchy answers. Also, some of the results would suggest further investigations in related fields while at times some of the results themselves could be improved by better experimental techniques. For these reasons, some further work is indicated in the following three areas:

(1) The nature of the slow step in adsorption could be investigated

(a) in the absence of salts

(b) in the presence of a non-specifically adsorbed salt such as cesium iodide.

This would help identify the nature of an ion-exchange reaction at the surface.

The influence of the slow step on the fast isotherm should also be studied with more care so as to follow changes in:

(a) intersections of isotherms

(b) the slope of isotherms

(2) More work is required also with regard to the nature of the fast adsorption isotherm.

(a) The specific effects of cations would be best analyzed with the series Li, K, Cs to emphasize differences.

(b) Strongly adsorbed organic ions should also be used in a further analysis of the effect of specific adsorption on the surface charge.

(c) Above all, the fast isotherm should be made more reproducible. At the origin of most experimental inaccuracies lies, it seems, an uncontrolled variable that was never investigated.

(3) Finally, the existence of surface hydroxyls on the surface, their lability at room temperature should be investigated with the help of infrared spectroscopy, while a quantitative evaluation of the surface hydration could be made with the help of thermogravimetric analysis.

VIII. BIBLIOGRAPHY

1. Graham, K. and Madeley, J.D., J. of Applied Chemistry (London), 12 (1962) 485.

2. Johansen, P.G. and Buchanan, A.S., Australian J. of Chemistry, 10 (1957) 398.

3. Purcell, C. and Sun, S.C., Transations of the Soc. of Min. Eng., 226 (1963) 6.

4. Parfitt, G. D., Unpublished Results (1966).

5. Parks, G. A., Chemical Review, 65 (1965) 177.

6. Parks, G. A. and de Bruyn, P. L., J. Phys. Chem., 66 (1962) 967.

7. Healy, T. W. and Fuerstenau, D. W., J. Colloid Science, 20 (1965) 763.

8. O'Connor, D. J., Johansen, P. G. and Buchanan, A. S., Trans. Faraday Soc., 52 (1956) 229.

9. Parks, G. A., Doctoral Dissertation, Massachusetts Institute of Technology (1960).

10. Mackor, E. L., Rec. des Travaux chimiques des Pays-Bas, 70 (1951) 763.

11a. Lÿklema, J., Kolloid Z., 175 (1961) 129.

11b. Lÿklema, J., Trans. Faraday Soc., 59 (1963) 418.

12a. Iwasaki, I. and de Bruyn, P. L., J. Phys. Chem., 62 (1958) 594.

12b. Freyberger, W. L. and de Bruyn, P. L., J. Phys. Chem., 61 (1957) 586.

13. Albrethsen, A. E., Doctoral Dissertation, Massachusetts Institute of Technology (1963).

14. Kruyt, H. R., "Colloid Science, Vol I., p. 159, Elsevier Publishers.

15. Ibid., p. 175.

16. Onoda, G. Y. Jr., and de Bruyn, P. L., Surface Science, 4 (1966) 48.

17. Korpi, G. S., Doctoral Dissertation, Stanford University (1965).

18. Onoda, G. Y. Jr., Doctoral Dissertation, Massachusetts Institute of Technology (1965).

19. Blok, L., Unpublished Data, Massachusetts Institute of Technology (1966).

20. Grahame, D. C., Chemical Reviews, 41 (1947) 441.

21. Hautefeuille, procédé de, Mellor treaties on inorganic and theoretical chemistry, Vol 7, p. 38.

22. Wilska Seppo, Acta Chemica Scandinavica, 8 (1954) 1796.

23. Weiser, H. B., Milligan, U. O. and Cook, E. I., J. of Phys. Chem., 45 (1941) 1227.

24. Paravano, N. and Schossberger, F., Acta Chemica Scandinavica, (1942) 1938.

25. Ermolseva, T. A. and Anufrieva, N. S., Chem. Abstract, 54 (1960) 23, 221.

26. Asher, R. C. and Gregg, S. J., J. Chem. Soc. (London) (1960) 5057.

27. Gregg, S. J. and Pope, M. I., Kolloid Z., 174 (1961) 27.

28. Latimer, W. M., "Oxidation Potentials", 2nd Edition, Prentice Hall (1952) 266.

29. Nabivanets, B.I. and Lukachima, V.V. 1, Ukraine Khim. Zh. 30 (1964) 1123.

30. Van Lier, J. A., de Bruyn, P. L. and Overbeek, J. Th., J. of Phys. Chem., 64 (1960), 1675.

31. Gebhart, J. and Herrington, K. D., J. Of Phys. Chem., 62 (1958) 120.

32. Salamitou, J., Doctoral Dissertation, Massachusetts Institute of Technology, (1966).

33. Yates, D.J.C., J. Phys. Chem., 65 (1961) 746.

34. Lewis, K. E. and Parfitt, G. D., Trans. Faraday Soc., 62 (1966) 204.

35. Kipling, J. J. and Peakall, D. B., J. Chem. Soc. (London) (1957) 834.

36. Blyholder, G. and Richardson, Y., J. Phys. Chem., 66 (1962) 2597.

37. Healey, F. H., Chessik, J. J. and Fraioli, A.V., J. Phys. Chem., 60 (1956) 1001.

38. Jurinak, J. J., J. Colloid Sci., 19 (1964) 477.

39. Prigogine, I., Mazur, P. and Deboy, R., J. Chimie physique, 50 (1953) 146.

40. Harned, H. S. and Davies, R. J., J. Amer. Chem. Soc., 65 (1943) 2030.

41. Alexander, G. B., Heston, W. H. and Iler, R. K., J. Phys. Chem., 58 (1954) 453.

42. Roller, P. S. and Ervin, G. E., J. Amer. Chem. Soc., 62 (1940) 461.

43. Van Lier, J. A., de Bruyn, P. L. and Overbeek, J. Th., J. Phys. Chem., 64 (1960) 1675.

44. Grahame, D. C. and Soderberg, B., J. Chem. Phys., 22 (1954) 449.

45. Payne, R., J. Phys. Chem., 69 (1965) 4113.

46. Loeb, A. L., Overbeek, J. Th. and Wiersema, P. H., The Electrical Double-Layer Around a Spherical Colloid Particle, M.I.T. Press (1961).

47. Verwey, E.J.W. and Overbeek, J. Th., The Theory of Stability of Lyophobic Colloids, Elsevier Publishers (1948) p. 29.

48. Frumkin, A. N., Trans. Faraday Soc., 36 (1940) 117.

49. Stern, O., Z. Elektrochemie, 30 (1924) 508.

50. Sluyters-Rehbach, M., Timmer, B. and Sluyters, J. H., Rec. des Trav. Chim. des Pays-Bas, 82 (1963) 553.

51a. Bockris, J. O'M., Devanathan, M.A.V. and Muller, K., Proc. Royal Soc., 274A (1963) 55.

51b. Delahay, P., Reference 58, p. 64.

52. MacDonald, J. R. and Barlow, C. A., Proceedings of the First Australian Conference on Electrochemistry, Pergamon Press.

53. Paulings, L., Nature of the Chemical Bond, Cornell University Press.

54. de Boer, J. H., J. Colloid and Interface Science, 21 (1966) 405.

55. Bjerrum, J., Schwarzenbach, G. and Sillen, L. G., Stability Constants of Metal-Ion Complexes, Vol. II, Publ. The International Union of Pure and Applied Chemistry, The Chemical Society (London) (1958).

56. Kargin, V. A. and Tolstaya, P. S., Zhur, Fiz. Khim., 13 (1939) 13.

57. Hurwitz, H.D., Sanfeld, A. and Steichen-Sanfeld, A., Electrochemica Acta, 9 (1964) 929.

58. Delahay, P., Double-Layer and Electrode Kinetics, Interscience Pub. (1965).

59. Rao, C. N., Canadian J. of Chemistry, 39 (1954) 498.

60. Hollabaugh, C. M. and Chessik, J. J., J. Phys. Chem., 65 (1961) 109.

61. Gregg, S. J., "Chemisorption", The Chemical Society Symposium, Butterworths (July 1956).

62. Cotton, F., Advanced Treatises of Inorganic Chemistry, Interscience Pub. (1963).

63. Haissensky, M., Nuclear Chemistry and its Applications", Addison-Wesley (1964) p. 544.

64. Zhuravlev, L. T. and Kiselev, A. V., Russian J. of Phys. Chem., 37 9 (1963) 1113.

65. Aldeman, R. G. and Emmett, P. A., J. Amer. Chem. Soc., 78 (1967) 2917.

66. Mills, G. A. and Hindin, S. G., J. Amer. Chem. Soc., 72 (1950) 5549.

67. Berthier, C., J. Chimie physique, 49 (1952) 527.

68. Feitknecht, Wyllenbach, A. and Buser, W., Reactivity of Solids, Symposium 1960, ed. by de Boer.

69. Zabrova, G. M. and Egorov, E. V., Russian Chemical Reviews, 30 (1961) 339.

70. Puskarev, V. V., Zhur, Neorg. Khem., 1 (1957) 178.

71. Amphlett, C. McDonald, L. and Redman, M., J. Inorg. Nuclear Chem., 6 (1958) 220.

72. Nelson, F. and Kraus, K. A., J. Amer. Chem. Soc., 77 (1955) 4508.

73. Nydahl, F. and Gustafson, L. A., Acta Chemica Scandinavica, 7 (1953) 143.

74. Winchel, A. N. and Winchel, H., Elements of Optical Mineralogy, Wiley & Sons, Publ.

75. Author's Unpublished Data.

76. Schewmon, Paul G., Diffusion in Solids, McGraw-Hill, p. 9.

77. Mill's, J. S., Philosophy of Scientific Method, Hafner, Publ. (1950) p. 227.

78. Bates, R. G., J. of Research, Nat. Bur. of Standards, 66A (1962) 179.

IX. APPENDICES

APPENDIX 1

LIST OF REAGENTS

Reagent	Quality	Manufacturer
NaCl	A.R.	Malinckrodt Chemicals
$NaNO_3$	A.C.S.	J. T. Baker
$NaClO_4$	A.R.	G. F. Smith
$LiNO_3$	A.C.S.	Malinckrodt Chemicals
$CsNO_3$	C.P.	Maywood Chemicals
NaI	A.R.	Malinckrodt Chemicals
HCl	A.R.	Anachemica, Montreal, Canada
HNO_3	A.R.	DuPont
$HClO_4$	A.R.	G. F. Smith Co.
2.5 dephenyloxazole (PPO)	technical	Pilot Chemicals
PBis 12-(5 phenyloxazolyle) Benzene POPOP	technical	Pilot Chemicals
Methanol	A.C.S.	J. T. Baker
Benzyl alcohol	A.C.S.	Merck
Tritiated water	-	New England Nuclear

APPENDIX 2

CALIBRATION OF ELECTRODES

Recent work by Bates[78] has established the pH (in terms of $\gamma_{NaCl} \cdot C_{HCl}$) of a series of standard buffers as a function of temperature. Care has been taken to minimize junction potential effects so that comparisons are permissible even with a cell having a liquid junction.

Three such buffers were prepared:

(1) Potassium acid phtalate (0.05 molar) with a pH of 4.008 at 25°C.

(2) Potassium dihydrogen phosphate (0.025 molar) and disodium hydrogen phosphate (0.025 molar) with a pH of 6.975 at 25°C.

(3) Borax (0.01 molar) with a pH of 9.180 at 25°C.

These buffers are used to determine the pH-millivolt slope of the electrodes.

Calibration is done by adding acid to water kept at a defined temperature to bring pH in the vicinity of 3.5 or lower. Ionic strength is varied and data is obtained in terms of ($-\log C_{H^+}$) versus electrode potential for various concentrations of salt.

The slope of electrodes is often checked against the buffer value when accurate activity coefficients are available. This is simply done by measuring the output voltage for a given concentration of acid and then adding base to approximately pH 10.5 where the electrode output is determined against a

known concentration of base. pH can be calculated from the expression

$$-\log K_w = pH - (-\log \gamma_{\pm} C_{OH^-}) \quad .$$

With two values of $pH = -\log \gamma_{\pm} C_H$ and two corresponding emf's the slope is calculated and found to be always within 0.1 mv of the slope measured with buffers.

Measurements of Activity Coefficients

Since one can determine the slope of electrodes when activity coefficients are available, and since one finds good agreement with the slope as obtained from buffers, one can reverse the logics and use the buffer slope to determine activity coefficients.

Values of the dissociation constant of water are obtained from the "Handbook of Chemistry" as $K_w = f(T)$. Determination of activity is done in the following way. A cell containing 300 cc of conductivity water is flushed at pH 4 overnight to remove dissolved CO_2. pH is then adjusted in the vicinity of 7.0 at a determined concentration of salt. Three additions of 100 μmoles of acid are made to the cell and corresponding emf's are recorded. pH is brought back to 7.00 again and this time three additions of 100 μmoles of base are made and emf's recorded again. The slope of the electrodes is obtained from two buffer readings.

With the first set of emf's and C_{H^+}, one calculates an average E° from the equation

$$E = E^\circ + (\text{slope}) \cdot (-\log C_{H^+}) \quad . \qquad (1)$$

The second set of emf's is introduced in equation (1) and values for ($-\log C_{H^+}$) are calculated; each corresponding to a value of ($-\log C_{OH^-}$), obtained from the amount of base added. Equation (2) gives directly values for $-2 \log \gamma_{\pm}$ which are then averaged.

$$K = (-2 \log \gamma_{\pm}) + (-\log C_{H^+} \cdot C_{OH^-}) \quad . \qquad (2)$$

Values for ($-\log \gamma_{NaCl}$) at various ionic strengths and temperatures are tabulated below.

	Ionic Strength		
Temperature	0.001M	0.01M	0.1M
25°C	0.02	0.05	0.11
50°C	0.02	0.05	0.14
75°C	"0.05"	"0.07"	0.15
95°C	0.01	0.05	0.13

APPENDIX 3

The calculation of isotherms is a rather tedious operation. It has been reduced to a simple data reduction operation through the use of a computer. The program is written in FORTRAN and results are given with a third decimal accuracy. The program is given below in a form suitable for card inputs.

```
*       XEQ
        DIMENSION COR(6), CON(6)
   20   FORMAT (6F5.2)
   21   FORMAT (6F10.2)
   22   FORMAT (F10.4, F10.2, F10.2, F10.2, F10.3, F10.3)
   23   FORMAT (F5.0, I1, 4X, F10.5, F10.2, F10.2)
   24   FORMAT (F5.0, F10.3, F10.3)
C       READ CONSTANTS
    9   READ 20, (COR(J), J=1,6)
        READ 21, (CON(J), J=1,6)
        READ 22, CA, SLOPE, CPH, CMV, MH, MOH
        DELGA = 0.0
        GAM = 0.0
C       READ DATA
    8   READ 23, EXP, ION, VOLU, DELH, VOLT
C       MAKE CORRECTIONS TO DATA
        IF (ION) 1,2,1
    1   I=ION
    2   VOLT=VOLT + COR(I)
        VOLU=VOLU/1000.
        IF (DELH) 14,13,11
   11   DELH = DELH* MH
        GO TO 13
   14   DELH = DELH * MOH
C       CLACULATION OF PH OR POH, CH OF COR
   13   PH= (( VOLT - CMV)/SLOPE) + CPH
        IF ( PH- 6.50 ) 4,3,3
    3   POH= CON(I) -PH
        COH= (10. ** (6. -POH))
        CH = 0.0
        GO TO 12
    4   CH= 10. ** ( 6. -PH)
        COH = 0.0
C       CHECK FOR FIRST DATA CARD
   12   IF (EXP) 5,6,5
    5   IF (EXP - 999. ) 7,6,6
C       CALCULATION OF DELTA GAMMA
    6   DELGA= DELH - (VOLU* (CH-COH) - VCHOH)
```

```
          GAM= GAM + DELGA
      7   VCHOH= VOLU* (CH- COH)
          GAMMA = GAM* CA
C         PRINT RESULTS
          PRINT 24, EXP, GAMMA, PH
C         CHECK FOR END OF ISOTHERMS OR DATA
          IF ( EXP - 999. ) 8,9.10
     10   CONTINUE
          CALL EXIT
          END
*         DATA
```

The last card *DATA indicates that data cards will now be fed. Both * XEQ and *DATA cards are required by the M.I.T. Computation Center, whether the program is in binary form or not.

In order to use the program to reduce the data to a printed output of ($-\log C_{H^+}$) versus adsorption ($\Gamma_H - \Gamma_{OH}$) in moles$\cdot 10^{+11}$ per cm^2, certain conditions must be met.

We will now illustrate the operations performed by the program in order to clarify the format to be used in punching the data.

To calculate ($-\log C_H$), the program makes use of the formula,

$$E = E^{\circ\prime} + k\ (-\log C_{H^+}) \qquad (1)$$

It is necessary to provide the computor with the actual slope of the electrodes (millivolt versus pH, , that is k. It is necessary also to submit to the program a value of E corresponding to a value ($-\log C_{H^+}$) so that the program can evaluate E°.

It was explained under Appendix 2 that E°' varies with ionic strength in Equation (1); therefore, this equation (1)

is only valid for one value of E°' given for one set of conditions. To correct for changes in ionic strengths or changes in the asymmetry potential of a glass electrode during a long experiment, E°' must be corrected. Correction factors must be added to the data for the changing conditions. It can be done by actually correcting E° or by correcting the data input E for each electrode reading, the latter is preferred.

An example will illustrate the point. If at 0.001M, it is found upon calibration of the electrodes that pH = 8.00 corresponds to an electrode output of 200 mv, these two values are called reference pH and reference millivolt. If now for the same pH the electrode output were to become 210 mv because of a different concentration of salt or any other reason, the correction is made by adding a correction factor of (-10 mv) to 210 mv or any other emf at the same ionic strength, such that the original equation can still be used. The opposite situation would rise, 190 millivolts corresponding to pH = 8.00 that the correction factor would be (+10 mv). Whenever the computor reads a millivolt output as a piece of data, there must be stored in the memory some correction factor applying to that point. The basic rule is, whenever an electrode output is read, the correction factor must be such that when added to the reading the basic relationship between the reference pH and the reference millivolt is always observed.

The data must also provide for values of :K where

$$K = (-\log C_{H+}) + (-\log C_{OH-}) \qquad (2)$$

K varies with ionic strength.

It is important to note here a characteristic of the calculations; for each piece of data, a value of K (defined as CON) is required which can be the same over many bits of data. The same holds for the correction factor, defined as COR. In the program, a value of CON is always associated with a corresponding value of COR.

We will now describe the format. The first three cards consist in operational data to be used to do the calculations.

(A) The first data card contains up to 6 correction factors or COR(J) where $0 < J < 7$. They can have any value including 0 but must always carry a decimal point.

(B) The second card contains values of K (or CON). Again, obviously from the preceding discussion, a maximum of 6 values are accepted, all with a decimal point. The first value CON (1) corresponds to the first correction factor COR (1) and so on. To change COR without changing CON requires repeating the old value of CON that will correspond to the new COR.

(C) The third card contains a constant (defined as CA) which will multiply adsorption to give as moles x $10^{+11}/cm^2$. It is calculated by:

$$k \cdot 10^{-11} = \frac{10^{-6}}{\text{specific area } (cm^2/gm \times Wt\ (gm)}$$

and also: (i) The EMF versus pH, slope of the electrode defined as SLOPE.

(ii) A reference pH defined as CPH.

(iii) A reference millivolt defined as CMV.

(iv) A correction factor for acid normality defined as MH, such that: $N_{acid} \times 10 = MH$.

(v) A correction factor for the normality of the base, defined as MOH, such that: $N_{base} \times 10 = MOH$.

We have given the content of the first three cards, now we will give the format used to punch the data on those cards.

First Card: 6 consecutive fields of 5 columns, where the correction factor always carries a decimal. Whenever a field is left out, it is taken as zero.

Second Card: 6 consecutive fields of 10 columns, where CON always carries a decimal point.

Third Card: 6 consecutive fields of 10 columns (decimal point required).

Following these cards are the data cards properly speaking. Each data card from now on has the same format which is described now consecutively:

(A) a field of 5 columns

(B) a field of 1 column

(C) 4 blanks (ignored by the computor)

(D) three consecutive fields of 10 columns

We will first describe the data which goes in "D". In the first field (column 11 to 20), the volume of the solution is expressed in cm^3 and must contain a decimal point (for instance 210.3 cc).

The second field (column 21 to 30) receives the amount of acid added (positive sign) or base (negative sign). The amount is expressed in μmoles and carries a decimal point (for instance, 21.0 μmoles).

The last field (column 31 to 40) receives the millivolt output after addition (decimal point required).

The first two fields in "A" and "B" are special and carry information to the computer pertaining to the experiment number and the ionic strength of a set of data.

The first field (column 1 to 5) receives the number of the experiment to facilitate identification. The number can have values between 1. and 998. (decimal point is required). The field is occupied only once for a titration on the first data card (excluding the first three cards already discussed). At the end of the titration two numbers can be placed 999. or 1000. 1000. indicates to the computer that calculations are over. 999. indicates that calculations are over for a set of isotherms but that a new set follows. In which case the computer clears its memory from all previous constants and expects an entirely independent set of data (including CON, COR, CPH, etc.). This number 1. to 1000. is defined as EXP in the program.

The second field (column 6) identifies which COR or CON is to be used on that piece of data given on the card. "1" indicates that the first COR and first CON are used, "2" the second values and so on. The number is given without decimal point and is defined as ION. Whenever this column is left blank, the computer uses the last value previously given. It is clear now that in a deck of data cards at the beginning of each different set of conditions, a value 0 < ION < 7

must be set. The rules are thus resumed:

First Card: 6 fields of 5 columns for COR (J) where $0 < J < 7$.

Second Card: 6 fields of 10 columns for CON (J) where $0 < J < 7$.

Third Card: 6 fields of 10 columns for CA, SLOPE, CPH, CMV, MH, MOH.

All data cards: 1 field of 5 columns EXP, 0<EXP<1000.
1 field of 1 column ION, 0<ION<7.
4 blanks.
3 consecutive fields of 10 columns, VOLU, DELH, VOLT.

Whenever EXP = 999., a new set of data starting with a "first card" is following.

Whenever EXP = 1000., the computer stops. Otherwise EXP is used only once on the <u>first</u> DATA CARD.

An example of fictitious data, one line to a card is given below:

```
 0.0        +0.5         +0.5        +2.4        -3.5
13.97          13.91        13.87               13.79    13.65
 0.312         -58.5         4.00              310.6      1.0     1.0
 1.   1        300.6         5.                 82.6
                300.7       -10.                40.6
                300.8        10.                88.2
                300.8        -1.4               82.8
      2         301.75        0.                302.1
                301.8         5.                306.1
      3         303.4         0.                307.2
      4         303.4         0.                291.3
      5         304.4      -100.                - 9.4
                304.5        10.                 10.2
999.            308.6       -10.                -9.4
    0.0  2.4
   12.26      11.91
     .650      -59.16          4.00              325.2   0.8450   1.926
   18.         1        300.         0.           140.
                        300.4        5.           170.2
               2        300.8       10.           160.4
 1000.                  300.8        8.25         180.6
```

The printed output comes as:

EXP_1	Γ_1	PH_1
	Γ_2	PH_2
	Γ_3	PH_3
999.	Γ_4	PH_4
EXP	Γ_1	PH_1
	Γ_2	PH_2
1000.	Γ_3	PH_3

APPENDIX 4

INTERACTION OF DOUBLE-LAYERS AT ELEVATED TEMPERATURES

When measuring pH at the higher temperatures of 75°C and 95°C in presence of precipitate, a special problem arises. Under the usual working conditions, stirring has no effect on the electrode response (less than 1.0 mv of variation) in a suspension kept at a fixed pH. Kruyt[14] warns of the Palmann error introduced when measuring pH of suspensions but at the low sol concentrations involved in all experiments the effect is not visible, though it should always be looked for whenever the amount of precipitate in a cell is large.

At higher temperatures, a different phenomenon occurs and is particularly annoying at low ionic strength. While the voltage output of electrodes dipped in a well-stirred suspension is stable (though varying the rate of stirring can change it by 0.1 to 1.5 millivolt), as soon as the stirrer is stopped the electrode starts drifting in a very unstable manner. The question now arises as to what causes this instability. We will describe first some experiments undertaken to clarify the problem.

First, a phosphate buffer was prepared as described in Appendix 2. One can check that its ionic strength, defined as $I = 1/2 \sum m_i z_i^2$ is 0.1M and its pH at 75°C, 6.905. In that particular experiment, a stirred or non-stirred buffer would give a voltage output of -751.2 millivolts. Now, a blank cell of pure water at an ionic strength of 0.1M of NaCl, when

adjusted by adding base to give an emf reading of -750 mv, will also show no effects due to stirring. That establishes the fact that the precipitate is responsible for the observed electrode instability.

A cell is, therefore, prepared with approximately one gram of precipitate and an ionic strength of 0.1M. pH is adjusted until the electrodes read -748.5 mv with the stirrer running. Upon stopping the stirrer, the voltage will drift to -801 mv in about 40 minutes and it is still drifting after that time. The original reading of -748.5 mv can be restored simply by stirring. This material is then filtered and introduced wet in the prepared buffer. With the material in the cell, the buffer would read -751.8 mv with the stirrer on and -752.7 without the stirrer, both readings being perfectly stable.

It can now be seen that if pH is kept absolutely constant by having the precipitate immersed in the buffer, no drift is observed when the stirrer is stopped. It can also be seen that stirring a precipitate may have it interact with the electrodes and change the reading, but the effect is small and can be overlooked. It is, therefore, concluded that the drift happens because of a true pH change in solution, and that pH change comes about because of the precipitate.

It is, therefore, suggested that as the material settles, the double layers are brought so close together that they interact. This results in the expulsion of counterions from the diffuse layer; the total counter charge is thus

reduced accordingly and potential-determining ions are released to the solution.

Such a phenomenon points to the danger of having too much material in a cell of a small volume, especially at high temperatures where the double layers stretch out in the solution.

APPENDIX 5

CRYSTAL STRUCTURES OF TITANIA AT ROOM TEMPERATURE

The rutile modification is characterized by a tetragonal unit cell containing two molecules, where:

$a = 4.49\text{Å}$
$c = 2.89\text{Å}$

The positions of the atoms are given by:

Ti = 000, 1/2, 1/2, 1/2
O = $\pm$ (uuO, u+1/2, 1/2-u, 1/2)

where u is usually small.

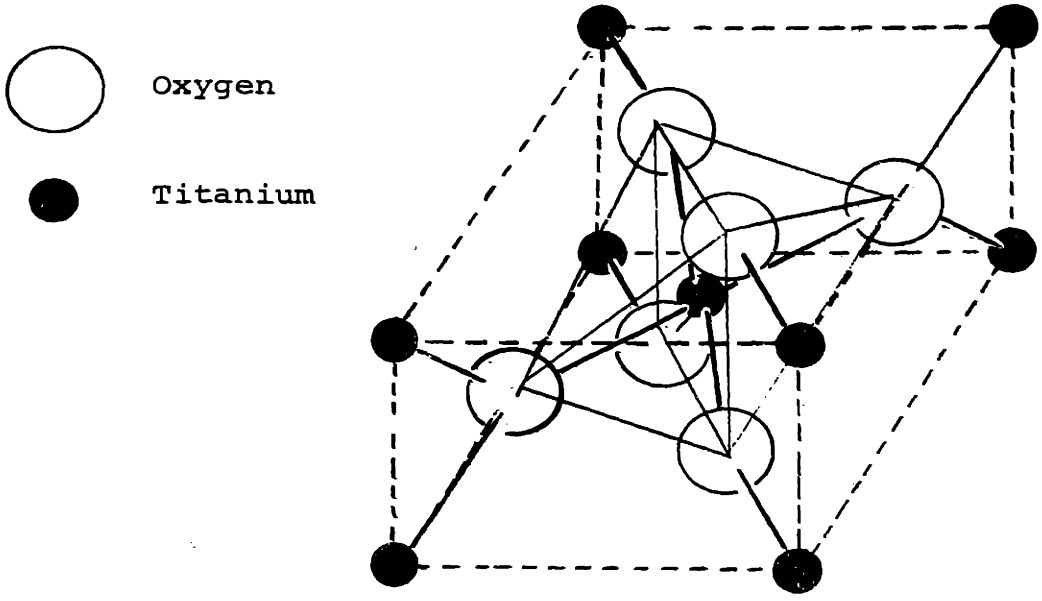

Figure 5-1. Crystal Structure of Rutile.

Figure 5-2 illustrates a (100) plane in the crystal while Figure 5-3 shows a (110) plane.

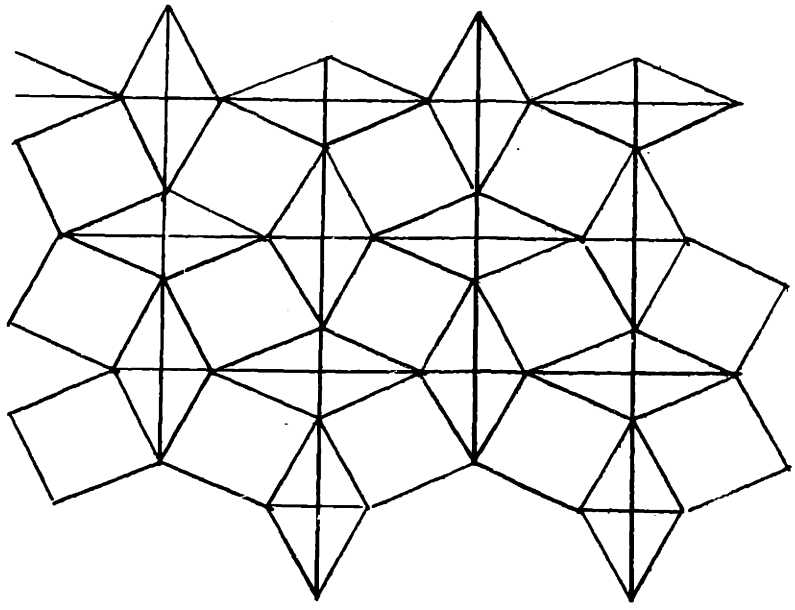

Figure 5-2. (100) Plane in Rutile.

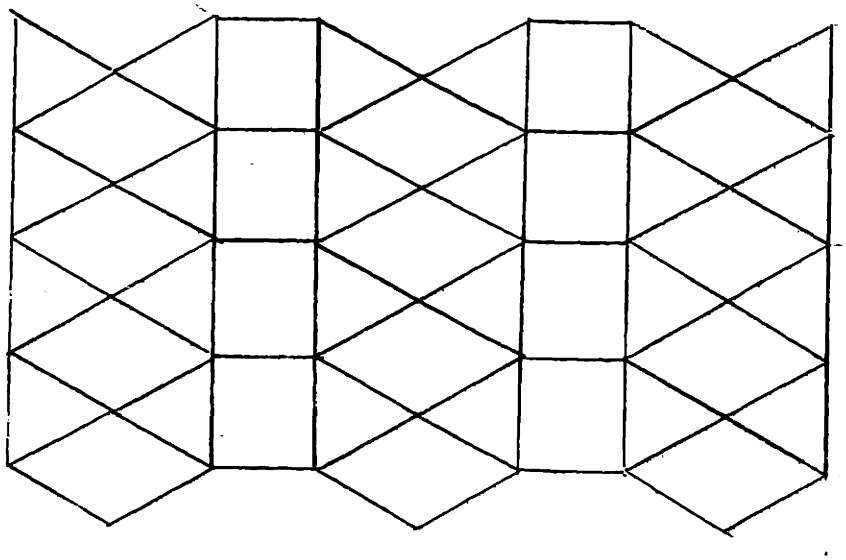

Figure 5-3. (110) Plane in Rutile.

The anatase modification is more difficult to illustrate. The unit cell is also tetragonal but it contains 4 molecules where:

$a = 5.36\text{Å}$

$c = 9.53\text{Å}$

The structure is best visualized by a stacking of Ti-O octahedra with four shared edges. Figure 5-4 describes such an octahedron where the heavy lines indicate the shared edges.

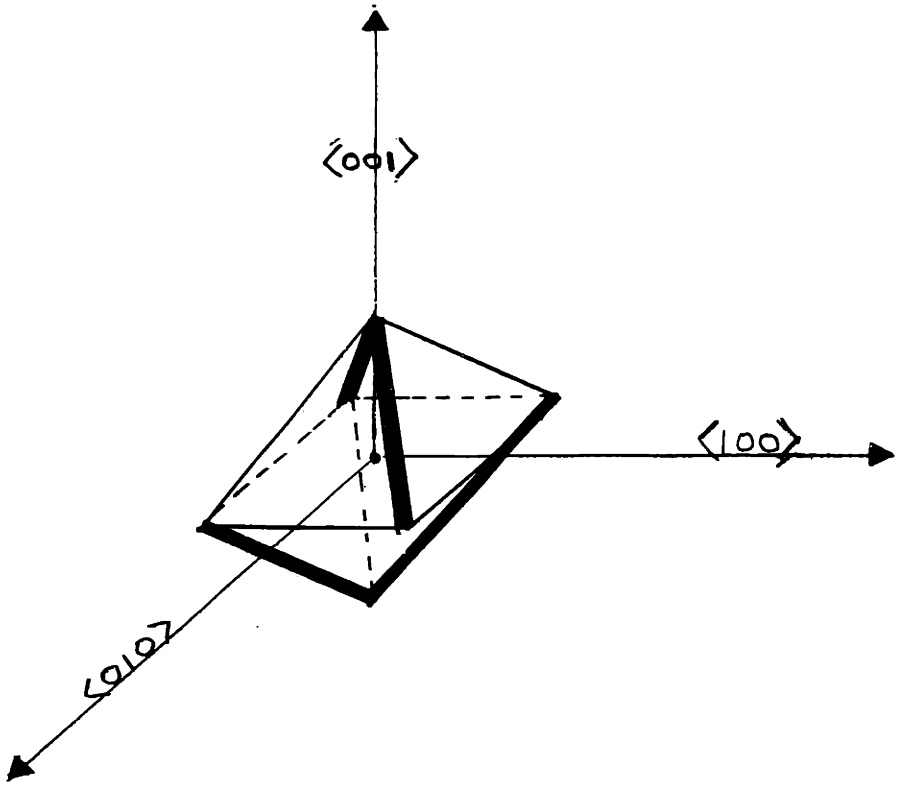

FIGURE 5-4. OCTAHEDRON, Ti^1-O^6, IN THE ANATASE STRUCTURE.

BIOGRAPHICAL NOTE

Yves Bérubé was born in Montreál on March 28, 1940. The author received a Bachelor of Arts in literature and philosophy from l'Université de Montreál in June 1961, whereupon he entered M.I.T. to obtain an S.B. in metallurgy in June 1963.

Since then he has pursued his graduate education at M.I.T. where he has held a merit scholarship from le Ministère des Richesses naturelles du Québec. He has been employed in the Department of Metallurgy as a research assistant.

He is married to Francine Leroux of Montreál, a graduate of M.I.T. in architecture. They have a daughter.